COMPUTER ENHANCEMENT OF LANDSAT DIGITAL DATA FOR THE DETECTION OF LINEAMENTS

By

FRANK MYNAR II

Bachelor of Science

University of Michigan - Flint

Flint, Michigan

1979

Submitted to the Faculty of the
Graduate College of the
Oklahoma State University
in partial fulfillment of
the requirements for
the Degree of
MASTER OF SCIENCE
July, 1982

COMPUTER ENHANCEMENT OF LANDSAT DIGITAL DATA FOR THE DETECTION OF LINEAMENTS

Thesis Approved:

Stephen J. Walsh
Thesis Adviser

John D. Vitek

Stephen J. Fadler

Norman N Durham
Dean of the Graduate College

ACKNOWLEDGMENTS

The completion of a thesis is not an easy task, nor is it a completely individual accomplishment. Along the way, there have been a number of people who have contributed in some manner to the generation of this final product. To all of them, my sincerest thanks:

Dr. Stephen J. Walsh, for his invaluable guidance as my major adviser, and, in his capacity as Director of the Center for Applications of Remote Sensing, for making the computer and processing system available to students like myself.

Dr. John D. Vitek and Dr. Stephen S. Stadler, the other members of my committee, for their many constructive comments in the course of my research and writing. To Jack, thanks also for catching my "LuLus", and for being responsible for bringing me to Oklahoma in the first place.

John Kerns, CARS' resident "computer whiz", for taking time out from his own thesis work to help me deal with the computers that seemed to be menacing me in all phases of this research. Without his constant help in guiding me through the intricasies of the computer world, I would probably have been here for another two years.

Tony Blanchard, Research Associate at CARS, for sharing with me his wealth of knowledge about Landsat, particularly

in the enhancement phase of this research.

The Department of Geography, for its financial support during my graduate studies, and for providing me with the computer time necessary for carrying out the study and producing this document.

My parents, Mr. and Mrs. Frank Mynar, for their never-ending support and encouragement, and for instilling in me the will to stick with whatever endeavor I undertake. Though physically many miles away these last two years, they were still near.

TABLE OF CONTENTS

LIST OF TABLES

LIST OF FIGURES

CHAPTER I

INTRODUCTION

General

Remote sensing techniques have become invaluable tools for use in the investigation of a wide variety of problems affecting man in his physical and cultural environments. One application of remote sensing technology is the identification of geologic features known as "lineaments" via satellite data. Lineaments can be concisely defined as surface manifestations of subsurface displacement (Gold, Parizek, and Alexander, 1973). This thesis is intended to assess the detection and discrimination of lineaments through the application of Landsat-satellite technology.

Objectives

The objectives of this study are twofold: (1) to apply a number of previously-developed computer enhancement techniques to Landsat digital data, in order to aid in the detection of lineaments; and (2) to evaluate the comparative utility of the various enhancement techniques for the purpose of lineament detection. This document does not attempt to analyze lineaments from a geologic point of view;

no direct concern is given to their origins or subsurface relationships.

Definition of Lineament

A number of different interpretations of the term "lineament" have been developed. In the Dictionary of Geological Terms (1976) lineaments are defined as straight or gently curved, lengthy features of the earth's surface, frequently expressed topographically as depressions or lines of depression. Billings (1972) describes lineaments as lines, resulting from natural processes, that may be observed or inferred, and are expressed as relatively straight lines on the surface. The surface features that make up a lineament are quite often geomorphic in nature, existing as landforms, linear boundaries between different types of terrain, or breaks within a uniform terrain (Sabins, 1978).

Some researchers have, in the past, defined lineaments in terms of size. Lattman (1958) differentiated between lineaments and fracture traces on this basis, defining lineaments as those linear features expressed continuously for at least one mile, and fracture traces as less than one mile long. Size similarly was used as a defining criterion by Gold, Parizek, and Alexander (1973), who stated that lineaments are generally five to several hundred miles long.

The term "lineament", as used in this research, will conform to a definition given by O'Leary, Friedman, and Pohn

(1976). This defintion states, in a clear, understandable manner, what a lineament is:

> . . . a mappable, simple or composite linear feature of a surface, whose parts are aligned in a rectilinear or slightly curvilinear relationship and which differs distinctly from the patterns of adjacent features and presumably reflects a subsurface phenomenon (p. 1467).

O'Leary, Friedman, and Pohn (1976) further elaborate on this definition, describing six characteristics associated with lineaments. By this definition, lineaments: (1) have geomorphic expression; (2) are composite, being either segmented or a complex of smaller features; (3) are characterized by alignment in a single direction; (4) are straight or slightly curved; (5) are regional in extent; and (6) are scale related.

Relevancy of Study

Value of Satellite Imagery for Lineament Detection

The detection of lineaments through remote sensing techniques has been a problem of considerable interest to geologists since the inception of aerial photography. The "bird's eye view" provided by aerial photography gave early interpreters the opportunity to detect features that could not ordinarily be seen from the ground. Not until the launch of the first Landsat satellite in 1972, however, was the true worth of remote sensing technology for lineament

detection fully realized. Upon interpretation of the first Landsat images, lineaments were readily visible, a condition that can be attributed to the oblique illumination, suppression of distracting details, and regional coverage characteristic of Landsat imagery (Sabins, 1978). Isachsen, Fakundiny, and Forster (1973) stated, in an early Landsat investigation, that the greatest geological contribution, by far, of satellite imagery was the detection of linear features. Goetz and Rowan (1981) remarked that one of the most striking results of Landsat image analysis is the discovery of numerous, previously unmapped regional linear features in both well mapped and poorly mapped areas. Rowan and Wetlaufer (1973) agreed that, while Landsat images provide useful information to several geologic applications, lineament analysis is benefitted particularly, because such features can be efficiently delineated by the satellite's synoptic view. Likewise, Hoppin (1973, p. 538) concluded that Landsat imagery provides an "unparalleled structural overview unobtainable by any other means".

Lack of Lineament Investigations Utilizing Digital Data

One predominant characteristic of nearly all of the early lineament-related studies involving Landsat imagery-- as well as most of the studies to date-- was that Landsat analog data, rather than digital data, was the primary interpretation medium. This is understandable in the early

studies, when computer processing technologies were relatively unavailable, but represents a serious gap in recent lineament research. Digital data is superior to analog data, in some respects, as it allows for resolution of the full level of detail originally sensed by the satellite. LARS Research Bulletin 919 (1975) stated that 9 inch by 9 inch format Landsat analog imagery, as well as 1:250,000 scale enlargements, do not adequately allow for detail extraction. Only through the use of computer analysis procedures can one make full use of the subtle detail contained in Landsat data.

Relatively few studies have made use of digital data for lineament detection purposes. Offield et al. (1977) utilized machine processing methods exclusively in an investigation of the geologic structure of Brazil. A combination of analog and digital methods was utilized by Podwysocki, Moik, and Shoup (1975) in their study of the Anadarko Basin of Oklahoma. Gold, Parizek, and Alexander (1973) also made use of both analog and digital data in a study of the application of satellite imagery to regional geologic mapping, a study which included the identification of lineaments. Goetz et al. (1973b) investigated lineaments and other aspects of geology from Landsat color composites that were enhanced by computer methods. The relative lack of studies utilizing digital data for purposes of lineament detection indicates that further work in this area is warranted.

Lack of Comparative Investigations of Digital Enhancement Techniques

Enhancement of digital data is a powerful technique in lineament analysis, primarily because of its flexibility. Virtually any enhancement desired can be executed without delays inherent in optical enhancement methods (Gillespie, 1980). While many image enhancements can be performed optically, Landsat images are best processed by computer methods (Offield et al., 1977). A review of the literature, however, has indicated that of the number of studies undertaken utilizing image enhancement techniques to aid in the detection of lineaments, relatively few have made use of digital techniques. Furthermore, of those studies that have used digital enhancement methods, nearly all have employed only one or two particular techniques in their research. Goetz et al. (1973b) made use of both a contrast stretch and directional filtering in enhancing lineaments, but made no attempt at comparing the results of the two techniques. Podwysocki, Moik, and Shoup (1975) applied only a directional filter enhancement. The most comprehensive application of a variety of digital enhancement techniques in a specific study situation was reported by Offield et al. (1977). In that study, the techniques of contrast stretching (linear and Gaussian), ratioing, and frequency filtering were applied to structural mapping in general, with a brief, qualitative comparison of the methods used. A comprehensive, comparative study of a variety of digital

image enhancement techniques applied specifically to the problem of lineament detection appears to have been a void in both remote sensing and geologic research.

Methodology

The research undertaken consists of three primary phases: (1) application of enhancement techniques; (2) interpretation of lineaments from the enhanced images; and (3) comparative analysis of the enhancement techniques utilized. Computer-assisted processing of Landsat digital data is the principal means of investigation in the first phase, with subsequent analysis of the processed data to follow.

Enhancement of the digital Landsat data is accomplished through the application of a variety of computer enhancement techniques to the data, in order to maximize the number of lineaments detected. The enhancements all involve techniques that have previously proven to be of value in lineament detection. Computer algorithms that digitally manipulate the satellite data are used for this purpose, with results being displayed on a COMTAL image processing system, using the Earth Resources Laboratory Applications Software (ELAS) package (Graham et al., 1980). Five primary enhancement techniques are applied: (1) mean value of all four bands; (2) histogram equalization; (3) band ratioing; (4) principal components analysis; and (5) high-pass digital filtering.

Interpretation of lineaments from the enhanced images, the second phase of this thesis, is accomplished manually. Visual identification of lineaments is done directly upon the COMTAL screen, with the resulting line segments mapped as a graphic overlay. One overlay is produced for each enhancement and for the unenhanced image. In addition, a lineament overlay is produced from a known-lineament map, which is used in the capacity of the "standard" against which the other interpretations are compared.

The final phase of the research, an analysis of the utility of the different enhancement techniques for the purpose of lineament detection, is designed to be as quantitative and objective as possible. Rather than visually comparing the lineaments mapped from two interpretations, a numerical means of comparative analysis is implemented. First, the beginning and endpoint locations of all lineaments mapped on each overlay are converted to digital format by means of a graphic digitizer. These data are then input to the computer, and run through a series of programs that summarize the data in terms of lineament length, number, and direction. Results from these programs are then input to another program, which calculates a "similarity coefficient" for two lineament interpretations. In this phase of the analysis, the interpretations resulting from the enhancements are compared, one by one, with each other, with the unenhanced data, and with the known-lineament map. Through an analysis of all interpretations

in this manner, a quantitative statement can be made regarding the enhancement techniques.

Study Area

Site Selection Requirements

Lineaments are expressed on the landscape as straight stream and valley segments, abrupt changes in valley alignment, aligned sink holes, and gaps in ridges, revealed on images as narrow bands or lines contrasting in tone from their surroundings (Gold, Parizek, and Alexander, 1973). Because of this topographic expression, lineaments are generally best interpreted on images depicting areas of rugged terrain. This fact was acknowledged by Podwysocki, Moik, and Shoup (1975) in their study of operator subjectivity in lineament mapping, where it was found that terrains of relatively low relief were less than ideal for a study requiring a high degree of objectivity in lineament detection. Thus, the first criterion for selection of a study area is an area of relatively rugged terrain.

A second criterion in site selection is an area previously mapped for geologic lineaments. In the analysis of the comparative utility of the various enhancement techniques, it is imperative that a lineament map of the study area be available. From the locations of known lineaments, interpretation results are assessed. Without a known-lineament map, there would be no standard against which to judge the enhancement interpretations.

Geographic Location

The study area with which this research deals is located in LeFlore County, in southeastern Oklahoma. Covering 169 square miles, the study area has dimensions of 13 miles by 13 miles. In terms of the Universal Transverse Mercator (UTM) grid coordinate system, the area is located in Zone 15, between 3,843,147 meters north and 3,864,067 meters north, and between 317,330 meters east and 338,250 meters east (Figure 1).

Topography

Located in the Ouachita Mountains, the area is characterized by relatively rugged terrain. Local relief is nearly 2,000 feet, with a low elevation of 500 feet and a high elevation of 2,448 feet. The study area is dominated by the Winding Stair Mountain Range of the Ouachitas, which encompasses all but the extreme northern extent of the region. This northern portion is nearly flat, and is marked by the presence of Wister Lake in the northeastern corner. The entire Winding Stair Mountain region of the study area is located in the Ouachita National Forest (Figure 2).

Geology

The Ouachita Mountains of Oklahoma and Arkansas are a small, exposed, central portion of a more extensive, elongate belt of folded and faulted Paleozoic rocks. This belt, called the Ouachita system, extends under the Gulf

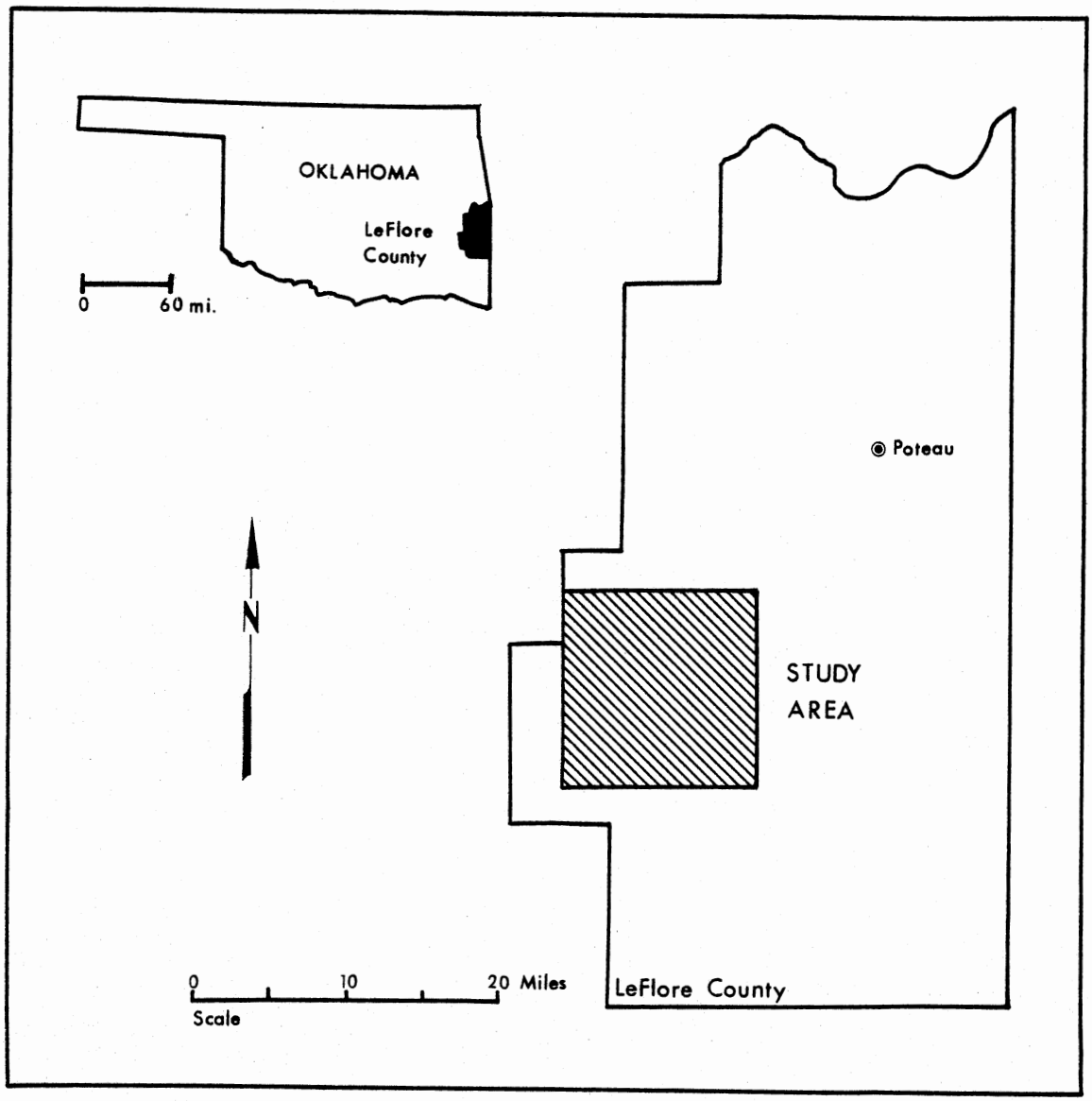

Figure 1. Study Area Location Map

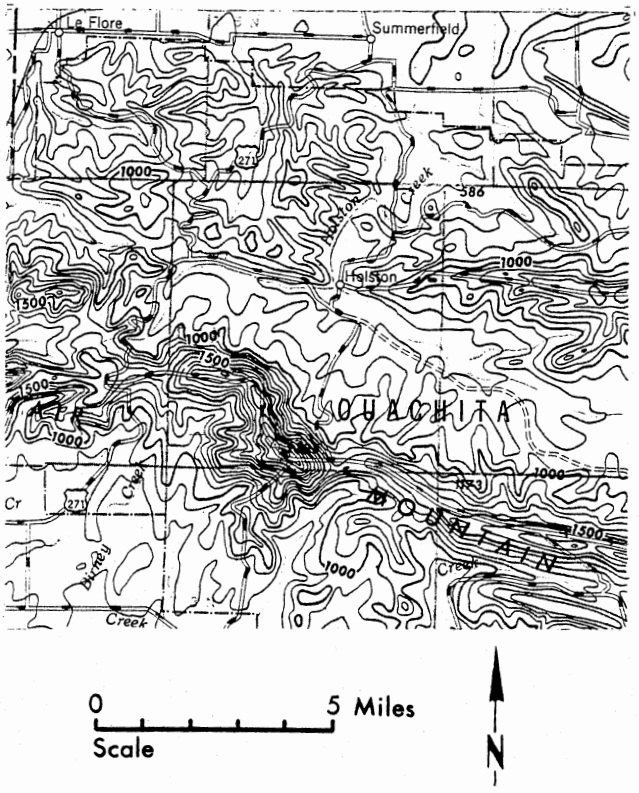

Source: U. S. G. S. Topographic Map, 1:250,000 Scale, McAlester, United States (1965).

Figure 2. Study Area Topographic Map

Coastal Plain, and stretches from Mississippi to west Texas (Melton, 1976). The Ouachitas of Oklahoma are characterized by abrupt structural contrasts, with areas of tightly folded and faulted sedimentary rocks located in close proximity to broad, relatively simple synclinal folds. This mountainous area is structurally divided into three zones: (1) a complex folded and faulted frontal zone between the Choctaw and Winding Stair faults; (2) a central, structurally less complex part, to the south; and (3) the Choctaw anticlinorium of older Paleozoic rocks, located near the Texas-Oklahoma border. The study area for this thesis is located in the frontal zone, and exhibits the complex structure of that zone, but is stratigraphically related to the central zone (Hart, 1963).

Exposed rocks in the Ouachita Mountains of Oklahoma are sedimentary in origin, of Late Mississippian and Early Pennsylvanian age. Such rocks belong to four principal units. From oldest to youngest, these units are the Stanley Group, Jackfork Group, Johns Valley Shale, and Atoka Formation. This rock sequence is composed of thousands of feet of rhythmically alternating sandstones and shales, with a few chert beds (Hart, 1963).

Organization

The remainder of this thesis details the methodology involved in applying enhancements and analyzing the results. An overview of Landsat data is given in Chapter II,

introducing basic concepts which will be incorporated into the methodological phases of the study. Chapter III discusses the enhancement procedures utilized, while Chapter IV details the interpretation of lineaments from the enhanced and unenhanced images. Chapter V discusses the analysis procedures through which the results of the enhancements are evaluated. Chapter VI presents a summary of the results obtained and conclusions drawn.

CHAPTER II

LANDSAT DATA OVERVIEW

Introduction

Landsat digital data comprises the primary data source in this study. To effectively understand the more complex manipulations of this data during enhancement, it is imperative that an understanding of the basic concepts underlying the Landsat system be gained. This chapter explores the fundamentals of the Landsat-satellite and the data that are obtained from it. Such information provides the building blocks from which the enhancement procedures are developed.

Landsat-Satellite

The unmanned satellite program, Landsat, was initiated under the name ERTS (Earth Resources Technology Satellite) in 1972. On July 23 of that year, the National Aeronautics and Space Administration (NASA) launched the first in a series of experimental satellites, ERTS-1. The goal of this program was to utilize information obtained from satellites for the monitoring and management of earth resources (Walsh, 1977). ERTS-1 was the first non-military, unclassified earth resources satellite, and thus changed the focus of

remote sensing through its global perspective of the earth (NASA, 1979). Two years after the launch of ERTS-1, it was renamed Landsat 1. Landsat 2, identical to its predecessor, was launched on January 21, 1975, and was followed by Landsat 3 on March 5, 1978. Landsat 1 ceased operation in early 1978, and Landsat 2 was officially retired in late 1981. Landsat 3, the only satellite in the series that is currently operational, is experiencing data collection and transmission problems. As a result, Landsat data are available only for selected locations in the continental United States, at the time of this writing.

Orbital Characteristics

The Landsat satellites orbit the earth in a sun-synchronous, near-polar, circular, north-to-south manner. Orbiting at an altitude of 570 miles, the satellites complete one revolution of the earth in 103 minutes, with 14 orbits a day being achieved (Figure 3). This orbit provides a repetitive coverage of 18 days, for an individual satellite. Landsat 2 was timed in its launch so that, in conjunction with Landsat 1, a particular ground area would be passed by a satellite every nine days. This timing was later changed to a six day/twelve day cycle between the two satellites. Since Landsat 1 ceased operation, Landsat 3 has been placed into a nine day orbital synchronization with Landsat 2, thereby ensuring repetitive coverage by one of the satellites at that time interval (NASA, 1979).

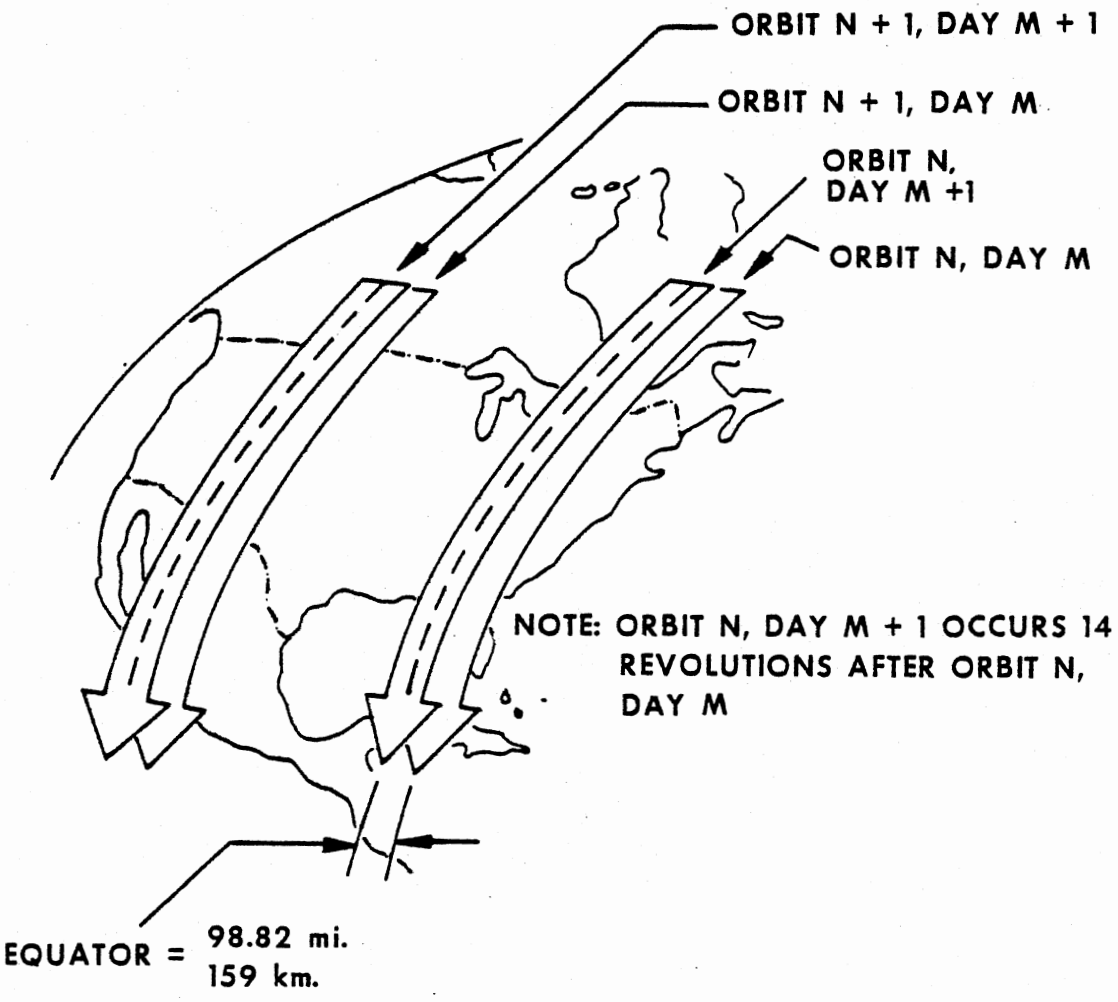

Figure 3. Landsat Ground Coverage Pattern

The sun-synchronous character of the Landsat orbit means that the satellites' orbital planes circle the earth at the same angular rate that the earth moves around the sun (NASA, 1979). The effect of such an orbit is that the spacecraft provide repeat coverage of ground points at the same local time each pass. Midmorning imagery is acquired at intermediate sun angles, a consistency which helps mitigate the effects of a variable sun angle (Sabins, 1978).

Each Landsat scene covers a ground area 115 miles by 115 miles, with coverage restricted to those areas of the earth's surface between 81 degrees north and south latitude (Figure 4) (Sabins, 1978). Due to orbital characteristics of the satellites, there is a sidelap between adjacent images, ranging from 14 percent at the equator to over 80 percent in the high latitudes. Forward overlap between successive images, introduced by processing methods, is 10 percent.

Scanner Systems

Two types of scanner systems are found on board the Landsat satellites, the return-beam vidicon (RBV) and the multispectral scanner (MSS). The RBV system consists of three cameras which, instead of using film to record the image, utilize a photosensitive tube upon which the image is formed. The tube is scanned by an electronic beam, with the resulting video signal transmitted to earth (Sabins, 1978). The MSS system makes use of an oscillating mirror to

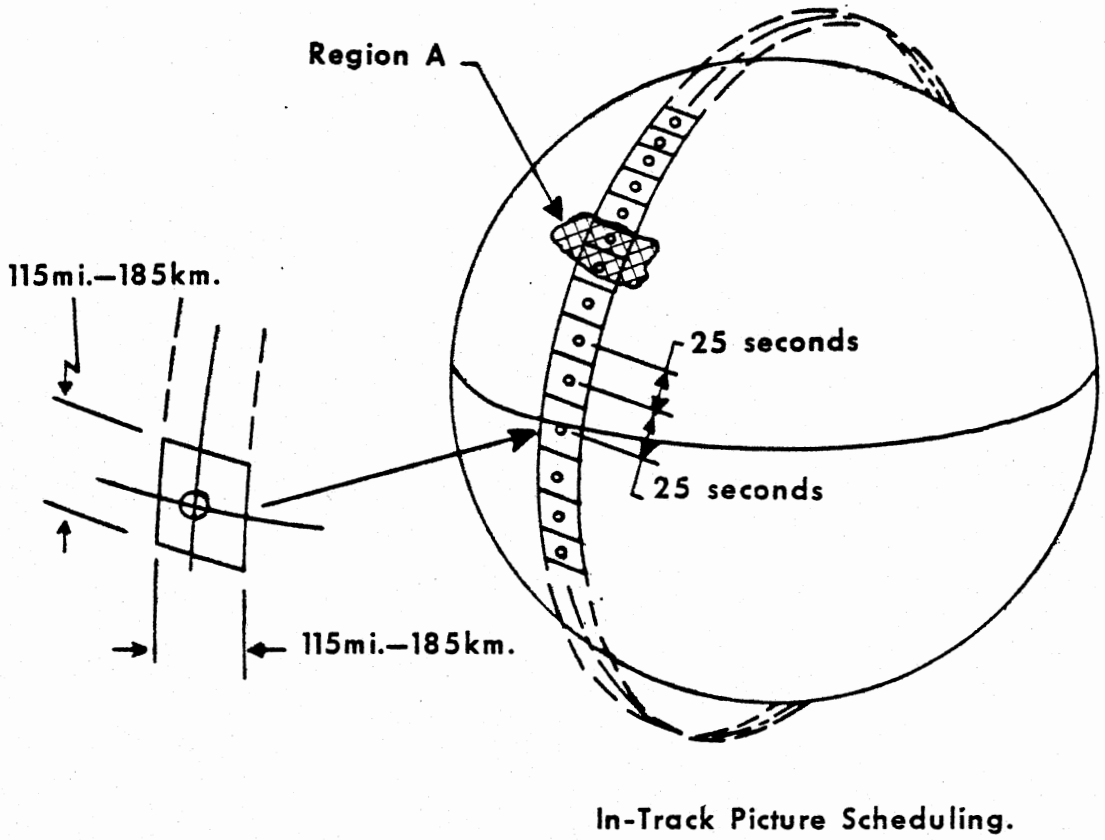

Figure 4. Landsat Tracking Scheme

continuously scan the earth's surface in a direction perpendicular to the path of travel of the satellite (Figure 5). The angle of view of the MSS scanner is 11.56 degrees, with a resulting scan of a 115 mile swath for one sweep of the mirror. Six lines are scanned for each sweep, with active scanning taking place only during the eastbound mirror sweep. After each sweep, the mirror retraces the scan (Figure 6). Scanning in this manner continues as the spacecraft progresses along its path, producing an image composed of 2,340 scan lines, each line comprised of between 3,000 and 3,450 elements of data (Figure 7) (Thomas, 1975, cited by Walsh, 1977).

Underlying the multispectral system of data collection is the assumption that a distinct amount of solar radiation is reflected by each ground object (Walsh, 1977). The MSS system operates in four spectral bands, with six detectors per band. Solar radiation reflected from the earth's surface is measured in a specific portion of the electromagnetic spectrum for each of the four bands (Table I). The unique amount of radiation of a particular wavelength that is reflected by an object for each of the bands is known as its "spectral signature". By recording such information in the four discrete wavelength bands of the electromagnetic spectrum (hence the term "multispectral"), the MSS can more readily differentiate between an object and those surrounding it, in terms of these reflectivity differences.

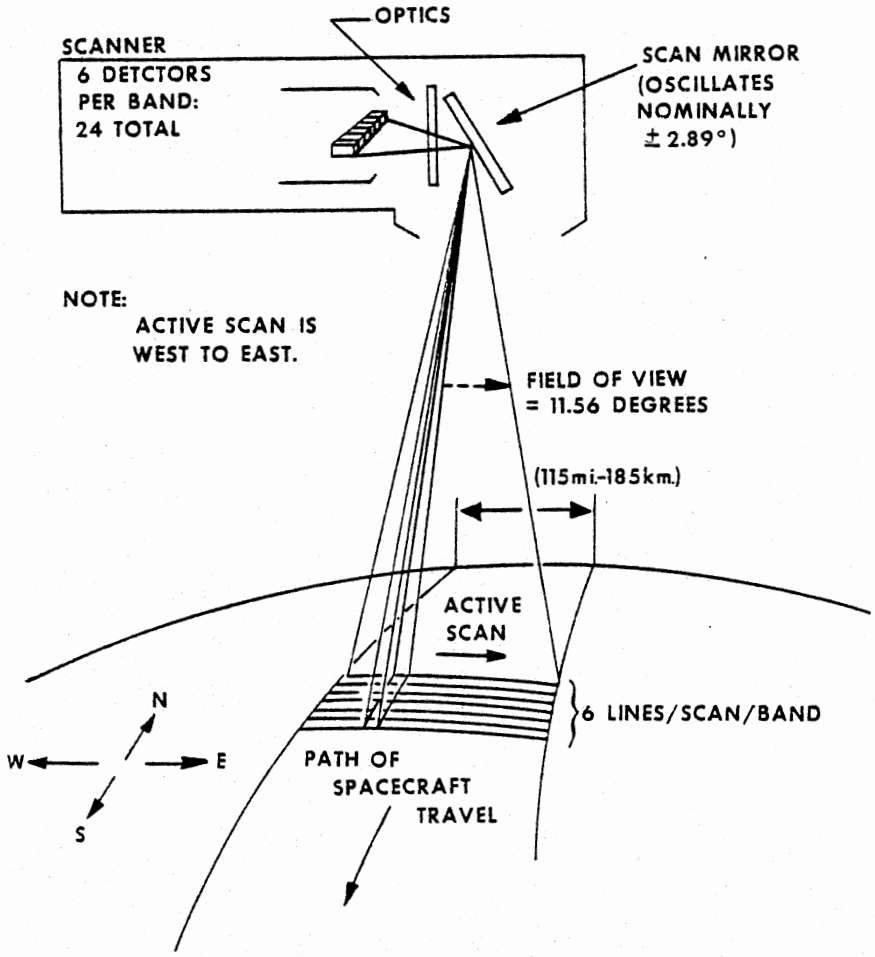

Figure 5. Landsat Scanning Arrangement

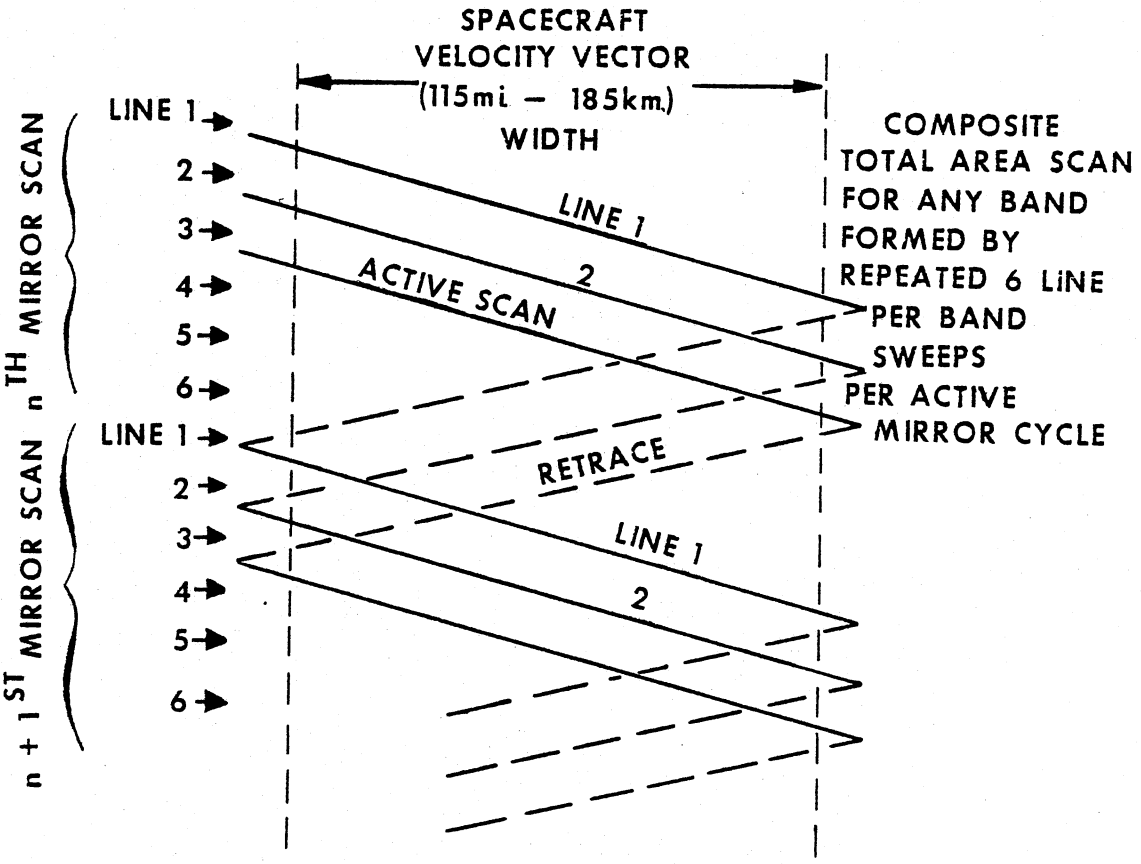

Figure 6. Ground Scan Pattern for a Single Landsat MSS Detector

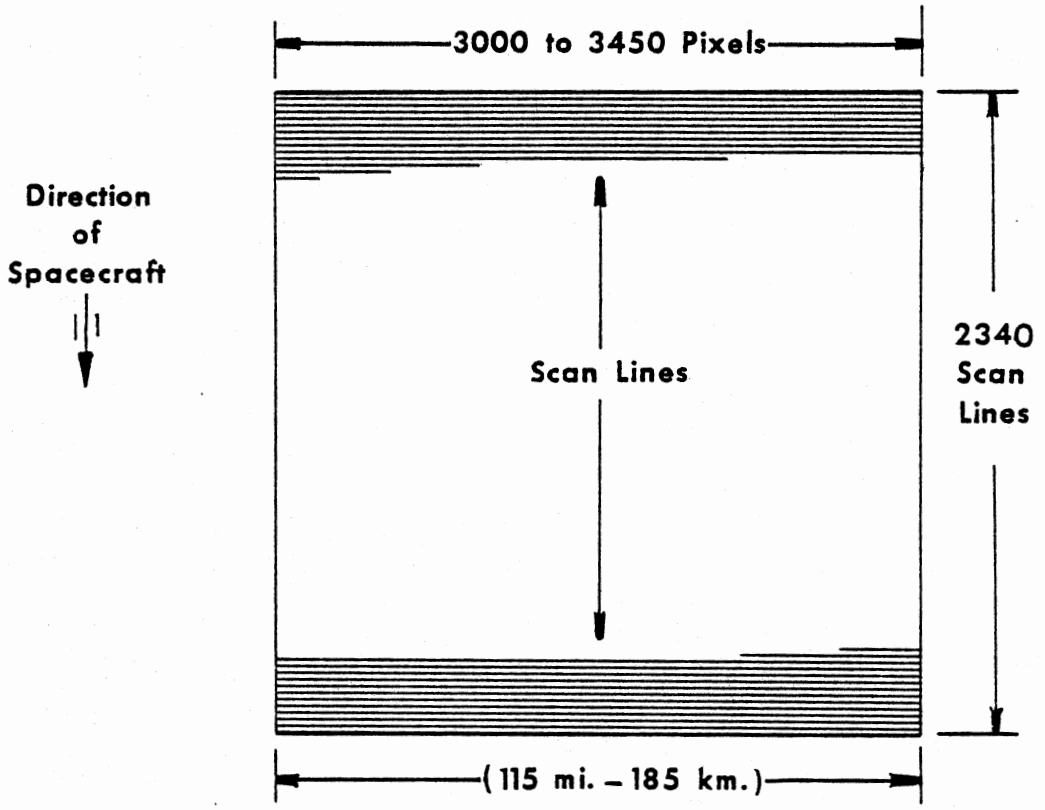

Figure 7. Landsat MSS Image Configuration

TABLE I

LANDSAT SPECTRAL BANDS

Band	Wavelength	Type of Radiation
4	0.5-0.6 um	Visible green
5	0.6-0.7 um	Visible red
6	0.7-0.8 um	Invisible reflected IR
7	0.8-1.1 um	Invisible reflected IR

Adapted from NASA (1979).

Nominal resolution of the Landsat MSS is 1.118 acres, this unit area being a "pixel" (picture element). The scanners on board the satellite sense radiant energy levels reflected from different surface features for each pixel in the Landsat scene, in each of the four spectral bands. A pixel's count value is recorded as the integration of reflectance values from all surface cover types within that 1.118 acre area. The reflectivities detected in each of the four bands for a particular pixel comprise the spectral signature for all cover types within that unit area (Walsh, 1977). Reflectivity levels, or "count values", are scaled from 0 to 127 for bands 4, 5, and 6, and from 0 to 63 for band 7. On these scales, higher magnitudes denote greater amounts of reflected energy.

In terms of the nominal instantaneous field of view of

the MSS, a pixel measures 79 meters by 79 meters. During the sensing process, the detectors record radiance values as electrical signals. Such signals are sent from the detectors in digital form. Output from the sensors is sampled, at a rate of approximately 100,000 times per second-- corresponding to a sample every 56 meters (NASA, 1979). As a result of this sampling, adjacent pixels along the scan line are overlapped, with a net gain of new information in each pixel of only 56 meters. Thus, the actual size of a picture element in a Landsat scene is 79 meters by 56 meters, rather than the originally-sensed 79 meters by 79 meters (Figure 8).

Summary

This chapter has provided a basic overview of the Landsat-satellite and the data that result from it. The concepts discussed here are vital in the application of Landsat data to the problem of lineament detection. The multispectral characteristic of the Landsat scanning system allows for the application of a variety of enhancement techniques that require the use of different wavelength bands. Rather than being limited to those techniques that utilize a single band of data, enhancements can be implemented utilizing different combinations of the bands. This allows for a wider range of manipulations to be performed on the data than would be possible without the MSS. The resolution of the satellite is also an important

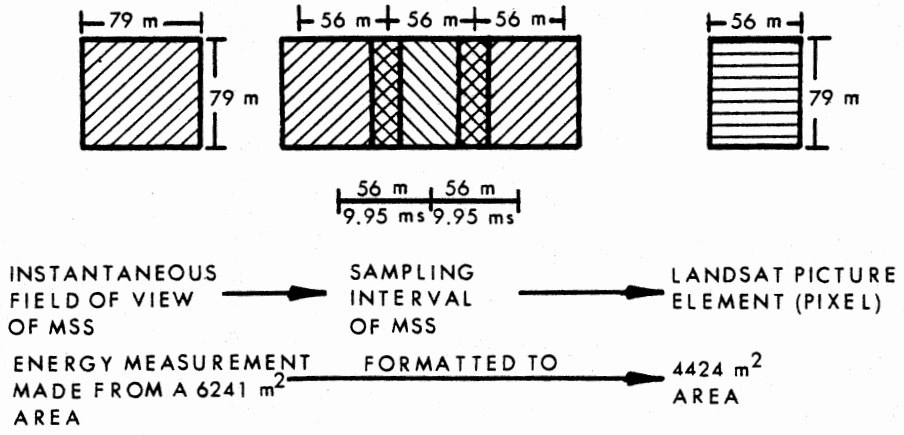

Figure 8. Formation of a Landsat Picture Element

concept, as it is sufficient to make visible the narrow tonal bands that mark the presence of lineaments. This resolution, when combined with the synoptic view provided by the Landsat-satellite, makes the data very useful for the detection of narrow, linear features such as lineaments. The high resolution allows for the identification of short lineaments, while the synoptic view provides a regional overview necessary for the identification of those lineaments that are much longer. The digital nature of the Landsat data, another concept introduced in this chapter, is also important to this study, as it makes possible the mathematical manipulation of the data that is the basis for all of the enhancements that are applied in this research.

The concepts discussed in this chapter, then, underlie the methodologies that follow in the remainder of this research. Principles explained here are utilized extensively in the next chapter, where the Landsat data are digitally enhanced for lineament detection purposes.

CHAPTER III

ENHANCEMENT PROCEDURES

Landsat Data Considerations

The nature of Landsat MSS data allows for some choices pertaining to data utilization. The multiple band capability of the scanning system provides for a choice of wavelength bands to be utilized for a particular research problem. Also, the repetitive coverage of the Landsat-satellite enables one to choose the season of the year during which the data are obtained, making possible the selection of the most useful date of information for a specific application. The objective of this study is to apply and evaluate various enhancement techniques, rather than to test the usefulness of the different MSS bands for lineament detection or to compare different dates of Landsat data for that purpose. A single date of imagery is utilized, with a single MSS band serving as the basis for the enhancements.

Previous studies utilizing Landsat data for lineament identification have generally favored the use of band 5 for that purpose. Sabins (1978) noted the value of band 5 data for general geologic mapping, as did Lee, Knepper, and Sawatzky (1974). Band 5 data were utilized for lineament

mapping in Nevada (Rowan and Wetlaufer, 1975) and in California (Lamar and Merifield, 1975). Band 5 and band 7 were demonstrated by Wobber and Martin (1973) to supply the greatest amount of geologic fracture detail.

Of the various enhancements implemented, not all utilize a single band of data, so the question of which band to enhance is not applicable to all enhancements. The principal components and mean value enhancements both utilize all four bands of the Landsat MSS data, while band ratioing involves the use of two of the four bands. A single band of data is enhanced only by the histogram equalization and high-pass filter techniques. Based upon the earlier studies discussed above, band 5 data are employed as the primary data set to which histogram equalization and high-pass filtering are applied. In addition, band 5 data are utilized as the unenhanced data against which all enhancements are compared.

The season of the year during which data are acquired is another important consideration for a lineament study, as it determines the angle at which solar radiation strikes the earth's surface. The angle of illumination is a crucial factor in the detection of lineaments. The subtle tonal and topographic alignments that mark lineaments on remotely-sensed data are best emphasized by a low sun angle (Lattman, 1958). While this statement was made in regard to aerial photography, rather than Landsat data, it was the only reference located pertaining to the season of acquisition of

remotely-sensed data, of any type. The statement, however, can still be considered relevant to Landsat data, as the principle is essentially the same. One would reason, then, that the winter season-- with a low sun angle-- would be preferential for data acquisition for a lineament study. A review of the literature, however, reveals little documentation to support such reasoning. Rarely, in fact, is the date of the data even stated in lineament studies. This lack of definitive support in the literature for a particular season necessitates that initially two dates of imagery be utilized in this study. High sun angle Landsat MSS data, acquired May 14, 1979, and low sun angle data, acquired November 28, 1972, are examined relative to one another for their worth in revealing topographic form. The data that are judged superior are utilized in the study.

Figures 9 and 10 show electrostatic printer/plotter output for the two dates of data. These plots are not completely indicative of the original data, as some clarity and detail have been lost in their generation and reproduction. Sufficient detail is retained in the plots, however, to indicate the differences between the two dates of data. A visual examination of these two figures is all that is necessary to see that the low sun angle data is markedly superior to the high sun angle data for revealing topography. The May, 1979 band 5 data (Figure 9) shows very little structure. Only the major surficial features can be seen, with the uniform illumination provided by the high sun

angle masking out nearly all details. The November, 1972 band 5 image (Figure 10) yields considerably greater amounts of structural information. Subtle details in topography are emphasized by the more oblique illumination resulting from the low sun angle. The superiority of the November data over the May data makes it clear that a low sun angle should be utilized for a lineament study in this particular geographic area. For this reason, all further work in this research makes use of November, 1972 Landsat MSS data.

Other Landsat data considerations come under the general category of "image restoration" (Sabins, 1978). Inherent in Landsat data, due to the mechanics of the imaging procedure, are a number of problems. Of these, the primary problems are "geometric distortions" and "sixth-line banding". Geometric problems arise from a number of systematic and nonsystematic distortions that are introduced during the scanning process. These distortions result in a Landsat image that is skewed relative to the actual orientation of the earth area that it represents. Such geometric distortions are readily corrected, by means of the "Geographical Referencing" module within the ELAS software package (Graham et al., 1980). This correction has been applied to the Landsat data utilized in this study. The sixth-line banding problem arises because one of the six MSS detectors for each spectral band has drifted to a higher or lower level, resulting in every sixth line of the data being brighter or darker than the other lines (Sabins, 1978).

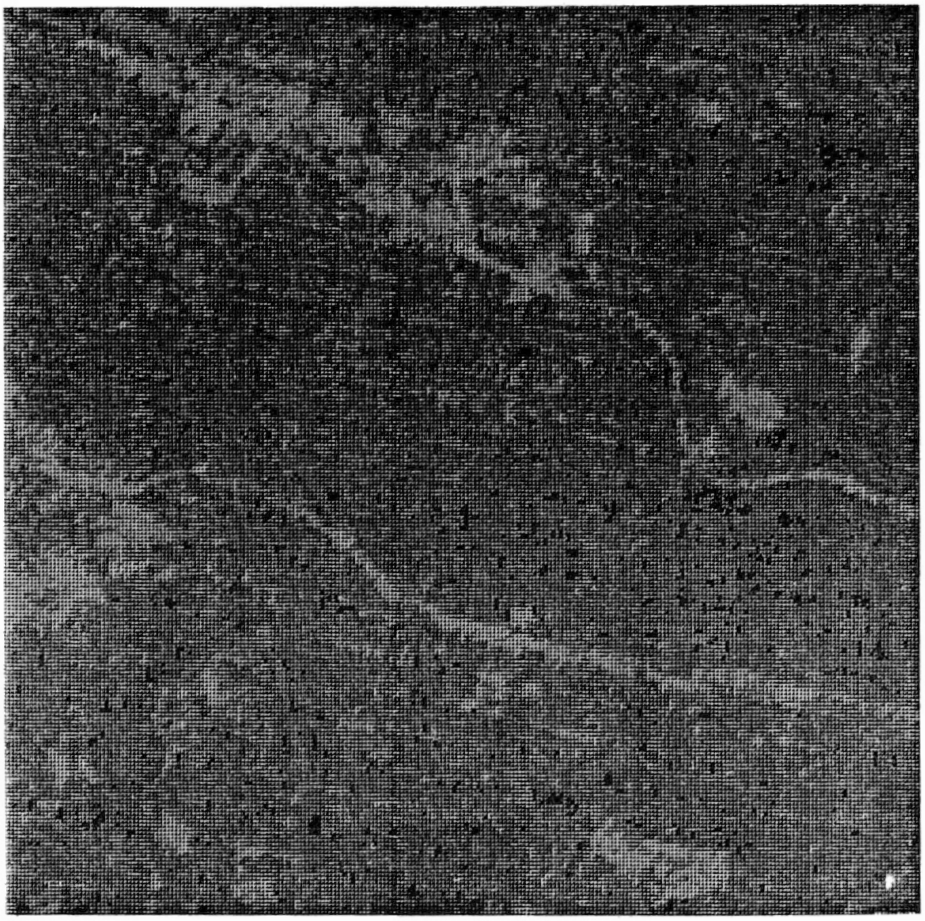

Figure 9. May 14, 1979 Landsat MSS Data, Band 5

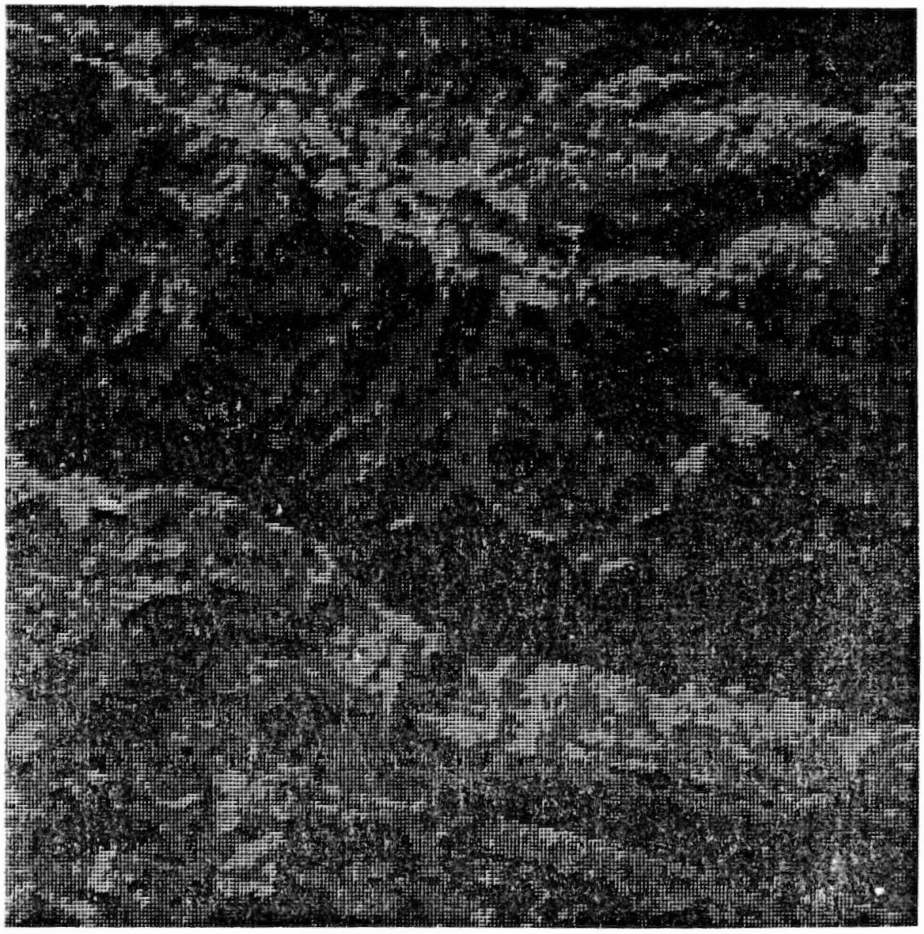

Figure 10. November 28, 1972 Landsat MSS Data, Band 5

This banding, showing up as noise or stripes on the image, can also be eliminated, using the "Destripe" procedure within ELAS (Graham et al., 1980). By removing the banding, however, some of the information contained in the original data is lost. For this reason, the Landsat data utilized in this research has not been destriped. It has been decided that the lineament information that might be masked out by the presence of stripes is a more minor loss than the lineament information that might possibly be removed by the destriping procedure.

Definition of Enhancement

"Enhancement", according to Andrews (1978a), refers to the manipulation of imagery to present to the viewer (or subsequent machine) additional information or insight into some factor concerning the preenhanced image. By this definition, any technique that provides improvement in the display of an image is an enhancement technique (Andrews, 1978b). Thus, the goal of enhancement is the improvement of image quality. Gillespie (1980) noted that because image quality is a subjective measure which varies from person to person, no clear-cut rules exist that one can follow to produce a single "best quality" image. The "best quality" image may require manipulations that result in a stretched gray scale, a sharpened edge, a delineated boundary, a compressed dynamic range, or a combination of these and other techniques (Andrews, 1978b).

Two general forms of image enhancement exist: (1) optical and (2) digital. Digital enhancement, utilized in this research, is performed on Landsat digital data by computer methods. As discussed in Chapter II, Landsat digital data consists of reflectivity count values, one value per picture element per band. These reflectance data are numerical, and thus can be treated in the same manner as any other numerical data. Enhancement of Landsat digital data can be accomplished by the mathematical manipulation of these reflectivity values. Specific manipulations have been demonstrated to have positive effects in terms of the detail in structure and topography shown by the Landsat data.

As discussed earlier, little research has been done in appraising the value of a number of different enhancement techniques for lineament detection, even though the worth of particular techniques has been demonstrated in various studies. This research makes such an appraisal. The first stage of this project, the application of enhancement techniques, is documented in the remainder of this chapter. The reasoning behind the use of each of the enhancements, and the methodologies involved in applying them to the data, are discussed.

All enhancements are generated from a Perkin Elmer 8/32 mini-computer, by means of the Earth Resources Laboratory Applications Software (ELAS) package (Graham et al., 1980). Results are displayed through a COMTAL image processing system. All processing is done at the Center for

Applications of Remote Sensing (CARS), Oklahoma State University.

Enhancement Descriptions

Mean Value of All Bands

The simplest of the five enhancements applied to the Landsat data is the "mean value of all bands". The utilization of this technique for image enhancement was suggested by W. Anthony Blanchard (personal communication, 1982). Although no additional documentation for the technique was found in the literature, the success reported by Blanchard merits the inclusion of the enhancement in this research.

The implementation of the mean value enhancement is relatively simple. Utilizing the "Programmable Calculator" (PCAL) module of the ELAS software system (Graham et al., 1980), the reflectance values for each of the four Landsat MSS bands are summed for each pixel. This sum is then divided by four, yielding a count value for each pixel that is the arithmetic mean of the four bands. The result of this operation is a new single-band data set, consisting of information compiled from all four of the original Landsat bands. When viewed on the image processing system's display screen, the image derived through this enhancement (Figure 11) appears, from an initial observation, to yield more structural detail than the unenhanced image.

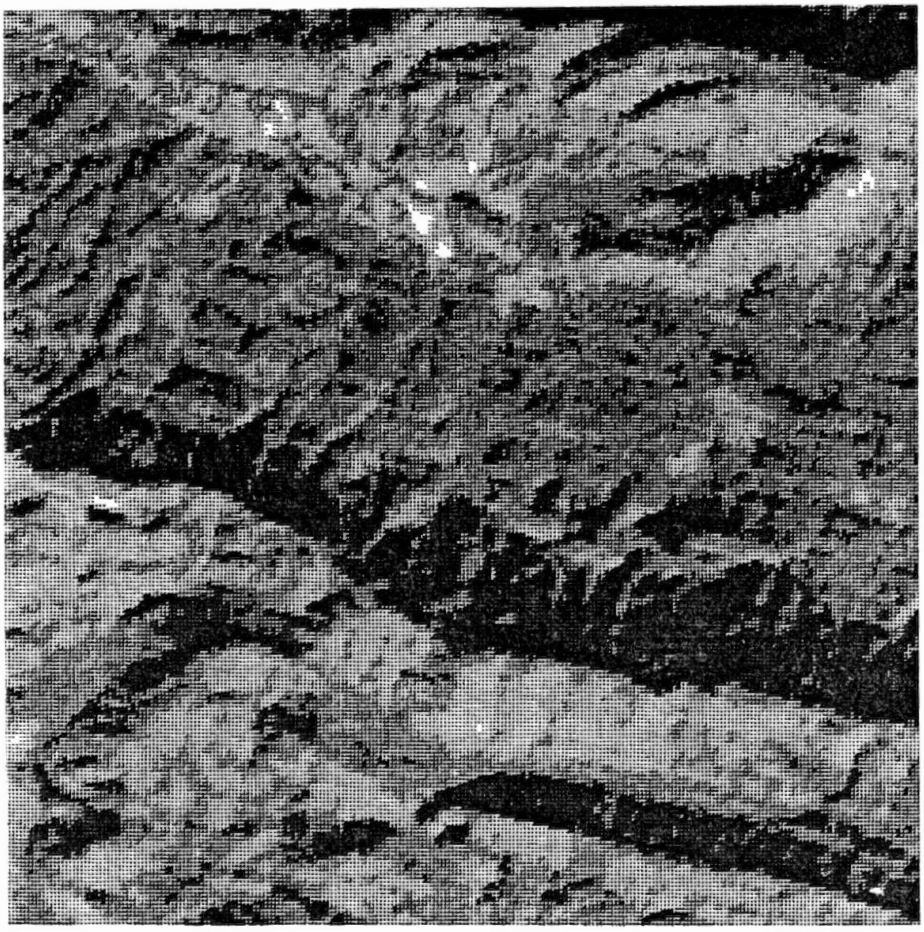

Figure 11. Mean Value of All Bands Enhanced Image

Principal Components Analysis

The second type of digital image enhancement applied is "principal components analysis". This technique is applied in order to correct for the poor visual display of the original Landsat data due to low contrast between objects (Fontanel, Blanchet, and Lallemand, 1975). Principal components analysis is based upon the principle that the original population density function of the Landsat data shows a strong correlation between channels (Gillespie, 1980). This means that the important information contained in all four MSS bands can be better represented in a new image statistically derived from the original data. According to Anuta (1977), this is a linear transformation that produces an uncorrelated multivariate image from the original correlated data set, the new image having certain ordered maximum variance properties which are desirable for subsequent analysis. This transformation is derived from covariance statistics of the original Landsat data. The first principal component is the most important result of the transformation, as that image contains most of the variability of all four original channels, and therefore most of the information contained in them (Anuta, 1977). Empirical evidence for this information content is shown in a study by Fontanel, Blanchet, and Lallemand (1975) that found that the first principal component contained 80 percent of the information contained in all four bands in the original data for a Landsat scene in southern France.

Principal components analysis is applied by means of the "General Algorithm for Statistical Processing" (GASP) module within the ELAS package (Graham et al., 1980). Input data consists of Landsat bands 4, 5, 6, and 7, which are statistically manipulated as described above. Output is a single-band data set, comprised of the first principal component, generated from all four bands. This enhanced image, as displayed by the image processing system, is shown in Figure 12.

Band Ratioing

A third enhancement implemented in this research is "band ratioing". With this technique, the reflectance value in one band is divided by the corresponding reflectance value in another band, for each pixel in the scene, and the results displayed (Sabins, 1978). Ratioing has been successfully applied in many geological investigations for detecting areas of mineral alteration and for mapping lithology (Rowan et al., 1973; Goetz et al., 1973a; Vincent, 1973). However, ratioing accentuates noise in the image, making interpretation difficult (Abrams, 1980). Ratioing also has the disadvantage of suppressing differences in albedo (Sabins, 1978). In terms of enhancement for lineament detection, ratioing appears to have limited utility, because the technique suppresses brightness information and thus displays only the most obvious structural lines (Offield et al., 1977). The simplicity of

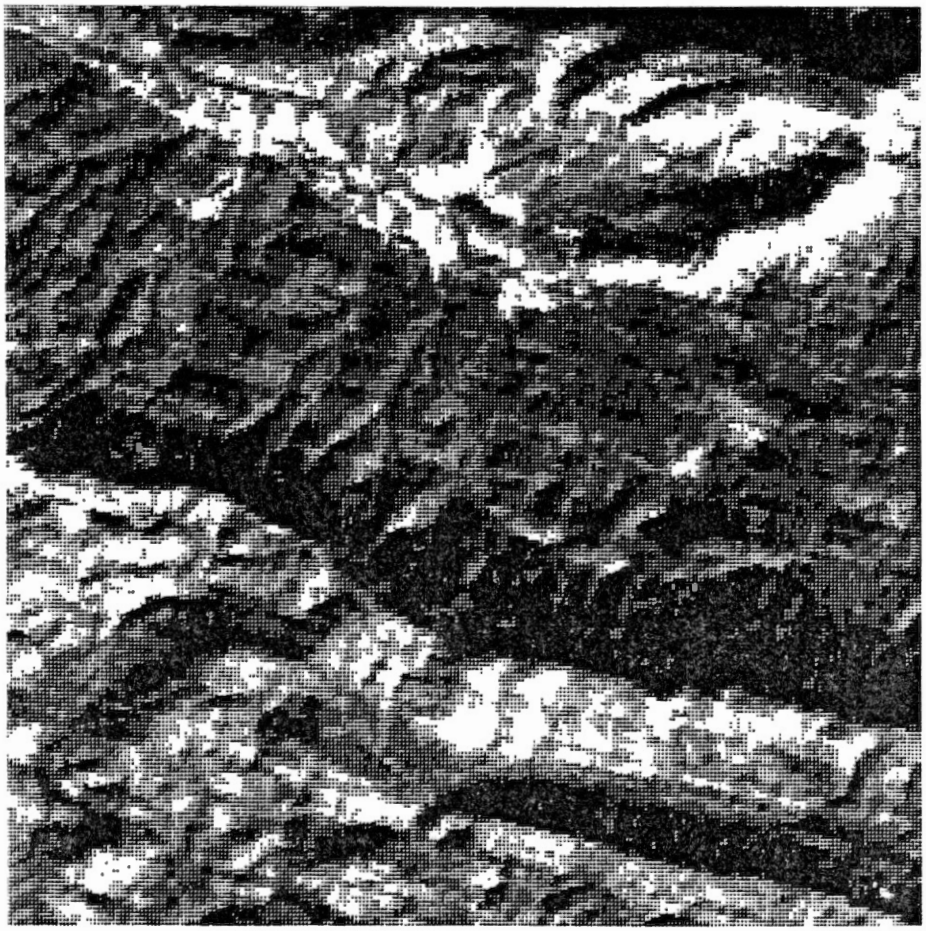

Figure 12. Principal Components Analysis Enhanced Image

applying the technique, along with the general acceptance of ratioing as a popular enhancement technique, warrants its inclusion as one of the enhancements applied and evaluated, despite reports of its questionable utility.

Little agreement has been found in the literature advocating the specific bands to be ratioed for enhancing geologic structure. The most definitive statement regarding this consideration was provided by Taranik (1978), who advocated the division of the pixel reflectance values in band 4 by twice the values in band 5. In ratioing, the ratioed values are generally multiplied by a constant so that all values lie between 0 and 255. With the ratio suggested by Taranik, this constant equates to 200 for the data used in this study, which is the equivalent of multiplying the ratio of band 4 to band 5 by 100. The latter ratio, when applied, requires one less mathematical operation, and is the ratio utilized here.

The ratio enhancement is obtained by using the "Programmable Calculator" (PCAL) module within ELAS (Graham et al., 1980). The reflectance value in band 4 is first divided by the value in band 5 for each pixel, after which the results of this operation are multiplied by 100. The resulting image, shown in Figure 13, is of rather poor quality, with much banding being evident.

Histogram Equalization

"Histogram equalization" is the fourth image

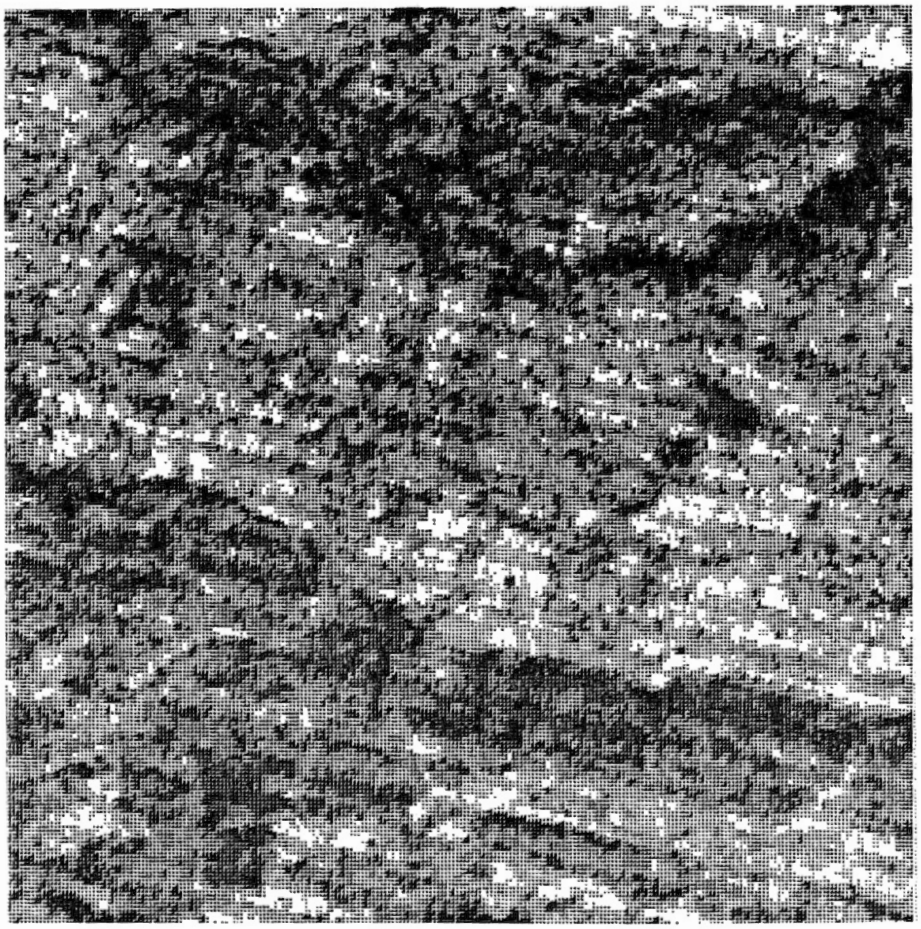

Figure 13. Band 4/Band 5 Ratio Enhanced Image

enhancement technique applied to the Landsat data. This is one type of contrast enhancement, designed to modify the data's reflectivity histogram, in effect "stretching" out the brightness values occurring in the data (Frei, 1978). As with any other contrast enhancement, this technique involves manipulating the distribution of reflectance values in the Landsat data in order to best utilize the entire brightness range of the display medium (Sabins, 1978). Such manipulation is helpful for the following reason: because of the nonvariable nature of exposure time in the Landsat multispectral scanner, the sensitivity of the sensor must be set so that it is not saturated by scenes of drastically different reflectivities. As a result, in any given scene, data are likely to occupy only a small portion of the available brightness range, causing the image to have a low contrast (Offield et al., 1977). Lineaments may not be distinguishable from their surroundings on these unenhanced images because their reflectivities may be too near the same values. Contrast enhancement can therefore highlight lineaments, by increasing the subtle tonal differences between the lineaments and their surroundings.

Histogram equalization, also referred to as "histogram flattening" (Eberlein et al., 1974) and as a "uniform distribution stretch" (Sabins, 1978), is best used when most of the original reflectance values are distributed over a narrow range in the middle of the grayscale (Andrews, 1978a). The original histogram is redistributed to produce

a distribution in which all brightness levels are spread over the available range as equally as possible (Frei, 1978). This method results in a spreading out of those values that occur most frequently in the original image, with the greatest contrast enhancement being applied there (Andrews, 1978a and Sabins, 1978). The histogram equalization enhancement causes considerable compaction of brightness values at the sparsely populated tails of the original histogram, with a resulting loss of contrast in the light and dark regions (Sabins, 1978).

The histogram equalization method of image enhancement is implemented by utilizing the "Programmable Calculator" (PCAL) module within the ELAS software system (Graham et al., 1980), operating on band 5 of the Landsat MSS data. Because of the operation characteristics of this module, it is not possible to subtract pixels from those count values having the highest population densities-- only addition is possible. As a result, the "equalization" of the histogram is accomplished by combining those count values with low population densities. Thus, the technique is, in essence, a "density slice", in which the original count values in the data are grouped together. Strictly speaking, the technique applied is not a true histogram equalization, but rather an approximation of that enhancement. The result of this technique is shown in Figure 14. As can be seen, this enhancement results in a loss of detail from the original

image, most likely attributable to the generalization necessary for its implementation.

High-Pass Digital Filtering

The final enhancement technique applied in this study is "high-pass digital filtering". This method is especially useful when a Landsat scene contains a high brightness range, in which case any contrast stretch performed would saturate large portions of the original population density histogram. Thus, digital filtering is used as an alternative to contrast enhancement, serving to suppress large changes in overall image brightness (Gillespie, 1980), while acting to sharpen or amplify boundary detail in the image (Condit and Chavez, 1979).

"Frequency" refers to the spatial scale of the brightness variations within the image. High frequency denotes rapid changes over a few pixels; low frequency means a gradual change over a large number of pixels (Condit and Chavez, 1979). A high-pass filter amplifies these high frequency variations within the Landsat data, filtering out the low frequencies. This amplification of higher frequencies is very important to lineament enhancement, as those features have high spatial frequency and short wavelengths, in contrast to major topographical features, such as mountains, that have low spatial frequency and very long wavelengths (Sabins, 1978). By suppressing the unwanted low frequencies and transmitting the desired high

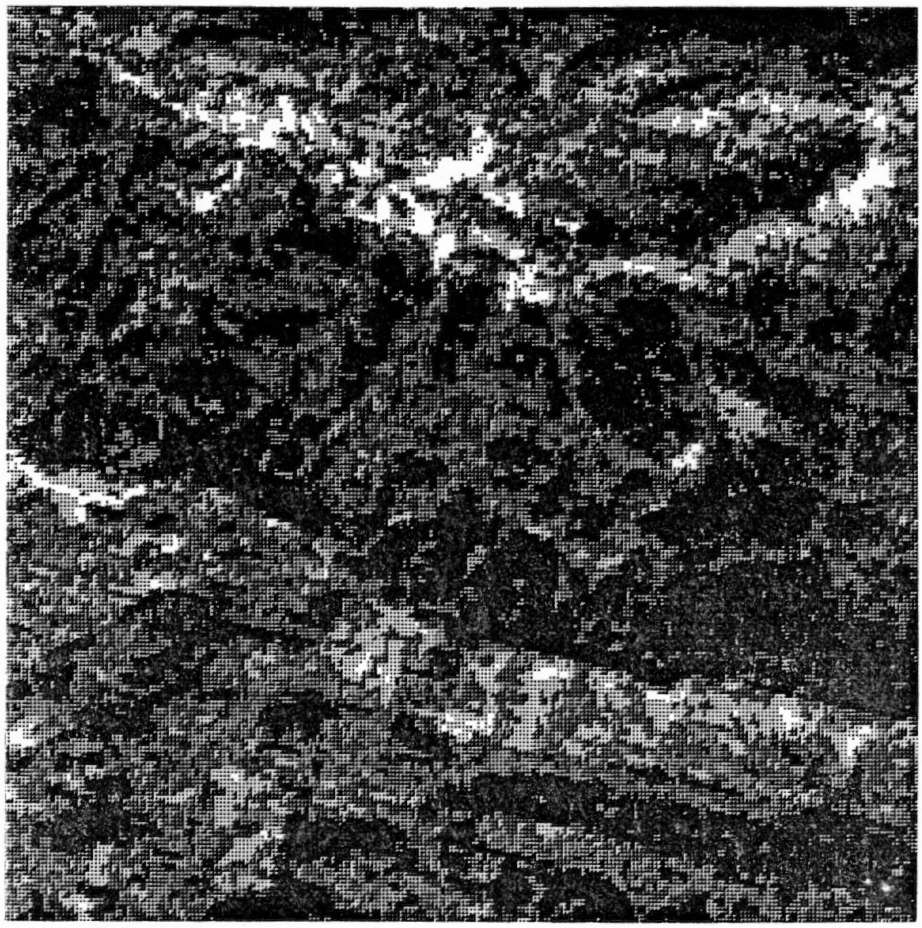

Figure 14. Histogram Equalization Enhanced Image

frequencies, high-pass filtering can greatly enhance lineaments.

High-pass filtering is applied to Landsat data by passing a window of predetermined size through the data. Within the window, an average of the reflectivities is taken, with the count value of the central pixel in the window being changed as a function of the average (Condit and Chavez, 1979). The window is moved through the data, being offset one pixel at a time. The size of the array of pixels examined in the window has a profound effect on the product output from the filter. A high-pass filter emphasizes features smaller than the size of the averaging window by calculating the average reflectivity within the window and subtracting this average from the value of the central pixel (Condit and Chavez, 1979). By passing the window in this manner, the count value for each pixel is altered on the basis of neighboring pixels, with the resulting data set being a filtered image.

The high-pass filter is implemented in this research by means of the "Spatial Filter" (FILT) module within ELAS (Graham et al., 1980), utilizing a procedure suggested by Condit and Chavez (1979). A smoothed (low-pass filtered) image is first generated from band 5 of the Landsat MSS data, using a nine pixel by nine pixel window size, with relative weights of each pixel equalling one and a total window weight of one. All of these values are empirically derived. The resulting image output from this operation is

then subtracted from the original band 5 data, yielding a high-pass filtered image. This image, shown in Figure 15, consists of only the details (high frequencies) present in the original image. As can be seen, the result is confusing, with only the high frequencies expressed and the larger patterns removed.

Summary

This chapter has discussed the enhancement procedures that are implemented in this study for lineament detection purposes. In all, five techniques are utilized: (1) mean value of all bands; (2) principal components analysis; (3) band ratioing; (4) histogram equalization; and (5) high-pass digital filtering. The next phase of this research, discussed in the following chapter, entails the interpretation of lineaments from each of these enhancements.

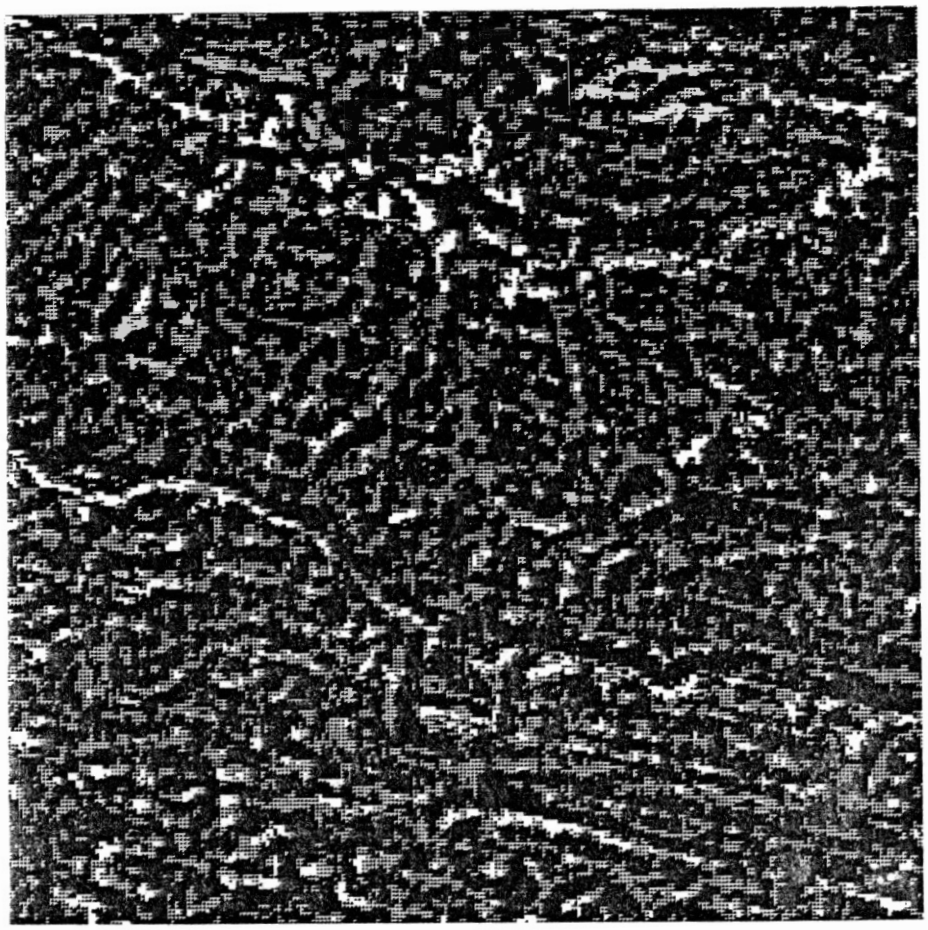

Figure 15. High-Pass Filter Enhanced Image

CHAPTER IV

INTERPRETATION PROCEDURES

Method of Interpretation

The unenhanced image, along with the images resulting from the five enhancement techniques applied to it, are interpreted for lineaments in the second phase of this research. This process is accomplished with each image being viewed, one at a time, on the display screen of the COMTAL image processing system. Lineaments are identified on the Landsat images on the basis of meeting one or more of a specific set of defining criteria, as suggested by Short and Lowman (1973): (1) lines of variable length, straightness, and continuity, as set apart by tonal contrasts in the image; (2) tonal discontinuities; (3) bands of variable width which contrast in tone to the areas immediately adjacent; (4) alignments of topographic forms; (5) alignments of drainage patterns; (6) association of vegetation along linear trends; and (7) co-alignment of cultural features with underlying structural and/or surrounding topographic control. In addition to these criteria, a minimum size limit is placed upon the lineaments, with only those segments approximately 0.5 miles or longer identified from the images. This size limit is

utilized in order to maintain a consistency among the interpretations.

Line segments that meet the above criteria for identification as lineaments are traced by the cursor on the COMTAL screen, with the processing system in the "write graphics" mode of the "Polygon Selection" (POLY) module (Graham et al., 1980). This results in the production of a graphic overlay of the lineaments interpreted from each image. These overlays are stored on the computer, and can be displayed alone or superimposed upon the Landsat data. The lineament interpretation overlays for each of the five enhancements, along with that from the unenhanced band 5 data are shown in Figures 16-21. In addition, the lineament overlay produced from a lineament map generated from another study is also shown, for comparative purposes, in Figure 22. This interpretation, to be discussed in greater detail in Chapter V, was derived by Melton (1976) from stereoscopic analysis of aerial photographs. It is used as the standard against which the other interpretations are evaluated.

Subjectivity of Interpretation Method

It should be emphasized that the method of lineament interpretation utilized in this research is subjective. Subjectivity is a recognized problem with the detection of lineaments from Landsat data, both analog and digital. This method of interpretation often leads to dissimilar results when two or more interpreters work from the same image, or

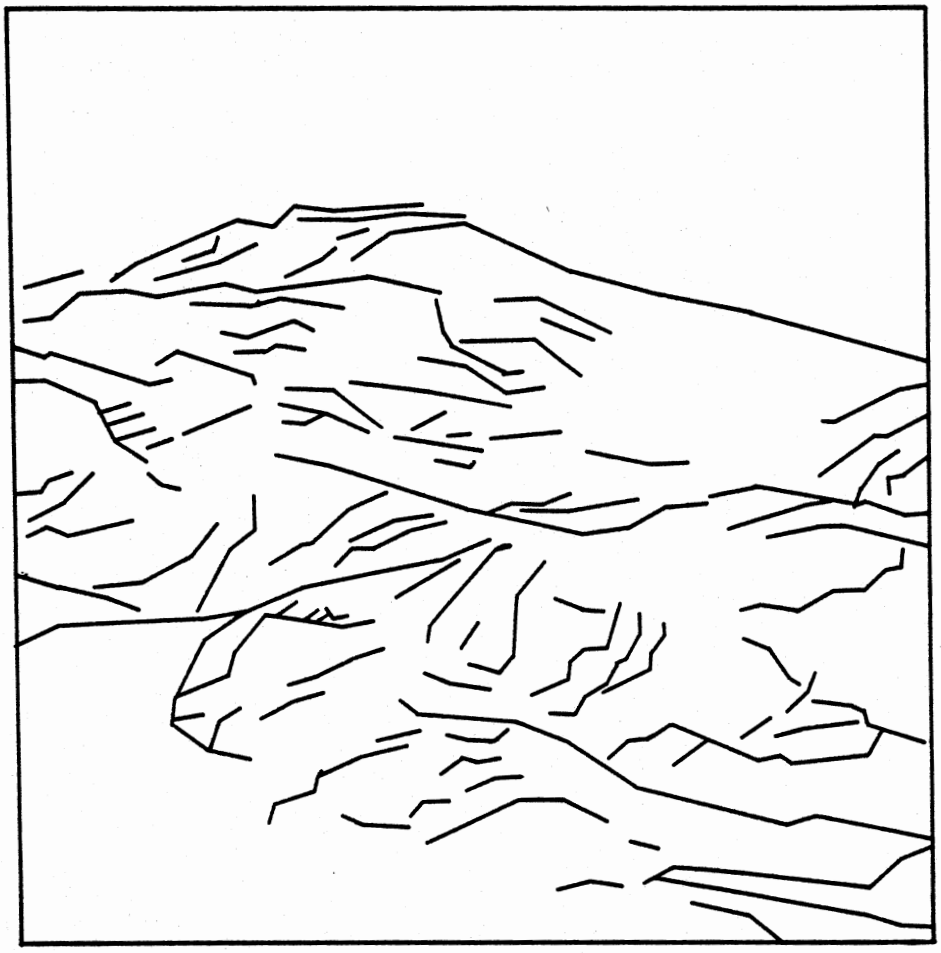

Figure 16. Unenhanced Band 5 Lineament Interpretation

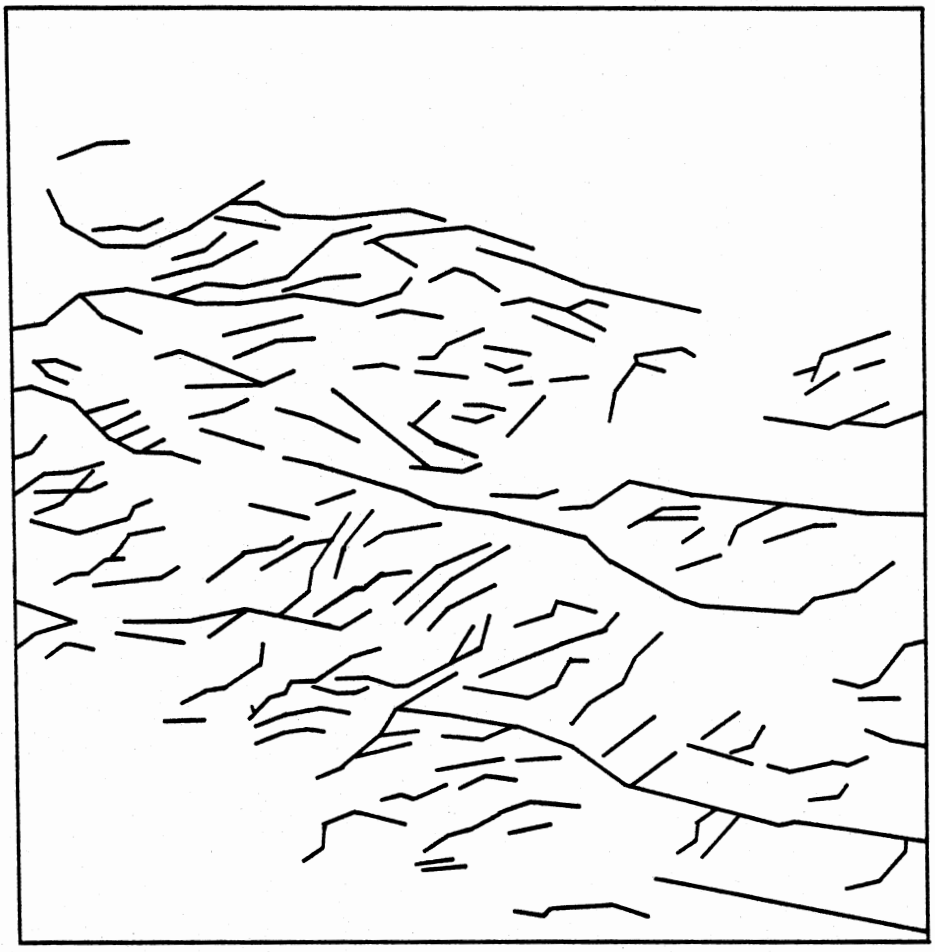

Figure 17. Mean Value Lineament Interpretation

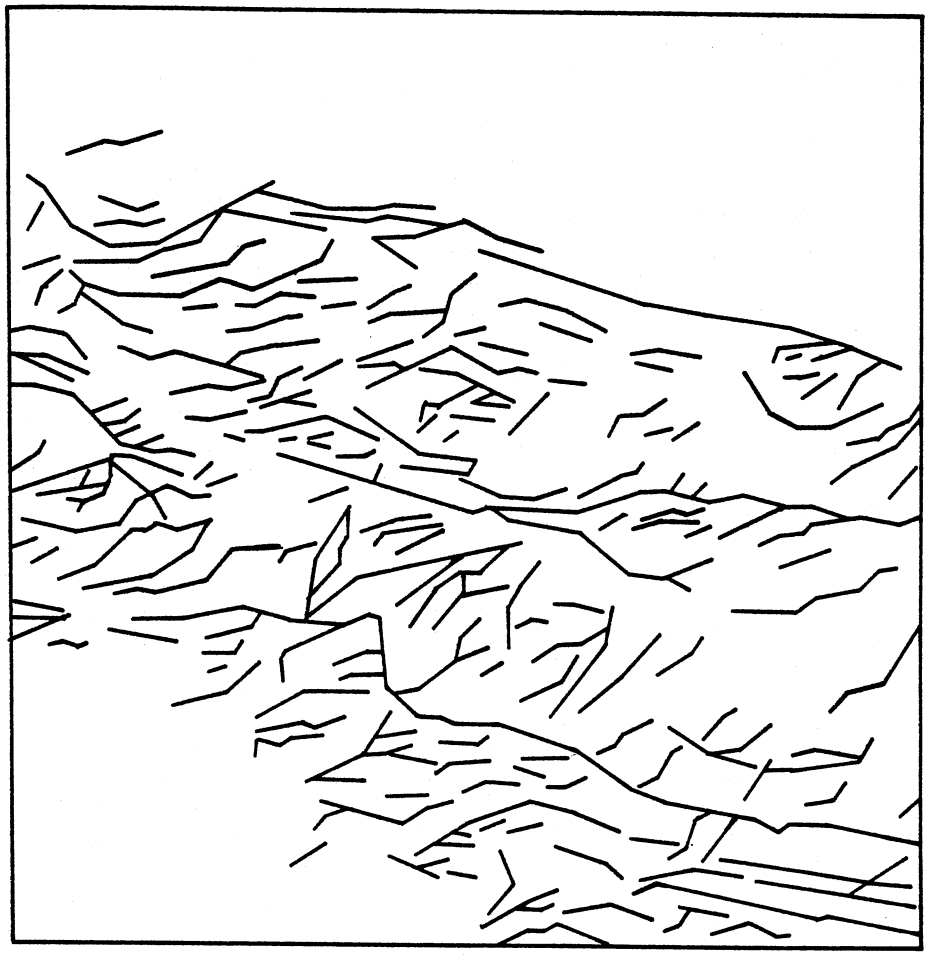

Figure 18. Principal Components Lineament Interpretation

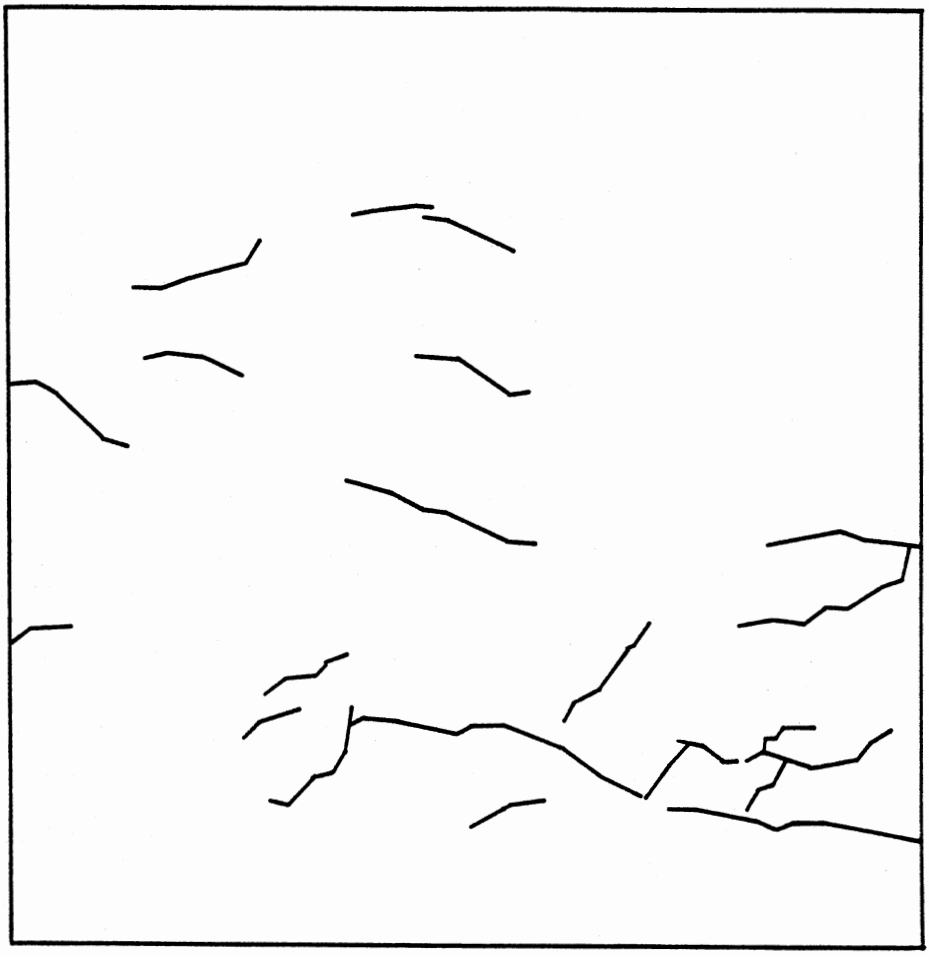

Figure 19. Band Ratio Lineament Interpretation

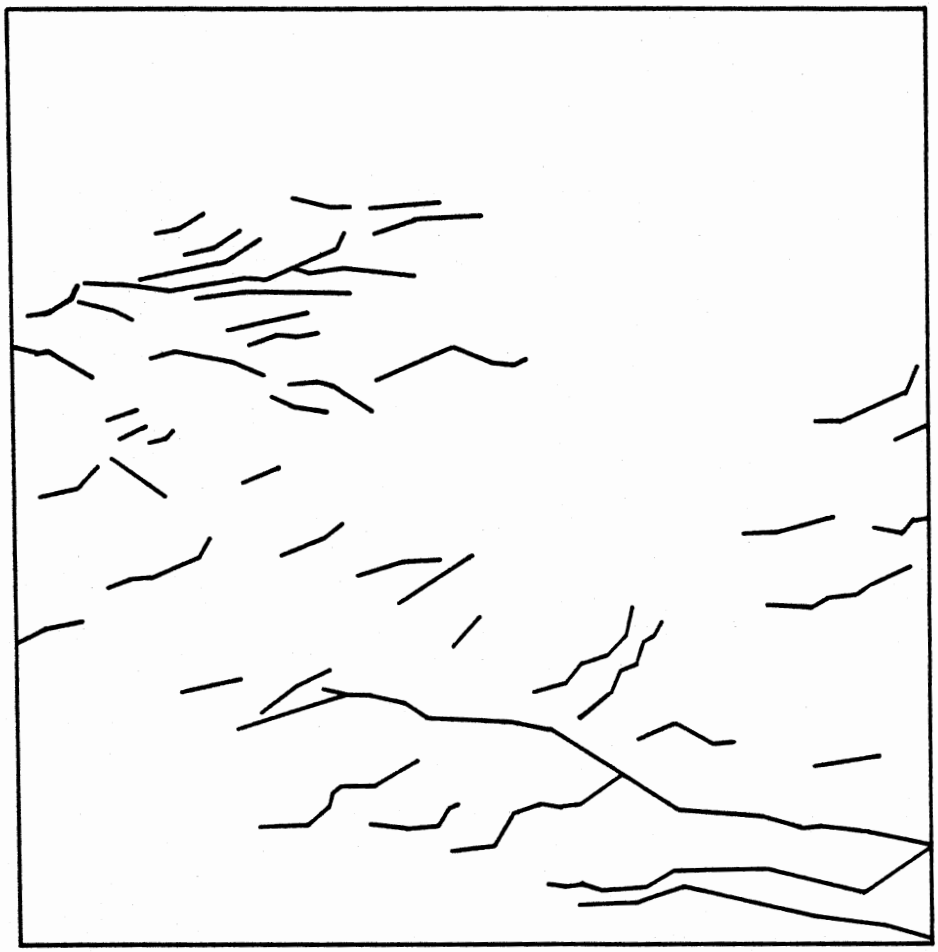

Figure 20. Histogram Equalization Lineament Interpretation

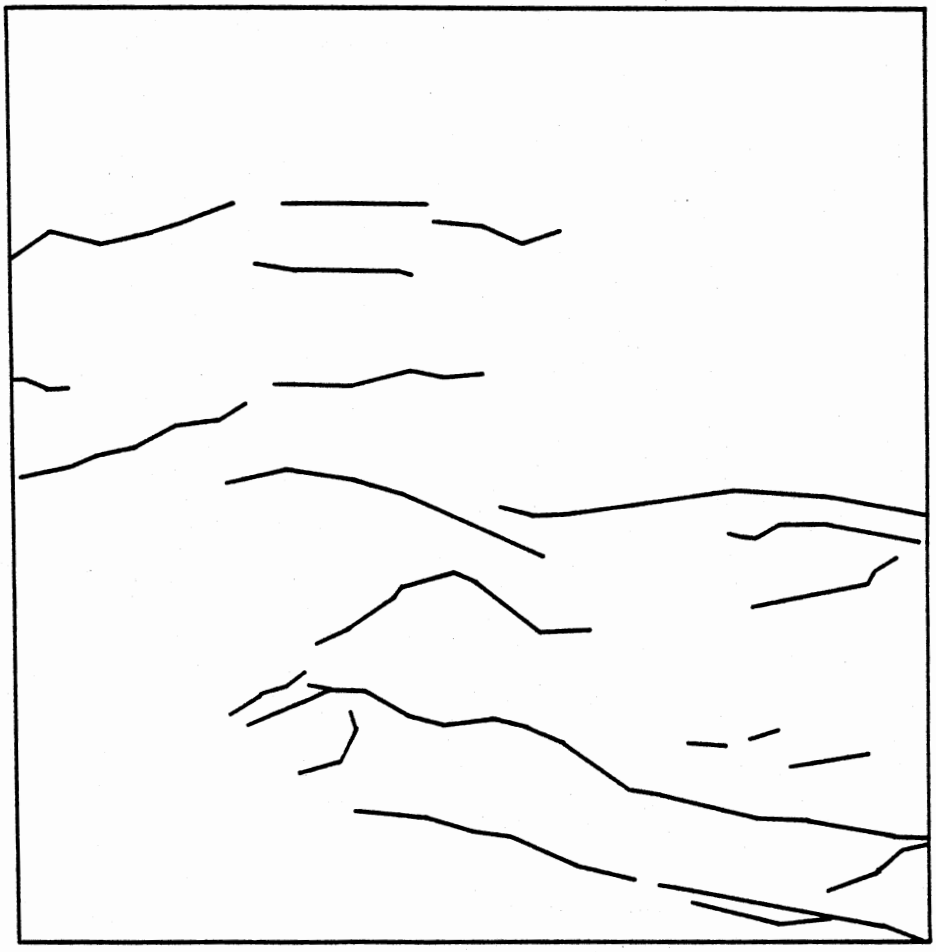

Figure 21. High-Pass Filter Lineament Interpretation

Figure 22. "Standard" Lineament Interpretation

even when one interpreter works from one image on several occasions (Huntington and Raiche, 1978). A study by Siegal (1977) quantified this subjectivity, finding a coincidence of individual lineaments recognized by five investigators interpreting the same image as being only four percent. Siegal attributed this discrepancy among lineament interpretations, in general, to the constant bias characteristics of operators, and to the inconsistencies within one interpreter and among a group of interpreters. He concluded that the number of lineaments recognized on a particular image depends primarily upon the individual doing the interpretation.

While the subjectivity among different interpreters is not a factor in this research-- since one investigator is interpreting all images-- the inconsistency within that one interpreter may be important. Such subjectivity might introduce complications into the comparison between enhancement methods. Interpretations of later-applied enhancement methods might possibly be biased toward the detection of more lineaments than in the earlier methods, because the locations of those lineaments found earlier may be remembered in later interpretations.

In an effort to mitigate this subjectivity in lineament interpretation as much as possible, specific measures are followed in this research. All images are interpreted under the same conditions of illumination. Lineaments are identified on all images by an identical set of defining

criteria. Once an interpretation is completed, it is not viewed again until all images are interpreted. While these measures may reduce the degree of subjectivity, it is unlikely that all subjectivity could ever be removed from this method of interpretation. The presence of subjectivity in the manual interpretation of Landsat imagery is acknowledged as unfortunate but unavoidable.

Summary

This chapter has described the procedures by which lineaments are interpreted from the enhanced and unenhanced images, and has presented the resulting interpretations. In the following chapter, these interpretations are subjected to a quantitative analysis, from which comparisons between the enhancement techniques will be made.

CHAPTER V

ANALYSIS PROCEDURES

Comparative Analysis of Enhancements

The final phase of this research involves the evaluation of the different enhancement techniques through an analysis of the lineament interpretations derived from each. This analysis is quantitative, and is accomplished with a series of computer programs. These programs serve two purposes: (1) they summarize the lineament data in a meaningful way; and (2) they allow for an objective comparison between the enhancements.

Summarization Programs

After the enhanced and unenhanced images are interpreted for lineaments, these interpretations are photographed. Utilizing a graphic digitizer, the locations of each of the line segments present on each photograph are recorded. A Cartesian coordinate system is superimposed upon each photograph, with the origin located in the upper left hand corner of the data. In this coordinate system, positive X is considered to the right, and positive Y is considered downward. This format is chosen in order to facilitate summarization of the lineament data by means of a

series of programs previously developed for lineament analysis. The digitizer is then used to record the X and Y locations of the beginning and endpoints of each line segment, relative to the origin of the coordinate system. All locations are recorded to a precision of 0.1 millimeter, which is sufficient to meet the accuracy requirements of the analysis programs, while allowing for the error introduced by the measurement process. Designed to be run on an IBM computer, the analysis programs require the manual transfer of the digitized data from the Perkin Elmer system of CARS, where all procedures discussed thus far have taken place, to the Oklahoma State University Computer Center, where final analysis is undertaken.

Summarization of the lineament interpretation data is done through the use of a series of two computer programs developed by Podwysocki. These programs, discussed in Podwysocki and Lowman (1974), were written in Fortran, and allow for a systematic and detailed analysis of lineament patterns that was not previously possible because of the large amounts of data involved in such an analysis. Input to these programs consists of the locations of digitized line segments, recorded from the lineament interpretations; output consists of frequency-azimuth histograms for each interpretation. A source listing of these programs is included in the Appendix.

VECTRANS, the first summarization program in the series, performs the initial data treatment. This program

converts the lineament data from the interpretations into a format acceptable for use in the second program, AZMAP. VECTRANS treats each lineament as a vector in map space, calculating, for each vector, the parameters of length, azimuth, slope, Y intercept, X midpoint, and Y midpoint (Podwysocki and Lowman, 1974). Figure 23 is a sample of output from the VECTRANS program.

Output from the VECTRANS program is input to the second program in the series, AZMAP. This program places a grid over the digitized data, parallel to the X and Y axes. The grid cell size over which the lineaments are summarized is specified by the user, in terms of the X and Y directions. The computer then automatically scans the lineament data, determining whether each line segment falls within a particular grid cell, incrementing the cell by user-supplied values in both directions, until the entire study area is covered. The program allows for summarization of lineaments in either of two ways. Subroutine PART considers only that portion of a lineament which lies within a particular grid cell, while Subroutine MID counts the whole lineament as occurring within the cell if its midpoint falls within that cell. The choice of which of these summarization options is used depends upon the size of the line segments mapped, grid cell size, and goals of the study (Podwysocki and Lowman, 1974). Also specified by the user is the number of azimuth (direction) classes into which the data are summarized. The Landsat data utilized are geometrically corrected, so that

BAND 5 -- LINEAMENT INTERPRETATION SUMMARY

VARIABLE INPUT FORMAT FOR X & Y IS

ALL VALUES WILL BE MULTIPLIED BY A FACTOR OF 1.00000

X1	Y1	X2	Y2	VECLEN	VECAZM	A	B	XMID	YMID
3.4	50.2	13.9	47.6	10.8	76.1	-0.248	51.0	8.6	48.9
19.0	49.1	23.9	46.0	5.8	57.7	-0.633	61.1	21.4	47.6
23.9	46.0	41.5	38.4	19.2	66.6	-0.432	56.3	32.7	42.2
48.1	39.5	41.5	38.4	6.7	279.5	0.167	31.5	44.8	38.9
48.1	39.4	52.1	36.7	4.8	56.0	-0.675	71.9	50.1	38.0
59.0	36.8	52.1	36.7	6.9	270.8	0.014	35.9	55.6	36.8
59.0	36.8	75.1	35.4	16.2	85.0	-0.087	41.9	67.1	36.1
32.0	45.7	37.5	43.5	5.9	68.2	-0.400	58.5	34.8	44.6
37.5	43.5	38.6	40.5	3.2	20.1	-2.727	145.8	38.1	42.0
27.1	49.1	38.6	45.5	12.1	72.6	-0.313	57.6	32.9	47.3
38.6	45.5	44.6	42.7	6.6	65.0	-0.467	63.5	41.6	44.1
38.3	62.7	52.5	38.1	28.4	30.0	-1.732	129.1	45.4	50.4
38.3	62.7	71.1	37.1	41.6	52.0	-0.780	92.6	54.7	49.9
82.7	37.6	71.1	37.1	11.6	272.5	0.043	34.0	76.9	37.4
50.0	48.7	57.0	45.4	7.7	64.8	-0.471	72.3	53.5	47.0
57.0	45.4	59.3	43.3	3.1	47.6	-0.913	97.4	58.1	44.3
59.3	43.3	59.6	41.5	1.8	9.5	-6.000	399.1	59.4	42.4
59.6	41.5	64.7	40.0	5.3	73.6	-0.294	59.0	62.1	40.8
62.5	45.1	69.5	40.5	8.4	56.7	-0.657	86.2	66.0	42.8
69.5	40.5	83.4	39.3	14.0	85.1	-0.086	46.5	76.4	39.9
102.2	47.6	83.4	39.3	20.6	293.8	0.441	2.5	92.8	43.4
166.6	63.9	134.0	55.0	33.8	285.3	0.273	18.4	150.3	59.4
134.0	55.0	117.8	51.8	16.5	281.2	0.198	28.5	125.9	53.4
117.8	51.8	102.2	47.6	16.2	285.1	0.269	20.1	110.0	49.7
3.5	56.5	8.1	55.9	4.6	82.6	-0.130	57.0	5.8	56.2
8.1	55.9	13.6	51.4	7.1	50.7	-0.818	62.5	10.8	53.6
13.6	51.4	21.8	51.1	8.2	87.9	-0.037	51.9	17.7	51.3
27.0	52.0	21.8	51.1	5.3	279.8	0.173	47.3	24.4	51.6
21.8	51.1	39.5	49.7	17.8	85.5	-0.079	52.8	30.6	50.4
46.0	51.0	39.5	49.7	6.6	281.3	0.200	41.8	42.8	50.3
46.0	51.0	65.7	48.4	19.9	82.5	-0.132	57.1	55.8	49.7
78.2	51.4	65.7	48.4	12.9	283.5	0.240	32.6	71.9	49.9
44.6	53.5	33.3	53.2	11.3	271.5	0.027	52.3	38.9	53.3
44.6	53.5	49.2	52.3	4.8	75.4	-0.261	65.1	46.9	52.9
60.9	54.0	49.2	52.3	11.8	278.3	0.145	45.2	55.0	53.1
43.4	59.6	39.3	58.8	4.2	281.0	0.195	51.1	41.3	59.2
43.4	59.6	51.9	56.6	9.0	70.6	-0.353	74.9	47.6	58.1
55.4	58.1	51.9	56.6	3.8	293.2	0.429	34.4	53.6	57.4
41.5	62.1	46.8	62.0	5.3	88.9	-0.019	62.9	44.1	62.1
46.8	62.0	48.6	61.0	2.1	60.9	-0.556	88.0	47.7	61.5
53.7	61.7	48.6	61.0	5.1	277.8	0.137	54.3	51.1	61.3
90.3	69.5	96.5	68.4	6.3	79.9	-0.177	85.5	93.4	68.9
90.3	69.5	82.6	64.6	9.1	302.5	0.636	12.0	86.4	67.1
82.6	64.6	74.7	63.3	8.0	279.3	0.165	51.0	78.6	63.9
90.3	66.1	92.9	65.6	2.6	79.1	-0.192	83.5	91.6	65.9
90.3	66.1	80.7	61.5	10.6	295.6	0.479	22.8	85.5	63.8
80.7	61.5	78.8	59.1	3.1	321.6	1.263	-40.4	79.8	60.3
78.8	59.1	77.3	52.4	6.9	347.4	4.467	-292.9	78.1	55.8
103.7	66.4	95.1	59.8	10.8	307.5	0.767	-13.2	99.4	63.1
82.0	60.2	95.1	59.8	13.1	88.3	-0.031	62.7	88.6	60.0
106.3	60.2	96.6	56.3	10.5	291.9	0.402	17.5	101.4	58.3
108.6	58.7	95.3	52.4	14.7	295.3	0.474	7.3	101.9	55.5
88.5	52.8	95.3	52.4	6.8	86.6	-0.059	58.0	91.9	52.6
149.2	75.0	146.9	74.9	2.3	272.5	0.043	68.5	148.0	74.9
149.2	75.0	161.8	68.8	14.0	63.8	-0.492	148.4	155.5	71.9
161.8	68.8	166.5	68.1	4.8	81.5	-0.149	92.9	164.1	68.4

Figure 23. Sample Output from VECTRANS Program

azimuths in the program are "true" azimuths on the earth's surface. The program allows for up to 90 azimuth classes, from 270 through 0 to 90 degrees.

The AZMAP program, then, scans the data, cell by cell, determining into which cell each lineament falls. If a line segment falls within a specific cell, its length is then added to the appropriate azimuth class within that cell, according to the subroutine selected. Data are summarized both in terms of density (total length of lineaments within each cell) and frequency (number of lineaments within each cell). Output from the program consists of density and numerical histograms, plotted for each cell of the data. In addition, the AZMAP program allows for an optional Chi Square test to be performed on the frequency-azimuth histogram for each grid cell, testing the distribution for randomness (Podwysocki and Lowman, 1974). Sample output for one grid cell generated from the AZMAP program is shown in Figure 24.

For the purposes of this research, a single grid cell is the optimal summarization unit, since an overall comparison of each of the interpretations is desired. Subroutine PART is utilized here, although with one cell, Subroutine MID would yield no different results. Azimuth class number is selected to be 18, so that data are summarized in 10 degree intervals.

Comparison Programs

Quantitative comparison between the different lineament

SAMPLE -- LINEAMENT INTERPRETATION SUMMARY

EACH GRID CELL IS 42 MM. (3.230 MILES) BY 42 MM. (3.230 MILES)

PROGRAM USES SUBROUTINE PART; CONSIDERS ONLY THAT PORTION OF EACH VECTOR WITHIN THE CELL

GRID CELL NUMBER: ROW 2, COLUMN 2 (43 <X< 85; 43 <Y< 85)

AZIMUTHS	CLASS LENGTH (IN MILES)		NUMERICAL FREQUENCY	
270.0-280.0	5.18	>XX	8	>****
280.0-290.0	4.38	>XX	8	>****
290.0-300.0	1.39	>	3	>*
300.0-310.0	1.09	>	2	>*
310.0-320.0	0.0	>	0	>
320.0-330.0	0.36	>	2	>*
330.0-340.0	0.0	>	0	>
340.0-350.0	0.53	>	1	>
350.0-360.0	0.0	>	0	>
0.0- 10.0	0.0	>	0	>
10.0- 20.0	0.0	>	0	>
20.0- 30.0	0.0	>	0	>
30.0- 40.0	1.03	>	1	>
40.0- 50.0	0.36	>	2	>*
50.0- 60.0	2.30	>X	2	>*
60.0- 70.0	1.68	>	6	>***
70.0- 80.0	1.06	>	2	>*
80.0- 90.0	2.35	>X	4	>**
TOTALS	21.71	EACH X = 2.00 MILES	41	EACH * = 2 UNITS

Figure 24. Sample Output from AZMAP Program

interpretations is accomplished by means of a method developed by Huntington and Raiche (1978). This method compares two interpretations at a time, basing the comparison on the lineament attributes of location, orientation, and length. From these attributes a "similarity coefficient", which is a measure of how well one lineament pattern overlays another, is calculated. By comparing the lineament patterns resulting from each of the enhancement techniques with each other, with the unenhanced data, and with the "standard" lineament interpretation, a quantitative measure of how the interpretations compare is made.

Huntington and Raiche have developed seven different levels of analysis to compare two lineament interpretations. These levels each require a slightly different methodology, and differ in the degree of detail that they consider. One of these levels requires the superimposition of an identical grid on each of the two interpretations. Within each cell of the grid, directional orientation of lineaments is divided into classes, with the total length of lineaments in each class computed. Thus, for each interpretation, information is compiled on total length of lineaments per azimuth class per cell (Huntington and Raiche, 1978). This measure for each cell is divided by a normalization factor, so that the similarity coefficient is in the range of 0 to 1. Next, the normalized total lineament length per direction class per cell is multiplied by that of the

corresponding cell in the other interpretation, with the product summed over all azimuth classes. The result of these calculations is a similarity coefficient for the two interpretations for that cell. This calculation can be expressed by the following equation:

$$C = \sum_{m=1}^{18} \left[\frac{a(m)}{\left\{ 1/2 \sum_{m=1}^{18} [a^2(m) + b^2(m)] \right\}^{1/2}} * \frac{b(m)}{\left\{ 1/2 \sum_{m=1}^{18} [a^2(m) + b^2(m)] \right\}^{1/2}} \right]$$

where:

c = cellular coefficient of similarity
a(m) = lineament length in azimuth class m, interpretation 1
b(m) = lineament length in azimuth class m, interpretation 2

This coefficient indicates how similar the lineament patterns in that cell are for the two interpretations, with a coefficient of 1 denoting perfect similarity and a coefficient of 0 denoting no similarity. By averaging these individual cellular coefficients of similarity over all cells in the study area, a mean similarity coefficient for the study area is obtained (Huntington and Raiche, 1978).

This technique of comparison is advantageous over the other six levels of detail discussed by Huntington and Raiche, in that a local comparison and scene-wide comparison can be made. If two lineament interpretations have a low overall coefficient of similarity, one can look at the coefficients of the individual cells to see in what portions of the image the lineament patterns differ. A drawback of

this level of detail is the tremendous number of calculations required. If the technique is programmed to be performed by computer, however, this drawback is mitigated. For this reason, a program has been written by the author to accomplish this lineament comparison.

The comparison program, SIMCO, utilizes as input data the output generated by the AZMAP program. This information consists of the total length of lineaments per azimuth class per cell, for each lineament interpretation. The program then normalizes this data, and computes both cellular and scene coefficients of similarity. Output from the program is a similarity coefficient map for the two interpretations, indicating the coefficients for each cell, along with the overall scene coefficient of similarity. As with AZMAP, the scene can be divided into any number of grid cells, and the number of azimuth classes is user-specified as well. Sample output from the SIMCO program is shown in Figure 25.

In keeping with the first three summarization programs, the SIMCO program as used in this research is implemented with a single grid cell, with 18 azimuth classes. While the use of a single grid cell eliminates the ability to analyze the lineament interpretations on a local basis, such detail is not essential to the objectives of this investigation. In comparing the interpretations for the various enhancements, all that is desired is an overall scene-wide appraisal, provided by a single-cell analysis. Additional

```
SIMCO -- SAMPLE OUTPUT

0.29  0.00  0.00  0.00

0.82  0.41  0.44  0.13

0.71  0.52  0.57  0.72

0.06  0.56  0.78  0.83

SCENE COEFFICIENT OF SIMILARITY = 0.43
```

Figure 25. Sample Output from SIMCO Program

detail, in this instance, only serves to complicate the analysis.

Through the use of the SIMCO program, it is possible to compare the similarities in lineament patterns between each of the the enhancement interpretations, and between the enhancements and the unenhanced interpretation. In addition, similarities between each of the interpretations and the known-lineament "standard" are determined. These comparisons indicate which enhancement techniques yield results which approximate those obtained from detailed lineament mapping by other means. The "standard" accepted in this research is a lineament map produced by Melton (1976). This map was produced in a manner different from the Landsat technique described here, as lineaments were interpreted from stereoscopic aerial photograph mosaics, at a scale of 1:20,000 or larger. As a result of the different interpretation methods and media, the lineament interpretations generated from this research cannot be directly compared with Melton's findings in assessing the absolute worth of the enhancement techniques. The enhancement interpretations, rather, are evaluated relative to one another in terms of how closely they correspond to this "standard". Perfect correspondence is not expected--the vast differences in scale and technique between aerial photograph and Landsat interpretation dictate this. It is probable that the larger scale of the aerial photography interpreted by Melton resulted in the detection of more

lineaments than the Landsat data interpreted in this research, but the degree of this difference is not known at this point. With Melton's interpretation accepted as the "standard", however, those enhancements most similar to it are deemed "best". In this manner, the evaluation of the different enhancement techniques, in terms of their relative utilities for regional lineament detection, is accomplished.

Results of Analysis

Results of Summarization Programs

The general results of the analysis performed by the summarization programs on the lineament interpretations derived from the unenhanced image, the five enhancements, and the "standard" lineament map are shown by Table II. As can be seen from this table, considerable differences exist between the total number of lineaments and the total length of lineaments found in the various interpretations. The "standard" lineament interpretation identifies many more lineaments than any of the other interpretations, a fact which is most likely attributable to the different interpretation methodology and medium used in its compilation. The principal components interpretation best approximates the lineament number and length totals derived in this "standard", while the band ratio and high-pass filter interpretations deviate farthest from it. In comparison with the interpretation resulting from the unenhanced data, the band ratio, histogram equalization, and

high-pass filter interpretations yield fewer lineaments, of less total length. The lineaments interpreted from the mean value enhancement are very nearly equal, in number and length, to those identified on the unenhanced image.

TABLE II

SUMMARY OF LINEAMENT INTERPRETATION DATA
FROM VECTRANS AND AZMAP PROGRAMS

Interpretation	Total Number of Lineaments	Total Length of Lineaments (mi)
Unenhanced Band 5	280	169.85
Mean Value	314	178.84
Principal Components	451	238.31
Band Ratio	88	39.87
Histogram Equalization	144	78.33
High-Pass Filter	83	68.60
"Standard" Map	633	400.85

Details of the individual interpretations are presented by the output from the AZMAP summarization program. Figure 26 depicts AZMAP output for the unenhanced band 5 lineament interpretation. As can be seen in this figure, most of the lineaments identified on this image occur within two general azimuthal orientations: 60 to 90 degrees and 270 to 290 degrees. A noticable lack of lineaments were detected in the 310 to 360 degree range.

BAND 5 -- LINEAMENT INTERPRETATION SUMMARY

EACH GRID CELL IS 168 MM. (12.919 MILES) BY 168 MM. (12.919 MILES)

PROGRAM USES SUBROUTINE PART; CONSIDERS ONLY THAT PORTION OF EACH VECTOR WITHIN THE CELL

GRID CELL NUMBER: ROW 1, COLUMN 1 (1 <X< 169; 1 <Y< 169)

AZIMUTHS	CLASS LENGTH (IN MILES)		NUMERICAL FREQUENCY	
270.0-280.0	21.12	>XXXXXXXXXX	33	>**********
280.0-290.0	31.00	>XXXXXXXXXXXXXXX	32	>**********
290.0-300.0	10.94	>XXXXX	16	>********
300.0-310.0	5.71	>XX	9	>****
310.0-320.0	0.25	>	1	>
320.0-330.0	0.85	>	3	>*
330.0-340.0	0.82	>	2	>*
340.0-350.0	0.75	>	2	>*
350.0-360.0	0.92	>	3	>*
0.0- 10.0	2.28	>X	7	>***
10.0- 20.0	3.05	>X	10	>*****
20.0- 30.0	3.23	>X	6	>***
30.0- 40.0	4.94	>XX	8	>****
40.0- 50.0	6.67	>XXX	15	>*******
50.0- 60.0	10.43	>XXXXX	17	>********
60.0- 70.0	23.25	>XXXXXXXXXXX	40	>**********
70.0- 80.0	19.45	>XXXXXXXXX	38	>**********
80.0- 90.0	24.19	>XXXXXXXXXXX	38	>**********
TOTALS	169.85	EACH X = 2.00 MILES	280	EACH * = 2 UNITS

Figure 26. AZMAP Output for Unenhanced Band 5 Interpretation

Output for the mean value interpretation is shown in Figure 27. The majority of the lineaments found in this interpretation are orientated toward 40 to 90 degrees and 270 to 300 degrees. Again, a marked absence of lineaments exists in the 0 to 40 degree range, along with 300 to 360 degrees.

Summarization output for the principal components interpretation is shown in Figure 28. Preferred orientations for lineaments in this interpretation are in the ranges 30 to 90 and 270 to 300 degrees, with few occurring in the 0 to 20 and 310 to 360 degree ranges.

Figure 29 shows output from the AZMAP program for the lineaments detected from the band ratio enhancement. Most lineaments in this interpretation are found orientated from 60 to 90 and 270 to 300 degrees. Again, few lineaments are found in the 0 to 20 and 310 to 360 degree orientations.

Orientations are similar in the histogram equalization interpretation, as shown by Figure 30. The majority of the lineaments are found in the 50 to 90 and 270 to 300 degree intervals, with few orientated between the ranges 0 to 40 and 300 to 360 degrees.

Output from the high-pass filter interpretation, shown in Figure 31, again indicates similar lineament orientations to those found in the other interpretations. Preferred lineament directions are 70 to 90 and 270 to 290 degrees, with a lack of lineaments orientated from 0 to 50 and 300 to 360 degrees.

MEAN VALUE OF ALL BANDS -- LINEAMENT INTERPRETATION SUMMARY

EACH GRID CELL IS 168 MM. (12.919 MILES) BY 168 MM. (12.919 MILES)

PROGRAM USES SUBROUTINE PART; CONSIDERS ONLY THAT PORTION OF EACH VECTOR WITHIN THE CELL

GRID CELL NUMBER: ROW 1, COLUMN 1 (1 <X< 169; 1 <Y< 169)

AZIMUTHS	CLASS LENGTH (IN MILES)		NUMERICAL FREQUENCY	
270.0-280.0	22.08	>XXXXXXXXXX	31	>***************
280.0-290.0	29.94	>XXXXXXXXXXXXX	39	>*******************
290.0-300.0	11.53	>XXXXX	18	>*********
300.0-310.0	3.76	>X	5	>**
310.0-320.0	1.91	>	4	>**
320.0-330.0	0.0	>	0	>
330.0-340.0	0.66	>	2	>*
340.0-350.0	0.0	>	0	>
350.0-360.0	3.61	>X	2	>*
0.0- 10.0	0.84	>	3	>*
10.0- 20.0	2.17	>X	6	>***
20.0- 30.0	2.34	>X	8	>****
30.0- 40.0	4.41	>XX	8	>****
40.0- 50.0	10.49	>XXXXX	21	>**********
50.0- 60.0	14.62	>XXXXXXX	29	>**************
60.0- 70.0	22.48	>XXXXXXXXXX	44	>*********************
70.0- 80.0	24.64	>XXXXXXXXXXX	50	>************************
80.0- 90.0	23.38	>XXXXXXXXXX	44	>*********************
TOTALS	178.84	EACH X = 2.00 MILES	314	EACH * = 2 UNITS

Figure 27. AZMAP Output for Mean Value Interpretation

PRINCIPAL COMPONENTS ANALYSIS -- LINEAMENT INTERPRETATION SUMMARY

EACH GRID CELL IS 168 MM. (12.919 MILES) BY 168 MM. (12.919 MILES)

PROGRAM USES SUBROUTINE PART; CONSIDERS ONLY THAT PORTION OF EACH VECTOR WITHIN THE CELL

GRID CELL NUMBER: ROW 1, COLUMN 1 (1 <X< 169; 1 <Y< 169)

AZIMUTHS	CLASS LENGTH (IN MILES)		NUMERICAL FREQUENCY	
270.0-280.0	28.85	>XXXXXXXXXXXXXX	45	>**********
280.0-290.0	37.66	>XXXXXXXXXXXXXXXXXX	50	>**********
290.0-300.0	13.57	>XXXXXX	26	>**********
300.0-310.0	6.99	>XXX	10	>*****
310.0-320.0	2.22	>X	4	>**
320.0-330.0	1.82	>	3	>*
330.0-340.0	0.45	>	1	>
340.0-350.0	0.0	>	0	>
350.0-360.0	2.73	>X	6	>***
0.0- 10.0	0.73	>	3	>*
10.0- 20.0	2.79	>X	6	>***
20.0- 30.0	4.33	>XX	15	>********
30.0- 40.0	11.86	>XXXXX	25	>**********
40.0- 50.0	12.06	>XXXXXX	28	>**********
50.0- 60.0	15.93	>XXXXXXX	38	>**********
60.0- 70.0	32.82	>XXXXXXXXXXXXXXXX	66	>**********
70.0- 80.0	32.43	>XXXXXXXXXXXXXXX	61	>**********
80.0- 90.0	31.06	>XXXXXXXXXXXXXX	64	>**********
TOTALS	238.31	EACH X = 2.00 MILES	451	EACH * = 2 UNITS

Figure 28. AZMAP Output for Principal Components Interpretation

BAND RATIO -- LINEAMENT INTERPRETATION SUMMARY

EACH GRID CELL IS 168 MM. (12.919 MILES) BY 168 MM. (12.919 MILES)

PROGRAM USES SUBROUTINE PART; CONSIDERS ONLY THAT PORTION OF EACH VECTOR WITHIN THE CELL

GRID CELL NUMBER: ROW 1, COLUMN 1 (1 <X< 169; 1 <Y< 169)

AZIMUTHS	CLASS LENGTH (IN MILES)		NUMERICAL FREQUENCY	
270.0-280.0	3.87	>X	9	>****
280.0-290.0	6.26	>XXX	10	>*****
290.0-300.0	5.36	>XX	9	>****
300.0-310.0	1.88	>	3	>*
310.0-320.0	0.92	>	1	>
320.0-330.0	0.0	>	0	>
330.0-340.0	0.0	>	0	>
340.0-350.0	0.0	>	0	>
350.0-360.0	0.18	>	1	>
0.0- 10.0	0.62	>	1	>
10.0- 20.0	0.45	>	1	>
20.0- 30.0	1.30	>	4	>**
30.0- 40.0	2.38	>X	7	>***
40.0- 50.0	1.63	>	4	>**
50.0- 60.0	1.78	>	4	>**
60.0- 70.0	2.72	>X	8	>****
70.0- 80.0	5.08	>XX	12	>******
80.0- 90.0	5.44	>XX	14	>********
TOTALS	39.87	EACH X = 2.00 MILES	88	EACH * = 2 UNITS

Figure 29. AZMAP Output for Band Ratio Interpretation

HISTOGRAM EQUALIZATION -- LINEAMENT INTERPRETATION SUMMARY

EACH GRID CELL IS 168 MM. (12.919 MILES) BY 168 MM. (12.919 MILES)

PROGRAM USES SUBROUTINE PART; CONSIDERS ONLY THAT PORTION OF EACH VECTOR WITHIN THE CELL

GRID CELL NUMBER: ROW 1, COLUMN 1 (1 <X< 169; 1 <Y< 169)

AZIMUTHS	CLASS LENGTH (IN MILES)		NUMERICAL FREQUENCY	
270.0-280.0	9.75	>XXXX	18	>*********
280.0-290.0	10.84	>XXXXX	17	>********
290.0-300.0	3.00	>X	6	>***
300.0-310.0	3.68	>X	3	>*
310.0-320.0	0.0	>	0	>
320.0-330.0	0.0	>	0	>
330.0-340.0	0.0	>	0	>
340.0-350.0	0.10	>	1	>
350.0-360.0	0.0	>	0	>
0.0- 10.0	0.16	>	1	>
10.0- 20.0	0.70	>	2	>*
20.0- 30.0	1.65	>	6	>***
30.0- 40.0	1.22	>	3	>*
40.0- 50.0	2.71	>X	8	>****
50.0- 60.0	7.70	>XXX	14	>*******
60.0- 70.0	11.52	>XXXXX	20	>**********
70.0- 80.0	12.33	>XXXXXX	20	>**********
80.0- 90.0	13.00	>XXXXXX	25	>**********
TOTALS	78.33	EACH X = 2.00 MILES	144	EACH * = 2 UNITS

Figure 30. AZMAP Output for Histogram Equalization Interpretation

HIGH-PASS FILTER -- LINEAMENT INTERPRETATION SUMMARY

EACH GRID CELL IS 168 MM. (12.919 MILES) BY 168 MM. (12.919 MILES)

PROGRAM USES SUBROUTINE PART; CONSIDERS ONLY THAT PORTION OF EACH VECTOR WITHIN THE CELL

GRID CELL NUMBER: ROW 1, COLUMN 1 (1 <X< 169; 1 <Y< 169)

AZIMUTHS	CLASS LENGTH (IN MILES)		NUMERICAL FREQUENCY	
270.0-280.0	15.43	>XXXXXXX	19	>*********
280.0-290.0	13.20	>XXXXXX	14	>*******
290.0-300.0	4.75	>XX	6	>***
300.0-310.0	2.92	>X	3	>*
310.0-320.0	0.0	>	0	>
320.0-330.0	0.0	>	0	>
330.0-340.0	0.0	>	0	>
340.0-350.0	0.26	>	1	>
350.0-360.0	0.0	>	0	>
0.0- 10.0	7.02	>XXX	1	>
10.0- 20.0	0.0	>	0	>
20.0- 30.0	0.63	>	2	>*
30.0- 40.0	0.21	>	1	>
40.0- 50.0	0.48	>	1	>
50.0- 60.0	3.04	>X	6	>***
60.0- 70.0	2.62	>X	5	>**
70.0- 80.0	10.13	>XXXXX	14	>*******
80.0- 90.0	7.92	>XXX	10	>*****
TOTALS	68.60	EACH X = 2.00 MILES	83	EACH * = 2 UNITS

Figure 31. AZMAP Output for High-Pass Filter Interpretation

The "standard" lineament interpretation, as shown by Figure 32, indicates a much more evenly distributed occurrence of lineaments over the compass directions than do the other interpretations. This might be attributed to the different methodology and medium utilized in the interpretation of lineaments found on this "standard". The conditions of solar illumination direction, angle of illumination, and look direction of the sensor, essentially fixed on the Landsat satellite, can be varied in the acquisition of aerial photographs. The difference in these parameters might be responsible for the differences in lineament distribution observed from the two types of imagery. The majority of lineament occurrences in the "standard" interpretation, however, still lie in the same general directions as in the other interpretations. Most lineaments are orientated in the 60 to 90 and 270 to 310 degree intervals, with fewest found in the 0 to 30 and 340 to 360 degree ranges.

The above lineament orientation observations, derived from output from the AZMAP program, are summarized in Table III. This table indicates that, while the different interpretations vary greatly in the total number and length of lineaments identified, they nonetheless do show agreement in terms of the directions in which the lineaments are orientated. In general, all seven interpretations show a preferred lineament orientation in the ranges 60 to 90 and 270 to 300 degrees.

```
                    LINEAMENT "STANDARD" MAP -- LINEAMENT INTERPRETATION SUMMARY
                    EACH GRID CELL IS  168 MM. ( 12.919 MILES  ) BY  168 MM. ( 12.919 MILES  )
                    PROGRAM USES SUBROUTINE PART; CONSIDERS ONLY THAT PORTION OF EACH VECTOR WITHIN THE CELL
GRID CELL NUMBER: ROW    1, COLUMN    1 (   1 <X<  169;    1 <Y<  169)

 AZIMUTHS    CLASS LENGTH (IN MILES  )                                  NUMERICAL FREQUENCY
 --------    -------------------------                                  -------------------
270.0-280.0     55.80   >XXXXXXXXXXXXXXXXXXXXXXXXXXX                        71     >***********************************
280.0-290.0     65.48   >XXXXXXXXXXXXXXXXXXXXXXXXXXXXXXXXXXX                84     >*****************************************
290.0-300.0     46.91   >XXXXXXXXXXXXXXXXXXXXXXX                            63     >*******************************
300.0-310.0     38.92   >XXXXXXXXXXXXXXXXXX                                 54     >**************************
310.0-320.0     18.00   >XXXXXXXXX                                          31     >****************
320.0-330.0     13.78   >XXXXXX                                             26     >**************
330.0-340.0     13.40   >XXXXXX                                             29     >****************
340.0-350.0      8.23   >XXXX                                               19     >**********
350.0-360.0      7.74   >XXX                                                13     >******
  0.0- 10.0      7.17   >XXX                                                19     >**********
 10.0- 20.0      6.57   >XXX                                                16     >*********
 20.0- 30.0      5.88   >XX                                                 15     >********
 30.0- 40.0     13.44   >XXXXXX                                             24     >*************
 40.0- 50.0     12.47   >XXXXXX                                             23     >************
 50.0- 60.0     13.35   >XXXXXX                                             21     >***********
 60.0- 70.0     23.98   >XXXXXXXXXXX                                        38     >*******************
 70.0- 80.0     26.63   >XXXXXXXXXXXXX                                      45     >************************
 80.0- 90.0     23.11   >XXXXXXXXXXX                                        42     >**********************
               -------                                                     ----
    TOTALS     400.85        EACH X =    2.00  MILES                      633           EACH * =    2 UNITS
```

Figure 32. AZMAP Output for "Standard" Interpretation

TABLE III

SUMMARY OF LINEAMENT ORIENTATION DATA
FROM AZMAP PROGRAM

Interpretation	Preferred Lineament Orientations (degrees)
Unenhanced Band 5	60-90, 270-290
Mean Value	40-90, 270-300
Principal Components	30-90, 270-300
Band Ratio	60-90, 270-300
Histogram Equalization	50-90, 270-300
High-Pass Filter	70-90, 270-300
"Standard" Map	60-90, 270-310

This general agreement in lineament orientation might be expected for the first six interpretations, since all deal with the same original Landsat data. These data were sensed under specific conditions of solar illumination and satellite look direction at the time of data acquisition. As a result, the lineament orientations observed from all of the Landsat interpretations will be similar, most likely being a function of those two parameters, which do not vary among the interpretations. The agreement between these Landsat interpretations and the "standard" interpretation must be attributed to some other factor, since the "standard" was probably derived under different conditions of illumination and look direction. By referring back to Figure 2, however, it can be seen that the general trend of

the geologic structure in the study area is northwest-southeast, which agrees with the orientation of many of the lineaments on both types of imagery. Thus, the similarity between the Landsat-derived and "standard" interpretation orientations appears to be a function of geologic structure.

Results of Comparison Programs

In the SIMCO program, each of the interpretations is compared, one by one, with the other six interpretations, and an overall coefficient of similarity is calculated for each interpretation pair. In all, there are 21 comparisons necessary in order to compare the seven lineament interpretations. The results of these comparisons are shown in Table IV. In this table, a similarity coefficient of 1.00 denotes perfect similarity between two interpretations; a coefficient of 0.00 denotes perfect dissimilarity.

From Table IV, several observations can be made regarding the seven interpretations: (1) of the five enhancements, the lineament interpretation pairs showing the greatest similarity are the principal components and mean value interpretations (similarity coefficient = 0.96) and the high-pass filter and histogram equalization interpretations (similarity coefficient = 0.85); (2) the enhancements showing the least similarity are the band ratio - mean value (0.38), and band ratio - principal components (0.29) pairs; (3) in comparison with the "standard" interpretation, the enhancements that show the least

TABLE IV

SUMMARY OF COEFFICIENTS OF SIMILARITY
FROM SIMCO PROGRAM

Lineament Interpretation							
U	M	P	R	E	F	S	
*	0.99	0.94	0.40	0.76	0.71	0.67	U
*	*	0.96	0.38	0.74	0.68	0.68	M
*	*	*	0.29	0.61	0.56	0.79	P
*	*	*	*	0.69	0.63	0.18	R
*	*	*	*	*	0.85	0.34	E
*	*	*	*	*	*	0.38	F
*	*	*	*	*	*	*	S

Interpretation Legend:

U = Unenhanced Band 5
M = Mean Value
P = Principal Components
R = Band Ratio
E = Histogram Equalization
F = High-Pass Filter
S = "Standard" Map

similarity are those resulting from the band ratio (0.18), histogram equalization (0.34), and high-pass filter (0.38) techniques; (4) those enhancements showing the most similarity to the "standard" interpretation are the principal components (0.79) and mean value (0.68) interpretations; and (5) the mean value and principal components interpretations show near-perfect similarity to the unenhanced image interpretation (similarity coefficients of 0.99 and 0.94, respectively). The significance of each of these observations is discussed in the following chapter, in terms of the conclusions that can be drawn from them regarding the effectiveness of the enhancement techniques.

Interpretation Composite Analysis

Rationale

From the analysis described above, one additional point can be investigated regarding the lineament enhancement techniques. The results of the analysis suggest that, of the techniques evaluated, only the principal components and mean value enhancements are of much utility, since they alone identify more lineaments than the unenhanced data. The other three enhancement techniques, histogram equalization, band ratioing, and high-pass filtering, appear to be of relatively little value, since they identify fewer lineaments than the unenhanced data. As a review of Table II indicates, these three techniques do result in the identification of some lineaments. The point can be raised

that if any of the lineaments identified by the three "less valuable" techniques are undetected by the principal components and mean value enhancements, then those techniques do indeed result in the gain of additional lineament information. If this is the case, then the histogram equalization, band ratio and high-pass filter enhancements are of some value for lineament identification. If the converse is true-- those lineaments identified by the three techniques are also identified by the "more valuable" techniques-- then no new information is gained, and the techniques can be considered essentially worthless.

In order to investigate this issue, the interpretation data are subjected to further analysis. The goal of this analysis is to ascertain the relative contribution of each enhancement technique toward a composite of all lineaments identified by the enhancements.

Methodology

The initial step in determining the relative lineament contributions of each of the enhancements is to overlay, on a light table, the lineament interpretations resulting from the five enhancements. The enhancements are first ranked, by use of Table II, in terms of the total number of lineaments identified. From most lineaments identified to least identified, this rank is: (1) principal components; (2) mean value; (3) histogram equalization; (4) band ratioing; (5) high-pass filtering. Next, the principal

components interpretation is placed over the mean value interpretation on the light table. Those line segments present on the mean value interpretation but not on the principal components interpretation are traced onto the principal components overlay, in red ink. This results in a composite of the lineaments identified by both the mean value and principal components techniques, with a distinction made for those lineaments added by the mean value enhancement. Beneath this principal components/mean value composite, the histogram equalization lineament interpretation is laid, with the line segments added by that technique traced, in another color ink, onto the composite. This procedure is continued for the final two enhancement interpretations. The result is a composite interpretation overlay showing the lineaments added to the "best" enhancement interpretation by the next "worst" interpretation in the rank, for all of the interpretations, with the principal components interpretation serving as the base. At this point, the unenhanced lineament interpretation is laid beneath the composite, with those line segments identified on the unenhanced data but not on any of the enhancements being added to the composite.

The second step in the analysis is the digitization of the line segments present on the composite overlay, making note of which segments are added by which enhancement interpretation. This digitization is completed in the same manner as in the initial analysis. Next, the beginning and

endpoints of the digitized line segments are input to the VECTRANS and AZMAP summarization programs. Data from the portion of the composite overlay added to the principal components interpretation by the mean value interpretation are first added to the principal components data set derived in the initial analysis. The summarization programs are then run on the new data set, with the result being number and length calculations for the principal components interpretation, plus the lineaments added to that interpretation by the mean value interpretation. By subtracting the totals from the principal components interpretation alone from these new totals, the number and length of lineaments added by the mean value enhancement are determined. In a similar manner, the data contributed by each of the other enhancements are added, step by step, to the new data set, with the summarization programs run for each step. The respective contributions of each enhancement are, in this way, calculated. In the end, this procedure results in a data set consisting of all lineaments identified by the five enhancements. The summarization programs are run on this data, with the resulting calculation of the total number of lineaments and the total length of lineaments identified by the five enhancements utilized (Figure 33).

Next, the portion of the composite contributed by the unenhanced data is added to the five enhancement data set. Again, the VECTRANS and AZMAP programs are run, with

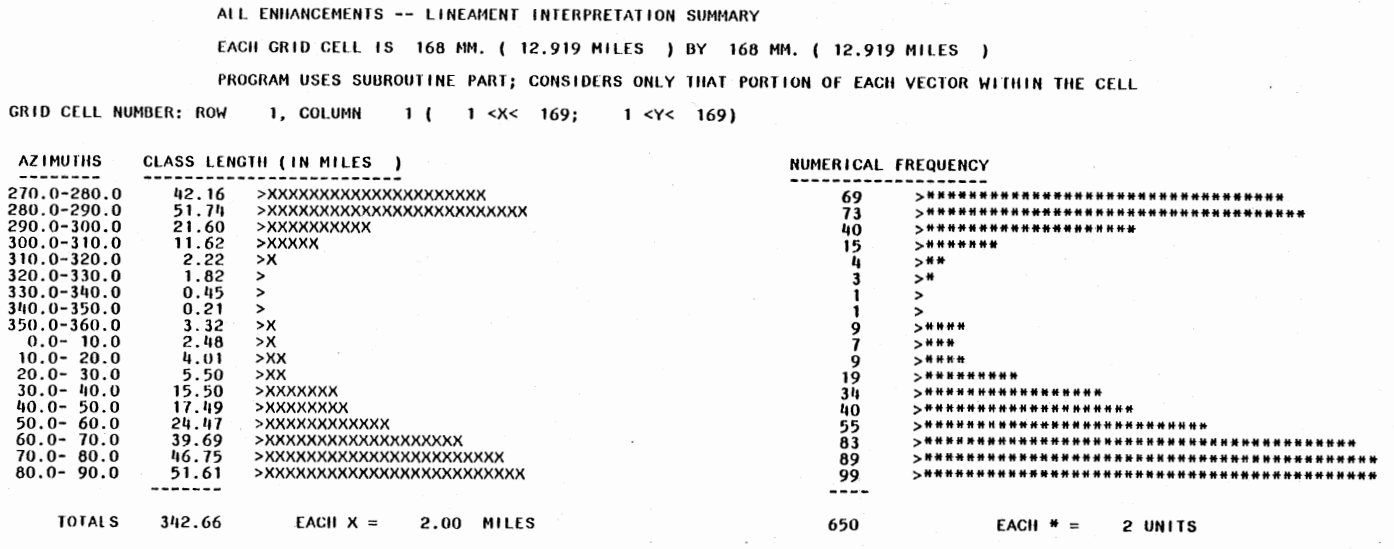

```
ALL ENHANCEMENTS -- LINEAMENT INTERPRETATION SUMMARY

EACH GRID CELL IS  168 MM. ( 12.919 MILES  ) BY  168 MM. ( 12.919 MILES  )

PROGRAM USES SUBROUTINE PART; CONSIDERS ONLY THAT PORTION OF EACH VECTOR WITHIN THE CELL

GRID CELL NUMBER: ROW    1, COLUMN    1 (   1 <X<  169;    1 <Y<  169)

 AZIMUTHS    CLASS LENGTH (IN MILES  )                    NUMERICAL FREQUENCY
 --------    -------------------------                    -------------------
270.0-280.0     42.16   >XXXXXXXXXXXXXXXXXXXX                  69     >**********************************
280.0-290.0     51.74   >XXXXXXXXXXXXXXXXXXXXXXXXX             73     >************************************
290.0-300.0     21.60   >XXXXXXXXXX                            40     >********************
300.0-310.0     11.62   >XXXXX                                 15     >********
310.0-320.0      2.22   >X                                      4     >**
320.0-330.0      1.82   >                                       3     >*
330.0-340.0      0.45   >                                       1     >
340.0-350.0      0.21   >                                       1     >
350.0-360.0      3.32   >X                                      9     >****
  0.0- 10.0      2.48   >X                                      7     >***
 10.0- 20.0      4.01   >XX                                     9     >****
 20.0- 30.0      5.50   >XX                                    19     >**********
 30.0- 40.0     15.50   >XXXXXXXX                              34     >*****************
 40.0- 50.0     17.49   >XXXXXXXX                              40     >********************
 50.0- 60.0     24.47   >XXXXXXXXXXXX                          55     >***************************
 60.0- 70.0     39.69   >XXXXXXXXXXXXXXXXXX                    83     >*****************************************
 70.0- 80.0     46.75   >XXXXXXXXXXXXXXXXXXXXXXX               89     >*********************************************
 80.0- 90.0     51.61   >XXXXXXXXXXXXXXXXXXXXXXXXX             99     >**************************************************
               -------                                       ----
    TOTALS     342.66       EACH X =    2.00  MILES          650          EACH * =    2 UNITS
```

Figure 33. AZMAP Output for "Enhancement" Interpretation Composite

summarization consisting of number and length of all lineaments detected from Landsat data, both unenhanced and enhanced (Figure 34). By subtracting from these "Landsat" interpretation calculations the "enhancement" interpretation calculations, the number and length of lineaments identified by the unenhanced data but not by the enhancements is determined.

Finally, the data generated by the interpretation composite analysis are input to the SIMCO comparison program. Similarity coefficients are calculated for three comparisons: (1) the lineaments identified by the composite of all enhancements compared to the unenhanced interpretation; (2) the "enhancement" composite compared to the "standard" interpretation; and (3) the "Landsat" interpretation (unenhanced and enhanced) compared to the "standard" interpretation. The results of these analyses are discussed below.

Results of Composite Analysis

The results of the analysis of the interpretation composite are summarized in Table V. As can be seen, the mean value enhancement results in the identification of 81 lineaments that are not identified by the "best" technique, the principal components enhancement. These additional lineaments are a total of 41.64 miles in length. The histogram equalization technique results in the identification of an additional 41 lineaments, 18.77 miles

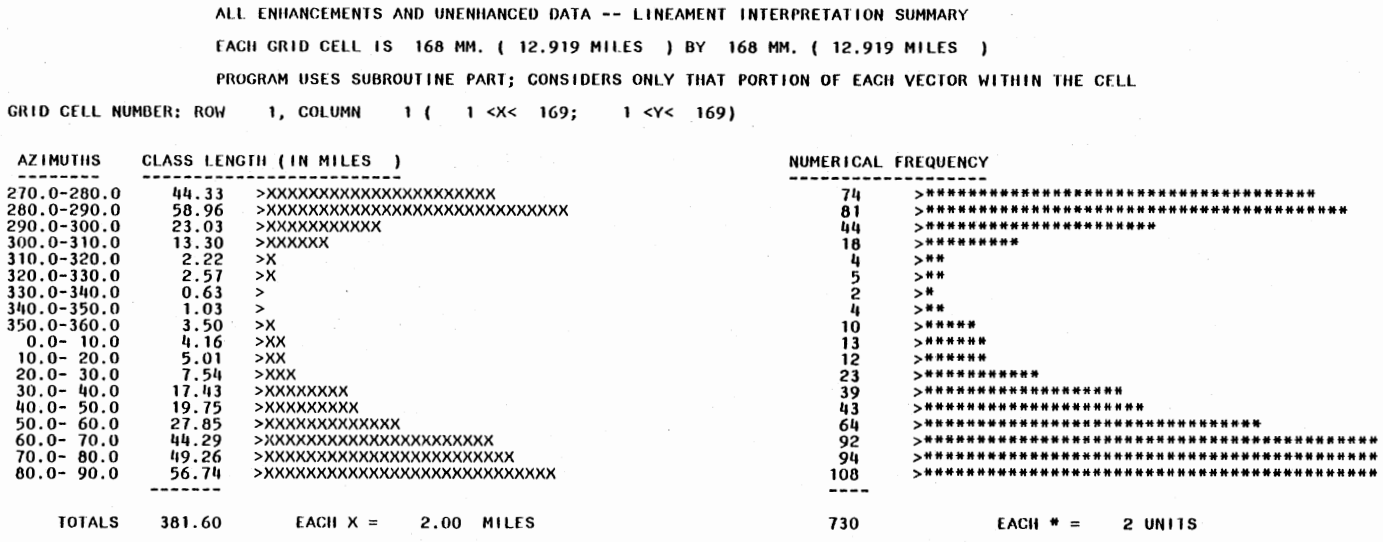

Figure 34. AZMAP Output for "Landsat" Interpretation Composite

in length, that are not found by the two "best" enhancements. The band ratio enhancement detects 45 additional lineaments (19.97 miles), while the "worst" technique, high-pass filtering, identifies 32 lineaments (23.97 miles) that are undetected by the four "better" techniques. Finally, the unenhanced data, when overlaid upon the enhancement composite, results in the identification of 80 lineaments, 38.94 miles in length, that are not detected by any of the five enhancements.

TABLE V

SUMMARY OF LINEAMENT INTERPRETATION DATA
FROM COMPOSITE ANALYSIS

Interpretation	Total Number of Lineaments Added By Interpretation	Total Length of Lineaments Added By Interpretation (mi)
Mean Value	81	41.64
Histogram Equalization	41	18.77
Band Ratio	45	19.97
High-Pass Filter	32	23.97
Unenhanced Band 5	80	38.94

In general, Table V shows that all of the enhancements do indeed result in the identification of some lineaments

that are not identified by any other interpretation. Of the three enhancement techniques whose worth is in question, the band ratio technique contributes the most additional data in terms of number of lineaments, followed by the histogram equalization and high-pass filter techniques, respectively.

The results of the comparative analysis of the interpretation composite data are shown in Table VI. From this table, in conjunction with Table IV, the following observations can be made: (1) the comparison of the enhancement composite with the unenhanced data (similarity coefficient = 0.80) yields less similarity than the initial comparison of the principal components interpretation alone with the unenhanced data (similarity coefficient = 0.94); (2) the comparison of the enhancement composite with the "standard" interpretation (0.87) yields greater similarity than the best initial comparison with the "standard", provided by the principal components enhancement alone (0.79); (3) the enhancement composite in conjunction with the lineaments added from the unenhanced data, when compared to the "standard" interpretation (0.87) yields no better similarity than the comparison of the enhancement composite alone with the "standard" (0.87).

Summary

This chapter has described the analysis of the original enhancement data and the enhancement composite, and has presented results of these analyses. The significance of

TABLE VI

SUMMARY OF COEFFICIENTS OF SIMILARITY
FROM COMPOSITE ANALYSIS

Lineament Interpretation				
U	S	E	L	
*	*	.80	*	U
*	*	.87	.87	S
*	*	*	*	E
*	*	*	*	L

Interpretation Legend:

U = Unenhanced Band 5
S = "Standard" Map
E = "Enhancement" Composite
L = "Landsat" Composite

these results are summarized in the next chapter, along with the conclusions and recommendations derived from this research.

CHAPTER VI

CONCLUSIONS AND RECOMMENDATIONS

Conclusions Drawn from Analysis

A number of conclusions can be drawn from the comparative analysis of the enhanced, unenhanced, and "standard" lineament interpretations. These conclusions are directed toward the specific lineament enhancements utilized and the general utility of computer enhancement procedures for lineament detection.

First, all enhancements identify lineaments orientated in the same general compass direction. Moreover, this direction is the same as that evident in the unenhanced and "standard" interpretations. Such consistency can imply: (1) that the lineaments identified on the various images, are, in general, the same ones; and/or (2) that the preferred lineament orientation is a function of the directions of illumination and observation. That is, with a constant direction of solar illumination on each of the images, certain orientations of lineaments are highlighted more than others, when viewed from a constant direction. This conclusion is consistent with findings reported by Podwysocki, Moik, and Shoup (1975). They found illumination

to be a major factor in lineament detection, with northeast and northwest trending lineaments generally being the most easily recognized, because of satellite pass-over time. Similar results are observed in this study, where lineaments orientated toward the east-northeast (60 to 90 degrees) and west-northwest (270 to 300 degrees) are found to be the most common.

A second conclusion is that, of the five enhancements applied, the principal components and mean value of all bands techniques have the most relative utility for lineament detection. These techniques, as discussed in Chapter V, most closely approximate the "standard" interpretation in terms of number of lineaments identified, total length of lineaments identified, and similarity coefficient. The analysis indicates that these two enhancements have more value than the other techniques evaluated. The unenhanced image, however, also has extremely close similarity with these two enhancement techniques. This implies that, while these techniques are better than the others tested, they serve to accomplish little more than does the unenhanced data. The "best" enhancement techniques result in the identification of only a slightly greater number and length of lineaments than are found on the unenhanced band 5 data for the season tested.

A third conclusion is that the enhancement techniques of band ratioing, histogram equalization, and high-pass digital filtering are relatively deficient as stand-alone

techniques of lineament identification. The analysis shows, in fact, that these enhancements, by themselves, actually hinder the lineament interpretation procedure rather than assist it. The unenhanced data results in the detection of more lineaments than do any of these three enhancements. Moreover, these enhancements show very poor correspondence to the lineament "standard", in terms of coefficient of similarity. Thus, it can be said that lineament interpretation can be better accomplished on the unenhanced data than through the use of any of the band ratio, histogram equalization, and high-pass filter enhancement techniques by themselves.

A fourth conclusion is that the development of a composite interpretation from the five enhancement interpretations has a positive effect on lineament detection. The composite more closely resembles the "standard" interpretation, in terms of similarity coefficient, than do any of the enhancements alone or the unenhanced data. In addition, more lineaments are identified on the composite than on any of the enhancements.

A fifth conclusion that can be reached is that the techniques of band ratioing, histogram equalization, and high-pass filtering are of value when used as a supplement to the principal components or mean value enhancements. While they are not useful as stand-alone techniques, these enhancements, as shown in the composite analysis, do each

result in the identification of additional lineaments that are undetected by the other enhancements.

A sixth conclusion is that, based upon the composite analysis, the use of the unenhanced data in conjunction with the enhancement composite yields some additional lineament information. This information, however, is not significant enough to cause the interpretation to be any more similar to the "standard" interpretation than is the enhancement composite alone.

Finally, the overall worth of the computer enhancement of Landsat digital data for purposes of lineament detection is, on the basis of this study, somewhat questionable. None of the five enhancements that were tested produced results markedly superior to those obtained from the unenhanced data. Additional testing must be done before any definitive statement can be made in this regard.

Limitations of Study

This study was hampered by two major limitations. As was acknowledged previously, the inherent subjectivity involved in the manual lineament interpretation procedures prevented a completely objective analysis of the different enhancement techniques. This subjectivity must be eliminated before any such comparison can be completely valid.

A second limitation was in the limited number of enhancement techniques applied and evaluated. The choice of

which techniques to be implemented in this research was limited by a number of factors, including: the human time required to develop and program the techniques; the computer time required to implement the techniques; the space required on the computer in which to apply the techniques to the data; and the lack of documentation in the literature in terms of the mechanics involved in various enhancement techniques. In addition, the large amounts of data generated by the enhancements and necessary for the analysis of the techniques dictated that the number of enhancements applied be limited in number. In order to keep the research within a manageable perspective, then, the number of techniques tested was restricted.

Recommendations

The recommendations for further study in the area of the computer enhancement of Landsat data for lineament detection are twofold, both directed toward overcoming the limitations of this study.

First, in order to analyze various interpretation techniques in a completely objective manner, the method of lineament interpretation utilized here must be improved upon. The manual interpretation procedure must be replaced by an automatic procedure, so that the element of human bias can be completely removed from the entire enhancement, interpretation, and analysis sequence. The automatic procedure, termed "line detection" in the literature, might

be accomplished in a variety of ways. Much work in the automatic detection of lines in satellite imagery has been done by VanderBrug (1975, 1976a, 1976b, 1977), who developed computer algorithms to accomplish that goal. Other automatic methods have been reported by Paton (1979), Wang (1977), and Xu, Li, and Flint (1981). Further research should be directed toward applying one of these methods in a comprehensive study of lineament enhancement techniques.

A second recommendation for further research is in the application of enhancement techniques. A wider variety of techniques need to be applied to the lineament enhancement problem. Research is needed on the variation of the direction of illumination. Implementation of a technique such as that described by Fukue, Shimoda, and Sakata (1981), in which an artificial "sun" is created, would make it possible to detect lineaments trending in all directions, rather than merely one or two. Such a technique would most likely yield better results in lineament analyses. Additional work is also needed in applying different types of contrast enhancements, such as Gaussian stretches, and in applying different types and sizes of digital filters.

Concluding Statement

This research provides a basic analysis of the computer enhancement of Landsat digital data for lineament detection purposes. Utilizing the methodologies developed and/or implemented here, in conjunction with the recommendations

suggested above, further research in this area could prove extremely valuable.

LITERATURE CITED

Abrams, Michael J. "Lithologic Mapping." Remote Sensing in Geology. Eds. Barry S. Siegal and Alan R. Gillespie. New York: John Wiley & Sons, 1980, pp. 381-418.

Andrews, Harry C. "Monochrome Digital Image Enhancement." Digital Image Processing. Ed. Harry C. Andrews. New York: Electrical and Electronics Engineers, Inc., 1978a, pp. 284-292.

Andrews, Harry C. "Image Enhancement (Introduction)." Digital Image Processing. Ed. Harry C. Andrews. New York: Electrical and Electronics Engineers, Inc., 1978b, p. 273.

Anuta, Paul E. "Computer-Assisted Analysis Techniques for Remote Sensing Data Interpretation." Geophysics, 42 (1977), 468-481.

Billings, Marland P. Structural Geology. 3rd Ed. Englewood Cliffs, New Jersey: Prentice-Hall, Inc., 1972, p. 208.

Blanchard, W. Anthony. Personal Interview. Center for Applications of Remote Sensing, Stillwater, Oklahoma, January, 1982.

Condit, Christopher D. and Pat S. Chavez, Jr. Basic Concepts of Computerized Digital Image Processing for Geologists. Washington: U. S. Government Printing Office, Geological Survey Bulletin 1462, 1979.

Dictionary of Geological Terms. Revised Ed. Garden City, New York: Anchor Press, 1976, p. 255.

Eberlein, R., G. J. VanderBrug, A. Rosenfeld, L. S. Davis. Edge and Line Detection in ERTS Imagery: A Comparative Study. College Park: University of Maryland Computer Science Center, Technical Report TR-312, 1974.

Fontanel, A., C. Blanchet, C. Lallemand. "Enhancement of Landsat Imagery by Combination of Multispectral Classification and Principal Component Analysis." Proceedings of the NASA Earth Resources Survey Symposium, IB (1975), pp. 991-1012.

Frei, Werner. "Image Enhancement by Histogram Hyperbolization." Digital Image Processing. Ed. Harry C. Andrews. New York: Electrical and Electronics Engineers, Inc., 1978, pp. 293-301.

Fukue, Kiyonari, Haruhisa Shimoda, Toshibumi Sakata. "Complete Lineament Extraction with the Aid of Shadow-Free Landsat Image." 1981 Machine Processing of Remotely Sensed Data Symposium Proceedings, (1981), pp. 94-99.

Gillespie, Alan R. "Digital Techniques of Image Enhancement." Remote Sensing in Geology. Eds. Barry S. Siegal and Alan R. Gillespie. New York: John Wiley & Sons, 1980, pp. 139-226.

Goetz, Alexander F. H. and Lawrence C. Rowan. "Geologic Remote Sensing." Science, 211 (1981), 781-791.

Goetz, Alexander F. H., Fred C. Billingsley, Donald P. Elston, Ivo Lucchita, Eugene M. Shoemaker. "Geologic Applications of ERTS Images on the Colorado Plateau, Arizona." Third Earth Resources Technology Satellite-1 Symposium, I (1973a), pp. 719-744.

Goetz, Alexander F. H., Fred C. Billingsley, Donald P. Elston, Ivo Luccita, Eugene M. Shoemaker. "Preliminary Geologic Investigations in the Colorado Plateau Using Enhanced ERTS Images." Symposium on Significant Results Obtained from the Earth Resources Technology Satellite-1, I (1973b), pp. 403-412.

Gold, D. P., R. R. Parizek, S. A. Alexander. "Analysis and Application of ERTS-1 Data for Regional Geologic Mapping." Symposium on Significant Results Obtained from the Earth Resources Technology Satellite-1, I (1973), pp. 231-245.

Graham, Marcellus H., Ronnie W. Pearson, Benjamin R. Seyfarth, Bobby G. Junkin, Maria T. Kalcik. Earth Resources Laboratory Applications Software. NSTL Station, Mississippi: National Aeronautics and Space Administration, National Space Technology Laboratories, Earth Resources Laboratory, 1980.

Hart, Orville Dorwin. Geology of the Eastern Part of Winding Stair Range, LeFlore County, Oklahoma. Norman: University of Oklahoma, Oklahoma Geological Survey Bulletin 103, 1963.

Hoppin, Richard A. "Structural Interpretations Based on ERTS-1 Imagery, Bighorn Region, Wyoming-Montana." Symposium on Significant Results Obtained from the Earth Resources Technology Satellite-1, I (1973), pp. 531-538.

Huntington, J. F. and A. P. Raiche. "A Multi-Attribute Method for Comparing Geological Lineament Interpretations." Remote Sensing of Environment, 7 (1978), 145-161.

Isachsen, Y. W., R. H. Fakundiny, S. W. Forster. "Evaluation of ERTS Imagery for Spectral Geological Mapping in Diverse Terranes of New York State." Third Earth Resources Technology Satellite-1 Symposium, I (1973), pp. 691-717.

Lamar, D. L. and P. M. Merifield. Application of Skylab and ERTS Imagery to Fault Tectonics and Earthquake Hazards of Peninsular Ranges, Southwestern California. Santa Monica: California Earth Science Corporation, Technical Report 75-2, 1975.

Laboratory for Applications of Remote Sensing, Purdue University. Natural Resource Mapping in Mountainous Terrain by Computer Analysis of ERTS-1 Satellite Data. West Lafayette, Indiana: LARS Information Note 061575, Research Bulletin 919, 1975.

Lattman, Laurence H. "Technique of Mapping Geologic Fracture Traces and Lineaments on Aerial Photographs." Photogrammetric Engineering, 24 (1958), 568-576.

Lee, Keenan, Daniel H. Knepper, Don L. Sawatzky. Geologic Information from Satellite Images. Golden: Colorado School of Mines, Remote Sensing Report 74-3, 1974.

Melton, Frank A. Stereoscopic and Mosaic Aerial-Photograph Study of the Central Ouachita Mountains in Oklahoma and Arkansas. Norman: Oklahoma Geological Survey, 1976.

NASA. Earth Resources Orientation and Training Course in Remote Sensing Technology, Landsat Series. NSTL Station, Mississippi: National Aeronautics and Space Administration, National Space Technology Laboratories, Earth Resources Laboratory, 1979.

Offield, Terry W., Elsa A. Abbott, Alan R. Gillespie, Sabino O. Loguercios. "Structural Mapping on Enhanced Landsat Images of Southern Brazil: Tectonic Control of Mineralization and Speculations on Metallogeny." Geophysics, 42 (1977), 482-500.

O'Leary, D. W., J. D. Friedman, H. A. Pohn. "Lineament, Linear, Lineation: Some Proposed New Standards for Old Terms." Geological Society of America Bulletin, 87 (1976), 1463-1469.

Paton, Keith. "Line Detection by Local Methods." Computer Graphics and Image Processing, 9 (1979), 316-332.

Podwysocki, Melvin H. and Paul D. Lowman, Jr. Fortran IV Programs for Summarization and Analysis of Fracture Trace and Lineament Patterns. Greenbelt, Maryland: Goddard Space Flight Center, NASA TMX-70596, 1974.

Podwysocki, Melvin H., Johannes G. Moik, Walter C. Shoup. "Quantification of Geologic Lineaments by Manual and Machine Processing Techniques." Proceedings of the NASA Earth Resources Survey Symposium, IB (1975), pp. 885-903.

Rowan, Lawrence C. and Pamela H. Wetlaufer. "Structural Geologic Analysis of Nevada Using ERTS-1 Images: A Preliminary Report." Symposium on Significant Results Obtained from the Earth Resources Technology Satellite-1, I (1973), pp. 413-423.

Rowan, Lawrence C. and Pamela H. Wetlaufer. Iron-Absorbtion Band Analysis for the Discrimination of Iron-Rich Zones. Washington: U. S. Government Printing Office, Geological Survey, Type III Final Report, Contract S-70243-AG, 1975.

Rowan, Lawrence C, Pamela H. Wetlaufer, F. C. Billingsley, Alexander F. H. Goetz. "Mapping of Hydrothermal Alternation Zones and Regional Rock Types Using Computer Enhanced ERTS MSS Images." Third Earth Resources Technology Satellite-1 Symposium, I (1973), p. 807.

Sabins, Floyd F., Jr. Remote Sensing, Principles and Interpretation. San Francisco: W. H. Freeman and Company, 1978.

Short, N. M. and P. D. Lowman, Jr. Earth Observations from Space: Outlook for the Geological Sciences. Greenbelt, Maryland: Goddard Space Flight Center, NASA X-650-73-316, 1973.

Siegal, Barry S. "Significance of Operator Variation and the Angle of Illumination in Lineament Analysis on Synoptic Images." Modern Geology, 6 (1977), 75-85.

Taranik, James V. Principles of Computer Processing of Landsat Data for Geologic Applications. Sioux Falls, South Dakota: U. S. Geological Survey, Open File Report 78-117, 1978.

Thomas, Valerie L. Generation and Physical Characteristics of the LANDSAT 1 and 2 MSS Computer Compatible Tapes. Greenbelt, Maryland: Goddard Space Flight Center, 1975.

VanderBrug, Gordon J. "Semilinear Line Detectors." Computer Graphics and Image Processing, 4 (1975), 287-293.

VanderBrug, Gordon J. "Experiments in Iterative Enhancement of Linear Features." 1976 Machine Processing of Remotely Sensed Data Symposium Proceedings, (1976a), pp. 4a-32 - 4a-44.

VanderBrug, Gordon J. "Line Detection in Satellite Imagery." IEEE Transactions on Geoscience Electronics, GE-14 (1976b), 37-44.

VanderBrug, Gordon J. "Linear Feature Detection and Mapping." (Ph.D. dissertation, University of Maryland, 1977.)

Vincent, Robert K. "Ratio Maps of Iron Ore Deposits, Atlantic City District, Wyoming." Symposium on Significant Results Obtained from the Earth Resources Technology Satellite-1, I (1973), pp. 379-386.

Walsh, Stephen J. "An Investigation into the Comparative Utility of Color Infrared Aerial Photography and LANDSAT Data for Detailed Surface Cover Type Mapping within Crater Lake National Park, Oregon." (Unpublished Ph.D. dissertation, Oregon State University, 1977.)

Wang, John Y. C. "Feature Extraction by Interactive Image Processing." Photogrammetric Engineering and Remote Sensing, 43 (1977), 1495-1501.

Wobber, Frank J. and Kenneth R. Martin. "Exploitation of ERTS-1 Imagery Utilizing Snow Enhancement Techniques." Symposium on Significant Results Obtained from the Earth Resources Technology Satellite-1, I (1973), pp. 345-351.

Xu, S. R., C. C. Li, N. K. Flint. "Extraction of Geological Lineaments from Landsat Imagery by Using Local Variance and Gradient Trend." 1981 Machine Processing of Remotely Sensed Data Symposium Proceedings, (1981), pp. 113-117.

APPENDIX

```
C
C
C            ****************************************
C                 VECTOR   TRANSFORM   PROGRAM
C            ****************************************
C
C       THE PROGRAM WAS WRITTEN BY MELVIN PODWYSOCKI OF THE
C       GEOSCIENCES DEPT., THE PENNSYVANIA STATE UNIVERSITY,
C       APRIL, 1972 FOR USE ON THE IBM 360/67 COMPUTER, AND WAS
C       MODIFIED IN APRIL, 1973 FOR USE ON OTHER COMPUTERS HAVING
C       THE EQUIVALENT CORE STORAGE OF 78K BYTES.
C
C     PROGRAM CALCULATES VECTOR LENGTH (VECLEN), AZIMUTH (VECAZM),
C     SLOPE (A), Y INTERCEPT (B) AND X & Y MIDPOINTS (XMID & YMID)
C     FOR EACH VECTOR GIVEN ITS BEGINNING (X1,Y1) AND END (X2,Y2)
C     POINTS IN MAP SPACE.  PROGRAM ASSUMES X IS + TOWARDS THE
C     RIGHT AND Y IS + DOWNWARD.  DUE NORTH-SOUTH AND EAST-WEST
C     DATA ARE TREATED AS SPECIAL CASES.  CONTROL CARDS ARE READ
C     FROM THE CARD READER WHILE DATA CARDS ARE READ FROM ANY UNIT
C     DECLARED BY 'ITAPE1' ON CONTROL CARD 3.  DATA CARDS ARE
C     GENERATED ON ANY UNIT DECLARED BY 'ITAPE2' IN A FORMAT
C     ACCEPTABLE TO "AZMAP" PROGRAM.  COORDINATES MUST BE IN
C     MILLIMETERS, IF NOT, CONTROL CARD 3 ALLOWS A TRANSFORMATION
C     TO BE PERFORMED.  PRINTED OUTPUT IS ALSO PRODUCED.
C
C                      (0,0)       X + ---->
C                        ------------------------
C                        |
C                        |
C                        |                              NORTH
C                      Y |
C                        |                               A
C                      + |          ALL VECTORS          |
C                        |          LIE IN THIS          |
C                      | |             AREA
C                      | |
C                      V |
C                        |
C                        |
C
C     ALL NUMERIC INPUT DATA IS RIGHT JUSTIFIED: "I" INDICATES
C     INTEGER FORMAT, "F" INDICATES FLOATING POINT FORMAT, "A"
C     INDICATES CHARACTER FORMAT, "#" PRECEDING NUMBERS INDICATES
C     COLUMNS USED FOR EACH PARAMETER.  TO SPECIFY NONUSE OF AN
C     OPTION, PUNCH 0 OR LEAVE BLANK.
C
C ********CONTROL CARD 1------TITLE CARD
C     TITLE WILL BE PRINTED AT BEGINNING OF PRINTED OUTPUT
C     (20A4,#1-80)
C ********CONTROL CARD 2------VARIABLE INPUT FORMAT CARD
C     TO READ X & Y VALUES FROM CARDS, FORMAT MUST BE ENCLOSED IN
C     PARENTHESES AND BEGIN IN #1. VALUES SHOULD BE READ IN THE
C     FOLLOWING ORDER: X1,Y1,X2,Y2 (20A4,#1-80)
C ********CONTROL CARD 3------OPTIONS CARD
C     ITAPE1=LOGICAL UNIT FOR READING DATA CARDS (I2,#1,2)
C     ITAPE2=LOGICAL UNIT FOR WRITING OUTPUT USEABLE BY "AZMAP"
C        (I2,#3,4)
C     NPRINT--PRINT COMMAND FOR OUTPUT (I1,1 IN #5)
C     NPUNCH--PUNCH COMMAND FOR OUTPUT ACCORDING TO FORMAT FOR
```

```
C        "AZMAP" PROGRAM ON ANY UNIT DECLARED BY 'ITAPE2'
C        (I1,1 IN #6)
C     NTRAN--TRANSFORMATION COMMAND TO CONVERT UNITS OF INPUT DATA
C        TO MILLIMETERS (I1,1 IN #7)
C     NOTE: THE FOLLOWING PARAMETER IS USED ONLY IF 'NTRAN' IS
C        PUNCHED 1. UNITS WILL BE CONVERTED TO MILLIMETERS FOR USE
C        IN "AZMAP". CONVERTED COORDINATE VALUE = ORIGINAL VALUE *
C        'CONV'
C     CONV=TRANSFORMATION FACTOR TO CONVERT UNITS ON INPUT DATA
C        TO MILLIMETERS (F6.2,#8-13)
C ********DATA CARDS-----
C     READ FROM ANY UNIT DECLARED BY 'ITAPE1'. END OF DATA CARDS
C        IS SIGNIFIED WHEN THE PROGRAM ENCOUNTERS A CARD WHOSE
C        VALUES OF X1,Y1.X2 & Y2 ARE ALL 0.0
C
 1        DIMENSION FMTRD(18),TITLE(18)
 2        DATA IREAD/10/,IPRINT/6/
C
C     READ CONTROL CARDS
C
 3        READ(IREAD,5)  (TITLE(L),L=1,18)
 4        READ(IREAD,5)  (FMTRD(L),L=1,18)
 5        READ(IREAD,7)  ITAPE1,ITAPE2,NPRINT,NPUNCH,NTRAN,CONV
 6        WRITE(IPRINT,9)  (TITLE(L),L=1,18),(FMTRD(L),L=1,18)
 7        IF(NTRAN.EQ.1) WRITE(IPRINT,10) CONV
 8        IF(NPRINT.EQ.1) WRITE(IPRINT,11)
C
C      READ X & Y COORDINATES FROM UNIT 'ITAPE1'
C
 9        NUM=0
10     12 READ(ITAPE1,FMTRD)  X1,Y1,X2,Y2
11        IF(X1.EQ.0..AND.Y1.EQ.0..AND.X2.EQ.0..AND.Y2.EQ.0.) GO TO 10
         *0
12        NUM=NUM+1
C
C     CONVERT DATA TO MILLIMETERS IF NECESSARY
C
13        IF(NTRAN) 20,20,15
14     15 X1=X1*CONV
15        Y1=Y1*CONV
16        X2=X2*CONV
17        Y2=Y2*CONV
C
C     ORDER BEGINNING AND END COORDINATES FOR "AZMAP" PROGRAM
C
18     20 IF(Y1.EQ.Y2.AND.X1.LT.X2) GO TO 22
19        IF(Y1-Y2) 21,23,23
20     21 Z2=Y2
21        Y2=Y1
22        Y1=Z2
23     22 Z1=X2
24        X2=X1
25        X1=Z1
C
C     CALCULATE VECLEN
C
26     23 VECLEN=SQRT(((X2-X1)**2)+((Y2-Y1)**2))
C
C     CALCULATE SLOPE 'A'
C
```

```
27          IF(X2-X1) 24,25,24
28       24 A=(Y2-Y1)/(X2-X1)
29          GO TO 30
30       25 A=-573.0
31          VECAZM=0.0
32          B=500000.
33          GO TO 50
      C
      C     CALCULATE VECAZM
      C
34       30 IF(A) 35,33,33
35       33 VECAZM=270.0 + ((ATAN(A)*180.)/3.14159)
36          GO TO 40
37       35 VECAZM=90. - ((ATAN(ABS(A))*180.)/3.14159)
      C
      C     CACULATE Y INTERCEPT 'B'
      C
38       40 B=(((Y1-Y2)*X2)/(X2-X1))+Y2
      C
      C     CALCULATE MIDPOINT OF VECTOR
      C
39       50 XMID=(X2+X1)/2.0
40          YMID=(Y2+Y1)/2.0
      C
      C     OUTPUT
      C
41          IF(NPRINT) 75,75,62
42       62 WRITE(IPRINT,65) X1,Y1,X2,Y2,VECLEN,VECAZM,A,B,XMID,YMID
43       75 IF(NPUNCH) 12,12,77
44       77 WRITE(ITAPE2,80) X1,Y1,X2,Y2,VECLEN,VECAZM,A,B,XMID,YMID
45          GO TO 12
46      100 WRITE(IPRINT,105) NUM
47        5 FORMAT (20A4)
48        7 FORMAT (2I2,3I1,F6.2)
49        9 FORMAT ('1',20A4/,'0','VARIABLE INPUT FORMAT FOR X & Y IS ',
         *20A4)
50       10 FORMAT ('0','ALL VALUES WILL BE MULTIPLIED BY A FACTOR OF ',
         *F12.5)
51       11 FORMAT ('0',4X,'X1',11X,'Y1',11X,'X2',11X,'Y2',9X,'VECLEN',
         *5X,'VECAZM',9X,'A',13X,'B',12X,'XMID',9X,'YMID'//)
52       65 FORMAT (' ',5(F7.1,6X),F5.1,6X,F8.3,6X,F9.1,2(6X,F7.1))
53       80 FORMAT (6F6.1,F9.4,F10.1,2F7.1)
54      105 FORMAT ('0','NUMBER OF VECTORS = ',I10)
55          STOP
56          END
```

```
C
C
C                    ****************************
C                          AZMAP       PROGRAM
C                    ****************************
C
C       THE PROGRAM WAS WRITTEN BY MELVIN PODWYSOCKI OF THE
C       GEOSCIENCES DEPT., THE PENNSYLVANIA STATE UNIVERSITY,
C       APRIL, 1972 FOR THE IBM 360/67 COMPUTER, AND WAS
C       MODIFIED IN APRIL, 1973 FOR USE ON OTHER COMPUTERS
C       HAVING THE EQUIVALENT OF 160K BYTES STORAGE.
C
C     PROGRAM SUMMARIZES FREQUENCY DISTRIBUTIONS OF VECTOR DATA IN
C     VARIABLE MAP GRID AND AZIMUTH CLASS SIZES. PROGRAM ALLOWS UP
C     TO 90 AZIMUTH CLASSES, FROM 270 THRU 0 TO 90 DEGREES,
C     SUMMARIZING DATA AS TOTAL LENGTH OF VECTORS/AZIMUTH CLASS
C     (DENSITY) OR NUMBER OF VECTORS/AZIMUTH CLASS (FREQUENCY).
C     UP TO 2000 VECTORS MAY BE USED. X AXIS IS + TO RIGHT & Y
C     AXIS IS + DOWNWARD. DATA ARE READ FROM CARDS GENERATED BY
C     VECTOR TRANSFORM PROGRAM. CONTROL AND TITLE CARDS ARE READ
C     FROM CARD READER WHILE DATA CARDS MAY BE READ FROM ANY UNIT
C     DECLARED BY 'ITAPE2' ON CONTROL CARD 1.
C
C     ALL NUMERIC INPUT DATA IS RIGHT JUSTIFIED: "I" INDICATES
C     INTEGER FORMAT, "F" INDICATES FLOATING POINT FORMAT, "A"
C     INDICATES CHARACTER FORMAT, "#" PRECEDING NUMBERS
C     INDICATES COLUMNS USED FOR EACH PARAMETER. TO SPECIFY
C     NONUSE OF AN OPTION, PUNCH 0 OR LEAVE BLANK.
C
C ********CONTROL CARD 1------OPTIONS CARD
C     XINC=INCREMENT OF X-AXIS TRAVERSE IN MILLIMETERS (I4,#1-4)
C     YINC=INCREMENT OF Y-AXIS TRAVERSE IN MILLIMETERS (I4,#5-8)
C     XSTART=STARTING POINT FOR X-AXIS TRAVERSE IN MILLIMETERS
C        (I4,#9-12)
C     YSTART=STARTING POINT FOR Y-AXIS TRAVERSE IN MILIMETERS
C        (I4,#13-16)
C     XSTOP=END OF X-AXIS TRAVERSE IN MILLIMETERS (I4,#17-20)
C     YSTOP=END OF Y-AXIS TRAVERSE IN MILLIMETERS (I4,#21-24)
C        NOTE: PROGRAM SUCCESSIVELY SCANS DATA IN MAP GRID CELLS
C        'XCELL' BY 'YCELL' IN SIZE, INCREMENTING BY 'XINC'
C        UNTIL 'XMAX' > 'XSTOP', WHEN 'YINC' IS INCREMENTED.
C        PROGRAM TERMINATES WHEN 'YMAX' > 'YSTOP'. NONE OF THE
C        ABOVE 6 VALUES CAN BE NEGATIVE.
C     AZCLAS=AZIMUTH CLASS WIDTH IN DEGREES (F3.1,#25-27)
C     AMPSCL=MAPSCALE IN UNITS/SCALE; SEE SCALE PARAM. BELOW
C        (F5.4,#28-32)
C     KTYPE--SELECTS SUBROUTINE FOR CLASSIFYING VECTOR DATA
C        (I2,#33-34)
C        PUNCH 1 FOR SUBR. PART. CONSIDERS ONLY THAT PART OF
C        VECTOR WHICH LIES WITHIN THAT CELL.
C        PUNCH -1 FOR SUBR. MID. CONSIDERS WHOLE VECTOR IN CELL
C        IF ITS MIDPOINT FALLS WITHIN THAT CELL.
C     NDHIST--PRINT COMMAND FOR DENSITY HISTOGRAM (I1,1 IN #35)
C     NFHIST--PRINT COMMAND FOR FREQUENCY HISTOGRAM (I1,1 IN #36)
C     NPUNCH--PUNCHED CARD OUTPUT FOR EACH GRID CELL AZIMUTH
C        DISTRIBUTION IS GENERATED AS PER CONTROL CARD 3 BELOW
C        (I1,1 IN #37)
C     DHINC=NUMERICAL VALUE OF EACH 'X' INCREMENT (ACCORDING TO
C        SCALE PARAMETER; SEE BELOW) FOR DENSITY HISTOGRAM
```

```
C        (F5.2,#38-42)
C     NFHINC=NUMERICAL VALUE OF EACH '*' INCREMENT FOR FREQUENCY
C        HISTOGRAM (I3,#43-45)
C     SCALE=SCALE UNITS FOR PRINTOUT I.E. MILES, MM., ETC.),
C        (2A4,#46-53)
C        NOTE: WHEN VECTORS ARE MEASURED ON A 1:24000 SCALE MAP
C        AND OUTPUT IS DESIRED IN MILES, 'AMPSCL'=.0149 (I.E.
C        1 MM.=.0149 MILES)
C     ITAPE1=LOGICAL UNIT FOR READING DATA CARDS GENERATED BY
C        "TRANSFORM" PROGRAM (I2,#54-55)
C     NCHI--COMMAND TO TEST FREQUENCY AND DENSITY DATA FOR
C        RANDOMNESS IN EACH GRID CELL (I1, 1 IN #60)
C     XCELL=CELL SIZE IN X DIRECTION (I4,#61-64)
C     YCELL=CELL SIZE IN Y DIRECTION (I4,#65-68)
C     NUM=NUMBER OF VECTORS (AS GIVEN IN TRANSFORM PROGRAM)
C        (I4,#69-72)
C ********CONTROL CARD 2------ TITLE CARD
C     TITLE WILL BE PRINTED AT TOP OF EACH HISTOGRAM (20A4,
C        #1-80)
C ********CONTROL CARD 3------VARIABLE OUTPUT FORMAT CARD
C     TO BE USED ONLY IF NPUNCH (CONTROL CARD 1) IS PUNCHED 1
C     PUNCHED OUTPUT WILL CONSIST OF A CELL ROW, COLUMN, X & Y
C        MIDPOINTS OF CELL, AND THE VALUE OF EACH AZIMUTH CLASS
C        SUMMATION AS PER VARIABLE 'ITYPE'. THE FOLLOWING
C        FORMAT IS SUGGESTED:
C                 (2I4,2F7.2,7F7.2/10F7.2/1F7.2)
C        NOTE: THE LAST SET OF VARIABLES MUST CORRESPOND TO THE
C        NUMBER OF AZIMUTH CLASSES (I.E. 180./'AZCLAS' =
C        NUMBER OF CLASSES).
C        IN THE ABOVE EXAMPLE IT'S 18. FOR DENSITY DATA IT SHOULD
C        BE AS ABOVE, BUT IN INTEGER FORMAT, I.E. (.........,
C        8I5/10I5)
C     FMTPCH--OUTPUT FORMAT FOR AZIMUTH CLASS DATA. MUST BE
C        ENCLOSED IN PARENTHESES AND START IN #1. (18A4, #1-72)
C ********CONTROL CARD 4------DATA SUMMARIZATION TYPE CARD
C     ITYPE--PUNCH 2 FOR DENSITY DATA (TOTAL LENGTH/AZIMUTH CLASS)
C        PUNCH 1 FOR FREQUENCY DATA (NUMBER OF VECTORS/AZIMUTH
C        CLASS)
C        OUTPUT WILL BE IN UNITS SPECIFIED BY 'AMPSCL' AND 'SCALE'
C        (I1,#77)
C ********DATA CARDS-----
C     VECTOR DATA INPUT FROM VECTOR TRANSFORM PROGRAM
C
C
1       DIMENSION TITLE(20),SCALE(2),FMTPCH(18),Z3(90)
2       COMMON X1(2000),Y1(2000),X2(2000),Y2(2000),VECAZM(2000),VECL
       *EN(2000),A(2000),B(2000),XMID(2000),YMID(2000),CLAMIN(90),CL
       *AMAX(90),AZLEN(90),NAZFRQ(90),XMIN,YMIN,XMAX,YMAX,FLAG,VLEN,
       *INUM
3       INTEGER XSTOP,YSTOP,XINC,YINC,XSTART,YSTART,XMIN,YMIN,XMAX,Y
       *MAX,FLAG,XCELL,YCELL
4       DATA IXS/1HX/,ISTARS/1H*/,IREAD/9/,IPRINT/6/,IPUNCH/10/
C
C     READ CONTROL INPUT INFORMATION AND TITLE CARD
C
5       READ(IREAD,5) XINC,YINC,XSTART,YSTART,XSTOP,YSTOP,AZCLAS,AMP
       *SCL,KTYPE,NDHIST,NFHIST,NPUNCH,DHINC,NFHINC,(SCALE(L),L=1,2)
       *,ITAPE1,NCHI,XCELL,YCELL,NUM
6       READ(IREAD,6) (TITLE(L),L=1,20)
7       IF(NPUNCH.EQ.1) READ(IREAD,7) (FMTPCH(L),L=1,18),ITYPE
```

```
 8          Z1=XCELL*AMPSCL
 9          Z2=YCELL*AMPSCL
10          IF(KTYPE) 19,9,19
11        9 WRITE(IPRINT,10)
12          STOP
      C
      C     READ DATA GENERATED BY VECTOR TRANSFORM PROGRAM
      C
13       19 DO 25 I=1,NUM
14          READ(ITAPE1,20) X1(I),Y1(I),X2(I),Y2(I),VECLEN(I),VECAZM(I),
           *A(I),B(I),XMID(I),YMID(I)
      C     WRITE(6,21) X1(I),Y1(I),X2(I),Y2(I),VECLEN(I),VECAZM(I),
      C    *A(I),B(I),XMID(I),YMID(I)
15       25 CONTINUE
      C
      C     GENERATE AZIMUTH CLASSES
      C
16       30 CLAMIN(1)=270.0
17          I=1
18          NCLASS=1
19          CLAMAX(I)=CLAMIN(I)+AZCLAS
20       40 IF(CLAMAX(I).GT.270.0.AND.CLAMAX(I).LE.360.0) GO TO 41
21          IF(CLAMAX(I)-90.0) 41,60,60
22       41 I=I+1
23          NCLASS=I
24          CLAMIN(I)=CLAMAX(I-1)
25          CLAMAX(I)=CLAMIN(I)+AZCLAS
26          IF(CLAMAX(I)-360.0) 40,50,50
27       50 NCLASS=I+1
28          I=NCLASS
29          CLAMIN(I)=CLAMAX(I-1)-360.0
30          CLAMAX(I)=CLAMIN(I)+AZCLAS
31          GO TO 40
      C
      C     SCAN AND SUMMARIZE DATA FOR EACH GRID CELL
      C
32       60 DO 300 YMIN=YSTART,YSTOP,YINC
33          YMAX=YMIN+YCELL
34          IF(YMAX-YSTOP) 62,62,400
35       62 DO 300 XMIN=XSTART,XSTOP,XINC
36          XMAX=XMIN+XCELL
37          IF(XMAX-XSTOP) 64,64,300
38       64 DO 65 L=1,90
39          AZLEN(L)=0.
40       65 NAZFRQ(L)=0
41          WVLEN=0.
42          NEWFRQ=0
43          DO 170 I=1,NUM
44          INUM=I
45          FLAG=0
46          IF(KTYPE)68,9,66
47       66 CALL PART
48          GO TO 69
49       68 CALL MID
50       69 IF(FLAG)70,75,70
      C
      C     TEST FOR F - W DATA
      C
51       70 IF(VECAZM(I)-270.) 76,71,76
52       71 IF(FLAG)72,170,73
```

```
53       72 WVLEN=WVLEN+VECLEN(I)
     C      WRITE(6,23) VECLEN(I),WVLEN
     C   23 FORMAT(1HO,'VECLEN= ',F6.1,2X,'WVLEN= ',F6.1)
54          GO TO 74
55       73 WVLEN=WVLEN+VLEN
56       74 NEWFRQ=NEWFRQ+1
     C
     C      ADD RESULTS TO APPROPRIATE AZIMUTH CLASS
     C
57       75 IF(I-NUM) 170,78,78
58       76 IF(I-NUM) 82,78,78
59       78 IF(AZLEN(1)-AZLEN(NCLASS)) 79,80,80
60       79 AZLEN(NCLASS)=AZLEN(NCLASS)+WVLEN
61          NAZFRQ(NCLASS)=NAZFRQ(NCLASS)+NEWFRQ
62          GO TO 81
63       80 AZLEN(1)=AZLEN(1)+WVLEN
64          NAZFRQ(1)=NAZFRQ(1)+NEWFRQ
65       81 IF(VECAZM(I).NE.270..AND.FLAG.NE.0.AND.I.EQ.NUM) GO TO 82
66          GO TO 170
67       82 DO 85 J=1,NCLASS
68          IF(VECAZM(I).GE.CLAMIN(J).AND.VECAZM(I).LT.CLAMAX(J)) GO TO
           *84
69          GO TO 85
70       84 NTYPE=J
71          GO TO 90
72       85 CONTINUE
73       90 IF(FLAG)100,170,150
74      100 AZLEN(NTYPE)=AZLEN(NTYPE)+VECLEN(I)
75          GO TO 160
76      150 AZLEN(NTYPE)=AZLEN(NTYPE)+VLEN
77      160 NAZFRQ(NTYPE)=NAZFRQ(NTYPE)+1
78      170 CONTINUE
     C
     C      OUTPUT
     C
79          TOTLN=0.
80          NFRQ=0
81          NXERR=0
82          NASTER=0
83          DO 180 N=1,NCLASS
84          TOTLN=TOTLN+AZLEN(N)
85          NFRQ=NFRQ+NAZFRQ(N)
86      180 CONTINUE
     C
     C      TEST FOR RANDOMNESS OF AZIMUTH DISTRIBUTIONS/CELL BY CHI
     C      SQUARE
     C
87          IF(NCHI) 184,184,181
88      181 CLASS=NCLASS
89          FRQ=NFRQ
90          DENEXP=TOTLN/CLASS
91          FRQEXP=FRQ/CLASS
92          DCS=0.
93          FCS=0.
94          DO 182 LCS=1,NCLASS
95          DCS=DCS+((AZLEN(LCS)-DENEXP)**2)/DENEXP
96          FCS=FCS+((NAZFRQ(LCS)-FRQEXP)**2)/FRQEXP
97      182 CONTINUE
98          NDF=NCLASS-1
99          DCHPRB=PRBCHI(DCS,NDF)
```

```
100         FCHPRB=PRBCHI(FCS,NDF)
      C
      C     PRINT DATA FOR EACH CELL
      C
101     184 NROW=(YMIN+YINC)/YINC
102         NCOL=(XMIN+XINC)/XINC
103         GXMID=(XMIN+XMAX)/2.
104         GYMID=(YMIN+YMAX)/2.
105         WRITE(IPRINT,185) (TITLE(L),L=1,20)
106         WRITE(IPRINT,186) XCELL,Z1,(SCALE(L),L=1,2),YCELL,Z2,(SCALE(
           *L),L=1,2)
107         IF(KTYPE) 195,9,196
108     195 WRITE(IPRINT,188)
109         GO TO 198
110     196 WRITE(IPRINT,187)
111     198 WRITE(IPRINT,190) NROW,NCOL,XMIN,XMAX,YMIN,YMAX
112         WRITE(IPRINT,200) (SCALE(L),L=1,2)
113         DO 230 I=1,NCLASS
114         Z3(I)=AZLEN(I)*AMPSCL
115         WRITE(IPRINT,205) CLAMIN(I),CLAMAX(I),Z3(I),NAZFRQ(I)
116         IF(NDHIST)220,220,214
117     214 NUMX=Z3(I)/DHINC
118         IF(NUMX)217,215,217
119     215 WRITE(IPRINT,216)
120         GO TO 220
121     217 IF(NUMX-50)219,219,218
122     218 NUMX=50
123     219 WRITE(IPRINT,286) (IXS,IUKA=1,NUMX)
124     220 IF(NFHIST)230,230,221
125     221 NUMAST=NAZFRQ(I)/NFHINC
126         IF(NUMAST)224,222,224
127     222 WRITE(IPRINT,223)
128         GO TO 230
129     224 IF(NUMAST-43)226,226,225
130     225 NUMAST=43
131         NASTER=1
132     226 WRITE(IPRINT,287) (ISTARS,LIBRAL=1,NUMAST)
133     230 CONTINUE
      C
      C     PUNCH CARD OUTPUT AS PER CONTROL CARD 2A
      C
134         IF(NPUNCH) 252,252,234
135     234 IF(ITYPE-1) 330,238,236
136     236 WRITE(IPUNCH,FMTPCH) NROW,NCOL,GXMID,GYMID,(Z3(KQA),KQA=1,NC
           *LASS)
137         GO TO 252
138     238 WRITE(IPUNCH,FMTPCH) NROW,NCOL,GXMID,GYMID,(NAZFRQ(KQA),KQA=
           *1,NCLASS)
      C
      C     PRINT SUMMARY DATA FOR EACH CELL
      C
139     252 WRITE(IPRINT,240)
140         TLENM=TOTLN*AMPSCL
141         WRITE(IPRINT,250) TLENM,NFRQ
142         IF(NDHIST)270,270,260
143     260 WRITE(IPRINT,265) DHINC,(SCALE(L),L=1,2)
144         IF(NXERR.EQ.1) WRITE(IPRINT,290)
145     270 IF(NFHIST)296,296,280
146     280 WRITE(IPRINT,285) NFHINC
147         IF(NASTER.EQ.1) WRITE(IPRINT,295)
```

```
148      296 IF(NCHI.EQ.1) WRITE(IPRINT,297) DCHPRB,FCHPRB
149      300 CONTINUE
150        5 FORMAT(6I4,F3.1,F5.4,I2,3I1,F5.2,I3,2A4,I2,4X,I1,3I4)
151        6 FORMAT(20A4)
152        7 FORMAT(18A4/I1)
153       10 FORMAT('1',30X,'NEITHER SUMMARIZATION TECHNIQUE (PART OR ',
             *'MID) WAS SPECIFIED.*****JOB ABORTED*****')
154       20 FORMAT(6F6.1,F9.4,F10.1,2F7.1)
      C   21 FORMAT(1H0,'DATA READ FROM TAPE ARE: ',6F6.1,F9.4,F10.1,2F7.1)
155      185 FORMAT('1',20X,20A4)
156      186 FORMAT('0',20X,'EACH GRID CELL IS ',I4,' MM. (',F7.3,2A4,
             *') BY ',I4,' MM. (',F7.3,2A4,')')
157      187 FORMAT('0',20X,'PROGRAM USES SUBROUTINE PART; CONSIDERS ',
             *'ONLY THAT PORTION OF EACH VECTOR WITHIN THE CELL')
158      188 FORMAT('0',15X,'PROGRAM USES SUBROUTINE MID; CONSIDERS ',
             *'WHOLE VECTOR AS BEING WITHIN CELL IF ITS MIDPOINT FALLS ',
             *'IN THE CELL')
159      190 FORMAT('0','GRID CELL NUMBER: ROW ',I4,', COLUMN ',I4,
             *' (',I4,' <X< ',I4,'; ',I4,' <Y< ',I4,')')
160      200 FORMAT('0',/,'  AZIMUTHS',4X,'CLASS LENGTH (IN',2A4,')',37X,
             *'NUMERICAL FREQUENCY',/,2X,'--------',4X,'------------',
             *'------------',37X,'--------------------')
161      205 FORMAT(' ',F5.1,'-',F5.1,2X,F8.2,57X,I4)
162      216 FORMAT('+',24X,'>')
163      223 FORMAT('+',87X,'>')
164      240 FORMAT(' ',14X,'-------',58X,'----')
165      250 FORMAT('0',5X,'TOTALS',2X,F8.2,56X,I5)
166      265 FORMAT('+',28X,'EACH X = ',F7.2,1X,2A4)
167      285 FORMAT('+',95X,'EACH * = ',I4,' UNITS')
168      286 FORMAT('+',24X,'>',50A1)
169      287 FORMAT('+',87X,'>',43A1)
170      290 FORMAT(' ','ONE OR MORE DENSITY HISTOGRAM CLASSES EXCEED ',
             *'LIMITS ALLOWED')
171      295 FORMAT(' ','ONE OR MORE FREQUENCY HISTOGRAM CLASSES ',
             *'EXCEED LIMITS ALLOWED')
172      297 FORMAT('0',13X,'RANDOMLY DISTRIBUTED DENSITY DATA PROB. = ',
             *F10.4,12X,'RANDOMLY DISTRIBUTED FREQ. DATA PROB. = ',F10.4)
173      315 FORMAT('1',30X,'"ITYPE" FOR PUNCHED OUTPUT NOT IN ',
             *'SPECIFIED RANGE.*****JOB ABORTED*****')
174      330 WRITE(IPRINT,315)
175      400 STOP
176          END
```

```
177           SUBROUTINE PART
      C
      C       SUBROUTINE 'PART' DETERMINES IF A VECTOR FALLS WITHIN A GRID
      C       CELL, AND IF SO, THE LENGTH OF THE PORTION WITHIN THE CELL.
      C
178           COMMON X1(2000),Y1(2000),X2(2000),Y2(2000),VECAZM(2000),VECL
             *EN(2000),A(2000),B(2000),XMID(2000),YMID(2000),CLAMIN(90),CL
             *AMAX(90),AZLEN(90),NAZFRQ(90),XMIN,YMIN,XMAX,YMAX,FLAG,VLEN,
             *I
179           INTEGER YMIN,XMIN,YMAX,XMAX,FLAG
180           REAL MINLEN
181           DATA IREAD/9/,IPRINT/6/,MINLEN/1.0/
      C
      C       DETERMINES IF WHOLE VECTOR IS WITHIN GRID CELL
      C
      C       ANY VECTOR < MINLEN (IN MM.) WILL NOT BE COUNTED
      C
182           IF(X1(I).GE.XMIN.AND.X1(I).LE.XMAX.AND.Y1(I).GE.YMIN.AND.Y1(
             *I).LE.YMAX.AND.X2(I).GE.XMIN.AND.X2(I).LE.XMAX.AND.Y2(I).GE.
             *YMIN.AND.Y2(I).LE.YMAX) GO TO 1
183           GO TO 2
184         1 FLAG=-1
185           RETURN
186         2 IF(A(I)) 3,20,3
187         3 IF(A(I).LE.-573..AND.X1(I).GE.XMAX) GO TO 422
188           IF(X1(I).EQ.XMAX.AND.A(I).GT.0.) GO TO 20
189           IF(X1(I).GE.XMIN.AND.X1(I).LT.XMAX.AND.Y1(I).GE.YMIN.AND.Y1(
             *I).LT.YMAX) GO TO 100
190           IF(X2(I).GE.XMIN.AND.X2(I).LT.XMAX.AND.Y2(I).GE.YMIN.AND.Y2(
             *I).LT.YMAX) GO TO 200
191           GO TO 300
192        20 IF(X1(I).GE.XMIN.AND.X1(I).LE.XMAX.AND.Y1(I).GE.YMIN.AND.Y1(
             *I).LT.YMAX) GO TO 100
193           IF(X2(I).GE.XMIN.AND.X2(I).LE.XMAX.AND.Y2(I).GE.YMIN.AND.Y2(
             *I).LT.YMAX) GO TO 200
194           GO TO 300
      C
      C       CALCULATES VECLEN WHEN VECTOR ORIGIN IS WITHIN GRID CELL
      C
195       100 IF(A(I))102,101,102
196       101 VLEN=X1(I)-XMIN
197           FLAG=1
198           RETURN
199       102 IF(X1(I).EQ.XMIN.AND.A(I).GT.0.) RETURN
200           Y=A(I)*XMIN+B(I)
201           IF(Y.LE.Y1(I).AND.Y.GE.Y2(I)) GO TO 105
202           GO TO 120
203       105 IF(Y.GE.YMIN.AND.Y.LE.YMAX) GO TO 110
204           GO TO 120
205       110 VLEN=SQRT((XMIN-X1(I))**2+(Y   -Y1(I))**2)
206           GO TO 440
207       120 Y=A(I)*XMAX+B(I)
208           IF(Y.LE.Y1(I).AND.Y.GE.Y2(I)) GO TO 125
209           GO TO 140
210       125 IF(Y .GE. YMIN .AND.Y .LE. YMAX) GO TO 150
211           GO TO 140
212       150 VLEN=SQRT((XMAX-X1(I))**2+(Y   -Y1(I))**2)
213           GO TO 440
214       140 X=(YMIN-B(I))/A(I)
```

```
215         IF(A(I))141,142,142
216     141 IF(X.GE.X1(I).AND.X.LE.X2(I)) GO TO 145
217         GO TO 170
218     142 IF(X.LE.X1(I).AND.X.GE.X2(I)) GO TO 145
219         GO TO 170
220     145 IF (X .GE. XMIN .AND. X .LE. XMAX) GO TO 165
221         GO TO 170
222     165 VLEN=SQRT((X   -X1(I))**2+(YMIN-Y1(I))**2)
223         GO TO 440
224     170 IF(A(I).GT.-573.) GO TO 175
225         VLEN=Y1(I)-YMIN
226         GO TO 440
227     175 IF(A(I).LT.-.018.AND.A(I).GT.0.) GO TO 180
228         VLEN=XMAX-X1(I)
229         GO TO 440
230     180 IF(A(I).LT.0..AND.A(I).GT..018) GO TO 185
231         VLEN=X1(I)-XMIN
232         GO TO 440
233     185 WRITE(IPRINT,190) X1(I),Y1(I),X2(I),Y2(I)
234         GO TO 422
        C
        C       CALCULATES VECLEN WHEN VECTOR END IS WITHIN GRID CELL
        C
235     200 IF(A(I))202,201,202
236     201 VLEN=XMAX-X2(I)
237         GO TO 440
238     202 Y=A(I)*XMIN+B(I)
239         IF(Y.LE.Y1(I).AND.Y.GE.Y2(I)) GO TO 205
240         GO TO 220
241     205 IF(Y .GE. YMIN .AND. Y .LE. YMAX) GO TO 210
242         GO TO 220
243     210 VLEN=SQRT((XMIN-X2(I))**2+(Y   -Y2(I))**2)
244         GO TO 440
245     220 Y=A(I)*XMAX+B(I)
246         IF(Y.LE.Y1(I).AND.Y.GE.Y2(I)) GO TO 225
247         GO TO 240
248     225 IF(Y.GE.YMIN.AND.Y.LE.YMAX) GO TO 250
249         GO TO 240
250     250 VLEN=SQRT((XMAX-X2(I))**2+(Y   -Y2(I))**2)
251         GO TO 440
252     240 X=(YMAX-B(I))/A(I)
253         IF(A(I))241,242,242
254     241 IF(X.GE.X1(I).AND.X.LE.X2(I)) GO TO 245
255         GO TO 270
256     242 IF(X.LE.X1(I).AND.X.GE.X2(I)) GO TO 245
257         GO TO 270
258     245 IF(X.GE.XMIN.AND.X.LE.XMAX) GO TO 265
259         GO TO 270
260     265 VLEN=SQRT((X   -X2(I))**2+(YMAX-Y2(I))**2)
261         GO TO 440
262     270 IF(A(I).GT.-573.) GO TO 275
263         VLEN=YMAX-Y2(I)
264         GO TO 440
265     275 IF(A(I).LT.-.018.AND.A(I).GT.0.) GO TO 280
266         VLEN=X2(I)-XMIN
267         GO TO 440
268     280 IF(A(I).LT.0..AND.A(I).GT..018) GO TO 285
269         VLEN=XMAX-X2(I)
270         GO TO 440
271     285 WRITE(IPRINT,290) X1(I),Y1(I),X2(I),Y2(I)
```

```
272          GO TO 422
      C
      C      "PASS" DETERMINES WHETHER VECTOR PASSES THROUGH CELL
      C      AND IF SO, ITS LENGTH WITHIN THE CELL
      C
273     300  FLAG=0
274          NCLC1=0
275          NCLC2=0
276          NCLC3=0
277          NCLC4=0
      C      IF(Y1(I).LE.YMIN) RETURN
278          IF(Y1(I).LT.YMIN) RETURN
279          IF(Y2(I).GE.YMAX) RETURN
280          IF(Y1(I).GE.YMIN.AND.Y1(I).LE.YMAX.AND.X1(I).LE.XMIN.AND.A(I
            *).GT.0.) RETURN
281          IF(Y1(I).GE.YMIN.AND.Y1(I).LE.YMAX.AND.X1(I).GE.XMAX.AND.A(I
            *).LT.0.) RETURN
282          IF(Y2(I).GE.YMIN.AND.Y2(I).LE.YMAX.AND.X2(I).LE.XMIN.AND.A(I
            *).LT.0.) RETURN
283          IF(Y2(I).GE.YMIN.AND.Y2(I).LE.YMAX.AND.X2(I).GE.XMAX.AND.A(I
            *).GT.0.) RETURN
284          IF(Y1(I).GE.YMAX.AND.X1(I).GE.XMAX.AND.A(I).LT.0.) RETURN
285          IF(Y1(I).GE.YMAX.AND.X1(I).LE.XMIN.AND.A(I).GT.0.) RETURN
      C      IF(Y2(I).LE.YMIN.AND.X2(I).LE.XMIN.AND.A(I).LT.0.) RETURN
286          IF(Y2(I).LE.YMIN.AND.X2(I).GE.XMAX.AND.A(I).GT.0.) RETURN
287          IF(Y2(I).LE.YMIN.AND.X2(I).LE.XMIN.AND.A(I).LT.0..AND.A(I
            *).GT.-573.) RETURN
288          IF(A(I).EQ.0.0.AND.X1(I).GE.XMAX.AND.X2(I).LE.XMIN.AND.Y1
            *(I).GE.YMIN.AND.Y2(I).LT.YMAX) GO TO 301
289          IF(A(I).EQ.0.0.AND.X2(I).GE.XMAX) RETURN
290          IF(A(I).EQ.0.0.AND.X1(I).LE.XMIN) RETURN
291          IF(A(I).GT.-573.) GO TO 303
292          IF(X1(I).GE.XMIN.AND.X1(I).LT.XMAX.AND.X2(I).GE.XMIN.AND.X2(
            *I).LT.XMAX.AND.Y1(I).GE.YMAX.AND.Y2(I).LE.YMIN.AND.A(I).LE.
            *573.) GO TO 302
293          RETURN
294     301  VLEN=XMAX-XMIN
295          GO TO 440
296     302  VLEN=YMAX-YMIN
297          GO TO 440
298     303  YXMIN=A(I)*XMIN+B(I)
299          IF(YXMIN.LE.Y1(I).AND.YXMIN.GE.Y2(I)) GO TO 305
300          GO TO 320
301     305  IF(YXMIN.GE.YMIN.AND.YXMIN.LE.YMAX) GO TO 310
302          GO TO 320
303     310  NCLC1=1
304     320  YXMAX=A(I)*XMAX+B(I)
305          IF(YXMAX.LE.Y1(I).AND.YXMAX.GE.Y2(I)) GO TO 325
306          GO TO 340
307     325  IF(YXMAX.GE.YMIN.AND.YXMAX.LE.YMAX) GO TO 330
308          GO TO 340
309     330  NCLC2=1
310          IF(NCLC1.GT.0.AND.NCLC2.GT.0) GO TO 335
311          GO TO 340
312     335  VLEN=SQRT((YXMAX-YXMIN)**2+(XMIN-XMAX)**2)
313          GO TO 440
314     340  XYMIN=(YMIN-B(I))/A(I)
315          IF(A(I))341,342,342
316     341  IF(XYMIN.GE.X1(I).AND.XYMIN.LE.X2(I)) GO TO 345
317          GO TO 380
```

```
318      342 IF(XYMIN.LE.X1(I).AND.XYMIN.GE.X2(I)) GO TO 345
319      345 IF(XYMIN.GE.XMIN.AND.XYMIN.LE.XMAX) GO TO 350
320          GO TO 380
321      350 NCLC3=1
322          IF(NCLC2.GT.0.AND.NCLC3.GT.0) GO TO 360
323          GO TO 365
324      360 VLEN=SQRT((XMAX-XYMIN)**2+(YMIN-YXMAX)**2)
325          GO TO 440
326      365 IF(NCLC1.GT.0.AND.NCLC3.GT.0) GO TO 370
327          GO TO 380
328      370 VLEN=SQRT((XMIN-XYMIN)**2+(YXMIN-YMIN)**2)
329          GO TO 440
330      380 XYMAX=(YMAX-B(I))/A(I)
331          IF(A(I))381,382,382
332      381 IF(XYMAX.GE.X1(I).AND.XYMAX.LE.X2(I)) GO TO 385
333          GO TO 422
334      382 IF(XYMAX.LE.X1(I).AND.XYMAX.GE.X2(I)) GO TO 385
335          GO TO 422
336      385 IF(XYMAX.GE.XMIN.AND.XYMAX.LE.XMAX) GO TO 390
337          FLAG=0
338          RETURN
339      390 NCLC4=1
340          IF(NCLC3.GT.0.AND.NCLC4.GT.0) GO TO 395
341          GO TO 400
342      395 VLEN=SQRT((XYMAX-XYMIN)**2+(YMAX-YMIN)**2)
343          GO TO 440
344      400 IF(NCLC2.GT.0.AND.NCLC4.GT.0) GO TO 405
345          GO TO 410
346      405 VLEN=SQRT((XMAX-XYMAX)**2+(YMAX-YXMAX)**2)
347          GO TO 440
348      410 IF(NCLC1.GT.0.AND.NCLC4.GT.0) GO TO 425
349          IF(NCLC1.GE.1.OR.NCLC2.GE.1.OR.NCLC3.GE.1.OR.NCLC4.GE.1) GO
            *TO 420
350      420 WRITE(IPRINT,430) NCLC1,NCLC2,NCLC3,NCLC4,X1(I),Y1(I),X2(I),
            *Y2(I)
351      422 FLAG=0
352          RETURN
353      425 VLEN=SQRT((XYMAX-XMIN)**2+(YMAX-YXMIN)**2)
354      440 FLAG=1
355          IF(VLEN.LT.MINLEN) FLAG=0
356          RETURN
357      190 FORMAT('0','********ERROR********* VECTOR ORIGIN ',
            *'SUBROUTINE. VECTOR DELIMITERS ARE',4(5X,F7.1),//,' ',
            *'**ERROR MESSAGE REFERS TO FOLLOWING PRINTED CELL**')
358      290 FORMAT('0','********ERROR********* VECTOR END SUBROUTINE. ',
            *'VECTOR DELIMITERS ARE',4(5X,F7.1),//,' ','**ERROR ',
            *'MESSAGE REFERS TO FOLLOWING PRINTED CELL**')
359      430 FORMAT('0','******ERROR****** SUBROUTINE VECTOR-PASS; ',
            *'VALUES OF NCLC1-4 ARE',4I5,'VECTOR DELIMITERS ARE',4F7.1)
360          END
```

```
      SUBROUTINE MID
C
C     SUBROUTINE 'MID' DETERMINES IF VECTOR MIDPOINT FALLS WITHIN
C     GRID CELL
C
      COMMON X1(2000),Y1(2000),X2(2000),Y2(2000),VECAZM(2000),VECL
     *EN(2000),A(2000),B(2000),XMID(2000),YMID(2000),CLAMIN(90),CL
     *AMAX(90),AZLEN(90),NAZFRQ(90),XMIN,YMIN,XMAX,YMAX,FLAG,VLEN,
     *I
      INTEGER XMIN,YMIN,XMAX,YMAX,FLAG
      IF(XMID(I).GE.XMIN.AND.XMID(I).LT.XMAX.AND.YMID(I).GE.YMIN.A
     *ND.YMID(I).LT.YMAX) GO TO 1
      FLAG=0
      RETURN
    1 FLAG=-1
      RETURN
      END

      FUNCTION PRBCHI (CHISQ,IDF)
C
C     WRITTEN BY H.D. KNOBLE & F.YATES BORDEN, THE PENNSYLVANIA
C     STATE UNIVERSITY, 1966
C     THIS FUNCTION COMPUTES BY THE APPROXIMATIONS ON PAGE 941
C     OF "HANDBOK OF MATHEMATICAL FUNCTIONS", U.S. DEPT. OF
C     COMMERCE, 1964. GIVEN A VALUE OF CHI-SQUARE AND ITS DEGREES
C     OF FREEDOM, FUNCTION PRBCHI COMPUTES THE PROBABILITY OF A
C     GREATER VALUE OF CHI-SQUARE. THE Z(ARGUMENT) FUNCTION IS
C     COMPUTED BY FORMULA 26.2.1, P. 931.
C
      INTEGER TEST
C     ALL REAL*8 ARGUMENTS CHANGED TO DOUBLE PRECISION BY M.
C     PODWYSOCK1.
      DOUBLE PRECISION DSQRT,DEXP,ARG,SCHISQ,XPLEVL
      DOUBLE PRECISION Q,R,S,T,U,V,V9,PROB,S2PI,Z005,APPROX
      DATA S2PI/2.5066282D00/
C
      Q(ARG)=(DEXP(-ARG*ARG*0.5)/2.5066282D00)*(T*(0.3193815D00+T*
     *(-0.3565638D00+T*(1.781478D00+T*(-1.821256D00+(1.330274D00*T
     *))))))
      XPL=2.57623596D00
      PRBCHI=0.0
      IF(CHISQ.LT.0.0) RETURN
      IF(IDF.LE.0) RETURN
  100 SCHISQ=CHISQ
      S=1.0
      V=IDF
      V9=2.0/FLOAT(9*IDF)
      U=-SCHISQ*0.5
      SCHISQ=DSQRT(SCHISQ)
      IF(DABS(U).LT.174.6) GO TO 110
C
C     174.6 IS THE LARGEST ARGUMENT THAT EXP WILL TAKE.
C
      PROB=0.0
      GO TO 240
C
C     CHECK FOR DEGREES OF FREEDOM GREATER THAN 100 OR GREATER
C     THAN 30
C
```

```
389      110 IF (IDF.GT.100) GO TO 200
390          IF (IDF.GT.30) GO TO 170
         C
         C     DEGREES OF FREEDOM LESS THAN OR EQUAL TO 30
         C
391          PROB=0.0
392          TEST=MOD(IDF,2)
393          IF (TEST.NE.0) GO TO 140
         C
         C     EVEN DEGREES OF FREEDOM ** LESS THAN OR EQUAL TO 30 **
         C     FORMULA 26.4.5, PAGE 941
         C
394          IRANGE=(IDF-2)/2
395          IF (IRANGE.EQ.0) GO TO 130
396          DO 120  I=1,IRANGE
397          IR=I+I
398          S=S*IR
399      120 PROB=PROB+SCHISQ**IR/S
400      130 PROB=DEXP(U)*(1.0+PROB)
401          GO TO 230
         C
         C     ODD DEGREES OF FREEDOM ** LESS THAN OR EQUAL TO 29 **
         C     FORMULA 26.4.4, PAGE 941
         C
402      140 IRANGE=(IDF-1)/2
403          IF (IRANGE.EQ.0) GO TO 160
404          DO 150  I=1,IRANGE
405          IR=I+I-1
406          S=S*IR
407      150 PROB=PROB+SCHISQ**IR/S
408      160 T=1.0/(1.0+0.2316419D00*SCHISQ)
409          PROB=2.0*(Q(SCHISQ))+2.0*(DEXP(U)/S2PI)*PROB
410          GO TO 230
         C
         C   ********** GREATER THAN 30 DEGREES OF FREEDOM **********
         C   AN APPROXIMATE VALUE OF CHISQ IS FIRST COMPUTED THEN
         C   COMPARED WITH THE GIVEN CHISQ. IF THE APPROX. VALUE IS
         C   GREATER THAN THE GIVEN VALUE, Q(CHISQ,IDF) IS RETURNED
         C   AS .995.
         C   ****************************************************************
         C   FOR GREATER THAN 30 OR LESS THAN OR EQUAL TO 100 DEGREES OF
         C   FREEDOM THE APPROX. VALUE OF CHISQ AT THE .995 LEVEL IS
         C   COMPUTED BY FORMULA 26.4.7, PAGE 941.  THE SIGN OF X(P) IN
         C   THE FORMULA WAS CHANGED FROM + TO - TO ALLOW COMPUTATION OF
         C   CHISQ AT THE .995 LEVEL RATHER THAN THE .005 LEVEL AS IS THE
         C   CASE WHEN THE SIGN IS +.
         C
411      170 APROX=((1.0-V9-XPL*DSQRT(V9))**3)*V
412          IF (APROX.LE.CHISQ) GO TO 180
413          GO TO 210
414      180 V=((CHISQ/V)**0.33333333D00-(1.0-V9))/DSQRT(V9)
415      190 T=1.0/(1.0+0.2316419D00*V)
416          PROB=Q(V)
417          GO TO 230
         C
         C   GREATER THAN 100 DEGREES OF FREEDOM.   THE APPROX. VALUE OF
         C   CHISQ IS COMPUTED BY FORMULA 26.4.16, PAGE 941.  THE SIGN OF
         C   X(P) WAS CHANGED FOR THE SAME REASON AS ABOVE.
         C
418      200 APROX=((-XPL+DSQRT(V+V-1.0))**2)*0.5
```

```
      C
419         IF (APROX.LE.CHISQ) GO TO 220
420     210 PROB=+0.995
421         GO TO 240
422     220 V=DSQRT(2.0D0*CHISQ)-DSQRT(2.0*V-1.0)
423         GO TO 190
424     230 IF (PROB.GT.0.995) GO TO 210
425     240 PRBCHI=PROB
426         RETURN
427         END
```

```
C
C
C              ****************************************
C                  COEFFICIENT OF SIMILARITY PROGRAM
C              ****************************************
C
C        THE PROGRAM WAS WRITTEN BY FRANK MYNAR II OF THE GEOGRAPHY
C        DEPT., OKLAHOMA STATE UNIVERSITY, MARCH, 1982 FOR USE ON
C        AN IBM 370/168 COMPUTER.
C
C     PROGRAM CALCULATES COEFFICIENTS OF SIMILARITY FOR TWO DIFFERENT
C     VECTOR INTERPRETATIONS, BY COMPARING THE INTERPRETATIONS CELL
C     BY CELL, AS DISCUSSED BY HUNTINGTON AND RAICHE IN " A MULTI
C     ATTRIBUTE METHOD FOR COMPARING GEOLOGICAL LINEAMENT INTERPRET-
C     ATIONS" (1978).  BOTH CELLULAR AND SCENE COEFFICIENTS OF
C     SIMILARITY ARE CALCULATED, BASED ON VECTOR LENGTH PER AZIMUTH
C     CLASS PER CELL.  A COEFFICIENT OF 1.00 INDICATES PERFECT
C     SIMILARITY BETWEEN THE TWO INTERPRETATIONS, WHILE A COEFFICIENT
C     OF 0.00 INDICATES PERFECT DISSIMILARITY.  DATA ARE READ FROM
C     CARDS GENERATED BY THE "AZMAP" PROGRAM.  CONTROL AND TITLE
C     CARDS ARE READ FROM CARD READER WHILE DATA CARDS MAY BE READ
C     FROM ANY UNITS DECLARED BY 'ITAPE1' AND 'ITAPE2' ON CONTROL
C     CARD 1.
C
C     ALL NUMERIC INPUT DATA IS RIGHT JUSTIFIED: "I" INDICATES INTEGER
C     FORMAT, "F" INDICATES FLOATING POINT FORMAT, "A" INDICATES
C     CHARACTER FORMAT, "#" PRECEEDING NUMBERS INDICATES COLUMNS USED
C     FOR EACH PARAMETER.
C
C ********CONTROL CARD 1------OPTIONS CARD
C     NCOLS=NUMBER OF COLUMNS IN CELL MATRIX, AS DEFINED IN "AZMAP"
C         (I3,#1-3)
C     NROWS=NUMBER OF ROWS IN CELL MATRIX, AS DEFINED IN "AZMAP"
C         (I3,#4-6)
C     NCELL=NUMBER OF CELLS (TOTAL) IN CELL MATRIX, AS DEFINED IN
C         "AZMAP" (I4,#7-10)
C     NCLASS=NUMBER OF AZIMUTH CLASSES, AS GIVEN IN "AZMAP"
C         (I2,#11-12)
C     ITAPE1=LOGICAL UNIT FOR READING DATA CARDS GENERATED BY "AZMAP"
C         PROGRAM, FOR VECTOR INTERPRETATION 1 (I2,#13-14)
C     ITAPE2=LOGICAL UNIT FOR READING DATA CARDS GENERATED BY "AZMAP"
C         PROGRAM, FOR VECTOR INTERPRETATION 2 (I2,#15-16)
C ********CONTROL CARD 2------TITLE CARD
C     TITLE WILL BE PRINTED AT TOP OF EACH COEFFICIENT OF SIMILARITY
C         MAP (20A4,#1-80)
C ********CONTROL CARD 3------VARIABLE INPUT FORMAT CARD
C     TO READ X & Y VALUES FROM CARDS GENERATED BY THE "AZMAP"
C         PROGRAM, THIS FORMAT MUST AGREE WITH THE 'FMTPCH'
C         FORMAT AS SPECIFIED ON CONTROL CARD 2A OF THE "AZMAP"
C         PROGRAM, WITH A SKIP FIELD INSERTED FOR THE FIRST 4
C         VARIABLES.  FORMAT MUST BE ENCLOSED IN PARENTHESES
C         AND BEGIN IN #1. (18A4,#1-72)
C ********CONTROL CARD 4------VARIABLE OUTPUT FORMAT CARD
C     TO PRINT COEFFICIENT OF SIMILARITY MAP FOR CELL MATRIX,
C         THIS FORMAT MUST AGREE WITH THE NUMBER OF VARIABLES
C         TO BE PRINTED ACROSS ONE LINE OF THE MATRIX (I.E.
C         'NCOLS').  FORMAT MUST BE ENCLOSED IN PARENTHESES
C         AND BEGIN IN #1.  (18A4,#1-72)
C
```

```
1           DIMENSION TITLE(20),FMTRD(18),FMPRT(18),AZLEN1(100),AZLEN2(100),
           *WSUM(250),DSUM(250),CCOEFF(250),PRT(100,100)
2           DATA IREAD/9/,IPRINT/6/
      C
      C     READ CONTROL CARDS
      C
3           READ(IREAD,5) NCOLS,NROWS,NCELL,NCLASS,ITAPE1,ITAPE2
4           READ(IREAD,6) (TITLE(L),L=1,20)
5           READ(IREAD,7) (FMTRD(L),L=1,18)
6           READ(IREAD,7) (FMPRT(L),L=1,18)
7         5 FORMAT(2I3,I4,3I2)
8         6 FORMAT(20A4)
9         7 FORMAT(18A4)
      C
      C     READ DATA OUTPUT FROM AZMAP, ONE CELL AT A TIME, FOR INTERP. 1
      C     AND INTERP. 2
      C
10          DO 200 N=1,NCELL
11          READ(ITAPE1,FMTRD) (AZLEN1(M),M=1,NCLASS)
12          READ(ITAPE2,FMTRD) (AZLEN2(M),M=1,NCLASS)
13          NDBUG=0
14          IF(NDBUG.EQ.0) GO TO 99
15          WRITE(6,101) (AZLEN1(M),M=1,NCLASS)
16          WRITE(6,101) (AZLEN2(M),M=1,NCLASS)
17        101 FORMAT(1H0,7F7.2/10F7.2/1F7.2)
      C
      C     COMPUTE COEFFICIENT OF SIMILARITY, ONE CELL AT A TIME
      C
18         99 WSUM(N)=0
19          DO 150 M=1,NCLASS
20          DSUM(N)=0
21          DO 100 I=1,NCLASS
22          DSUM(I)=AZLEN1(I)**2+AZLEN2(I)**2
23          DSUM(N)=DSUM(I)+DSUM(N)
24          NDBUG=0
25          IF(NDBUG.EQ.0) GO TO 100
26          WRITE(6,103) DSUM(N)
27        103 FORMAT(1H0,F7.2)
28        100 CONTINUE
29          IF(DSUM(N).EQ.0.) GO TO 50
30          WSUM(M)=(AZLEN1(M)/((.5*DSUM(N))**.5))*(AZLEN2(M)/((.5*DSUM(N))
           ***.5))
31          WSUM(N)=WSUM(M)+WSUM(N)
32        150 CONTINUE
33          CCOEFF(N)=WSUM(N)
34          GO TO 200
35         50 CCOEFF(N)=0.
36          NDBUG=0
37          IF(NDBUG.EQ.0) GO TO 200
38          WRITE(6,102) (CCOEFF(J),J=1,NCELL)
39        102 FORMAT(1H0,9(F4.2,2X))
40        200 CONTINUE
      C
      C     COMPUTE SCENE COEFFICIENT OF SIMILARITY
      C
41          CSUM=0
42          DO 300 N=1,NCELL
43          CSUM=CSUM+CCOEFF(N)
44        300 CONTINUE
45          SCOEFF=CSUM/NCELL
```

```
      C
      C     MAP COEFFICIENT OF SIMILARITY FOR CELL MATRIX
      C
46          WRITE(IPRINT,11) (TITLE(L),L=1,20)
47       11 FORMAT(1H1,20X,20A4)
48          L=1
49          DO 500 J=1,NROWS
50          DO 500 K=1,NCOLS
51          PRT(J,K)=CCOEFF(L)
52      500 L=L+1
53          DO 600 J=1,NROWS
54      600 WRITE(IPRINT,FMPRT) (PRT(J,K),K=1,NCOLS)
      C
      C     PRINT SCENE COEFFICIENT OF SIMILARITY
      C
55          WRITE(IPRINT,21) SCOEFF
56       21 FORMAT(1HO,'SCENE COEFFICIENT OF SIMILARITY = ',F4.2)
57          STOP
58          END
```

VITA

Frank Mynar II

Candidate for the Degree of

Master of Science

Thesis: COMPUTER ENHANCEMENT OF LANDSAT DIGITAL DATA FOR THE DETECTION OF LINEAMENTS

Major Field: Geography

Biographical:

Personal Data: Born in Flint, Michigan, April 6, 1957, the son of Mr. and Mrs. Frank Mynar.

Education: Graduated from Hamady High School, Flint, Michigan, in June, 1975; received Bachelor of Science degree from the University of Michigan - Flint, in December, 1979; completed requirements for the Master of Science degree at Oklahoma State University in July, 1982.

Professional Experience: Graduate research assistant, Center for Applications of Remote Sensing, Department of Geography, Oklahoma State University, May, 1980 - May, 1982.

Professional Organizations: Member, Association of American Geographers; member, American Society of Photogrammetry.